Natural Resources Canada Ressources naturelles Canada

GEOLOGICAL SURVEY OF CANADA
OPEN FILE 8878

Hydrogen sulfide (H_2S) in the Montney Formation, Western Canada Sedimentary Basin (WCSB) - investigating a complex issue, workshop proceeding

Edited by
O.H. Ardakani and P.K. Pedersen

2022

Canada

GEOLOGICAL SURVEY OF CANADA
OPEN FILE 8878

Hydrogen sulfide (H_2S) in the Montney Formation, Western Canada Sedimentary Basin (WCSB) - investigating a complex issue, workshop proceeding

Edited by
O.H. Ardakani[1,2] and P.K. Pedersen[2]

[1]Geological Survey of Canada, 3303-33rd Street N.W., Calgary, Alberta
[2]Department of Geoscience, University of Calgary, 2500 University Drive N.W., Calgary, Alberta

2022

Permanent link: https://doi.org/10.4095/329782

Recommended citation
Ardakani, O.H. and Pedersen, P.K. (ed.), 2022. Hydrogen sulfide (H_2S) in the Montney Formation, Western Canada Sedimentary Basin (WCSB) - investigating a complex issue, workshop proceeding; Geological Survey of Canada, Open File 8878, 68 p. https://doi.org/10.4095/329782

Contents

List of presentations

Speaker	**Affiliation**	**Title**	**Theme**
Gabrielle Scheffer	University of Calgary	Microorganisms from the Montney formation: where are they coming from and what can they do?	Diagenetic and Geochemical Controls
Mastaneh Liseroudi	University of Calgary	Diagenetic and geochemical controls on H_2S distribution in the Montney Formation, Peace River Region, Western Canada	
Jaime Cesar	Natural Resources Canada – Geological Survey of Canada, Calgary	Organic geochemistry of the Montney Formation. New insights on the source of hydrocarbons, their accumulation history and post accumulation processes	
Andrew Kingston	Natural Resources Canada – Geological Survey of Canada, Calgary	Tracing the subsurface sulfur cycle using isotopic and elemental fingerprinting: From the micro to the macro scale	
Andy Mort	Natural Resources Canada – Geological Survey of Canada, Calgary	Controls on the distribution and composition of gas and condensate in the Montney Resource Play	Distribution and Mapping
Pablo Silva	University of British Columbia	Distribution of H_2S in the Triassic of Western Canada-Old Problems and New Ideas	
Andrew Kingston	Natural Resources Canada – Geological Survey of Canada, Calgary	Hydrogen Sulfide (H_2S) Distribution in the Triassic Montney Formation of the Western Canadian Sedimentary Basin	
Paulina Wozniakowska	University of Calgary	Identification of regional structural corridors in the Montney play using trend surface analysis combined with geophysical imaging	Structural and Stratigraphic Controls
Samantha Mackie	University of Calgary	Stratigraphy and Facies Heterogeneities in the Montney Formation of Northeastern British Columbia: Relation to H_2S Distribution	

Hydrogen sulfide in Montney, previous and current knowledge, the way forward – Introduction

Omid H. Ardakani[1,2], *Per K. Pedersen*[2]
[1]*Natural Resources Canada, Geological Survey of Canada, Calgary*
[2]*Department of Geoscience, University of Calgary, Calgary*

Non-hydrocarbon gases in sedimentary basins

Generation of petroleum fluids due to the increased temperatures associated with progressive burial of organic-rich source rocks within sedimentary basins is well established (Seewald, 2003). However, the role of inorganic sedimentary components in organic transformations associated with hydrocarbon generation is not well understood (Seewald, 2003). Conversion of metastable macromolecular kerogen to thermodynamically favored lower molecular mass compounds occur in response to the removal of kinetic barriers, as temperatures increase with progressive burial in sedimentary basins (Tissot and Welte, 1984; Seewald, 2003; Peters et al., 2004). Water also plays a significant role in these processes, facilitating reaction mechanisms and may contribute hydrogen and oxygen for the formation of hydrocarbons and oxygenated alteration products. Non-hydrocarbon generated gases, hydrogen sulfide (H_2S), carbon dioxide (CO_2), and nitrogen (N_2), are common major accompanying gases in petroleum-rich sedimentary basins (Tissot and Welte, 1984; Cooles et al., 1987; Seewald, 2003) including Western Canada Sedimentary Basin (WCSB) (Hitchon et al., 1999; Hutcheon, 1999 and references therein).

The origin, source, and formation mechanism of non-hydrocarbon gases in sedimentary basins may provide patterns of fluid flow, water-rock interaction and diagenesis processes that control formation and/or dissolution of cement that in turn control porosity and permeability of sedimentary rocks. (Surdam et al., 1989; Hutcheon, 1999). Some non-hydrocarbon gases like CO_2 originate through the generation of petroleum and hydrocarbon gases, thus providing some information of the microbial and thermal evolution of sedimentary basins, whereas other non-hydrocarbon gases like H_2S can be generated through water-rock interaction.

Microbial processes within sedimentary basins are one of the major controlling factors of diagenetic processes in sedimentary basins in addition to the generation of natural gas through bacterial methanogenesis (Lovley and Chapelle, 1995; Martini et al., 2003; McIntosh et al., 2004 among many others). Microbial sulfate reduction (MSR) is one of the major known metabolic processes in the subsurface (Amrani, 2014; Fike et al., 2015). This process, along with other microbial activity that contributes to diagenesis in sedimentary basins, are a common source of sulfide mineralization (Cavalazzi et al., 2014). The most abundant sulfide minerals in organic-rich shales, in particular, is pyrite where a supply of organic matter fuels microbial activity (Raiswell and Berner, 1986). Another major sulfate-reduction process in sedimentary basins at temperatures higher than ~90°C is thermochemical sulfate reduction (TSR) which plays a key role in H_2S generation when iron is not available (Krouse et al., 1988; Machel, 2001; Amrani, 2014; Fike et al., 2015). Among non-hydrocarbon gases H_2S—a highly toxic and corrosive gas—has adverse environmental and economic impacts; for the latter, high concentrations of H_2S in hydrocarbon decreases its heat value (Worden et al., 1996).

Hydrogen sulfide in WCSB – Previous studies

Previous major studies on the origin and distribution of non-hydrocarbon gases including H_2S in the WCSB were mainly focused on the Alberta Basin (Hutcheon, 1999). Several studies reported isotopic analyses of hydrocarbon and non-hydrocarbon gases, particularly CO_2 and H_2S, and their distribution in the Alberta Basin (Krouse, 1983; Krouse et al., 1988; Cody, 1993; Machel et al., 1995; McLellan, 1995; Kirste et al., 1997; Desrocher et al., 2004). Major H_2S or sour hydrocarbon-bearing strata in the WCSB include 1) Devonian and Mississippian reservoirs in the Paleozoic, 2) the Montney and Halfway formations of the Triassic; the Mannville and Colorado groups of the Cretaceous in the Mesozoic (Hutcheon, 1999).

Simpson (1999) reported H_2S concentration up to 30 mole% with a small number of values ranging between 30 and greater than 80 mole% in Devonian reservoirs of southwestern Alberta within the WCSB. The H_2S concentration in the Mississippian reservoirs is lower than Devonian reservoirs but reaches 15 mole% with local maximum values of up to 20 mole% in western Alberta (Hutcheon, 1999). The H_2S concentration in Lower and Middle Triassic reservoirs (Montney through Halfway formations respectively) reach 29 mole% (Kirste et al., 1997; Hutcheon, 1999; Desrocher et al., 2004). H_2S concentration in the Mannville Group in southern Alberta ranges from 0 to 1 mole% (Cody et al., 1999). In comparison to the Mannville Group, H_2S concentration in the Colorado Group is negligible (Mclellan, 1995). Both MSR and TSR has been suggested as the main diagenetic processes responsible for the generation of H_2S in the WCSB (Krouse et al., 1988; Machel et al., 1995a,b; Desrocher, 1997; Kirste et al., 1997; Desrocher et al., 2004). These abundant studies shows that H_2S in the WCSB has been a challenge for the industry throughout the hydrocarbon resource extraction history of the WCSB.

H_2S origin and distribution in the Montney Formation – Current studies

Since the discovery of gas in Triassic reservoirs at Whitelaw, Alberta in 1950, Triassic reservoirs of west-central Alberta have been the focus of natural gas exploitation (Edwards et al., 1994). Advancement in directional drilling and hydraulic fracturing of tight reservoirs made the Lower Triassic Montney Formation a prolific unconventional resource in North America (National Energy Board, 2013; USGS, 2019). The Lower Triassic Montney Formation, part of the greater Triassic petroleum system of the WCSB, is considered to be world-class, as it is the most prolific unconventional tight gas and hydrocarbon liquids play in the WCSB;estimated natural gas, oil, and liquid condensate reserves of 450 TCF, 1,125, and 1.7 MMB, respectively (National Energy Board, 2013; USGS, 2019).

The local high concentration of H_2S in the Montney Formation in southwestern Alberta, and to a lesser degree in northeast British Columbia, have raised economic and environmental concerns. Initial studies on the distribution and origin of H_2S in the Triassic of the WCSB using H_2S sulfur isotope data suggested MSR as the main process involved in H_2S generation in the Doig and Halfway formations, whereas the basal Doig anhydrite was suggested to be the source for sulfate-rich fluids. Conversely the H_2S in Montney is thought to be primarily produced by TSR during maximum burial (Kirste et al., 1997; Desrocher et al., 2004).

The University of British Columbia in a project funded by Geoscience BC investigated the H_2S distribution in several major unconventional resources (i.e., Montney, Doig, and Duvernay formations) in northeastern British Columbia and northwestern Alberta (Chalmers et al., 2019, 2020, 2021; Silva and Bustin, 2021). In another project, in order to better understand the main source(s) of sulfate-rich fluids as well as the main H_2S generation mechanism(s), Natural Resources Canada (NRCan) in collaboration with the University of Calgary and Ovintiv (formerly Encana) investigated the regional digenetic controls including water-rock interaction, and sulfur cycle on H_2S generation in the Montney Formation. In those studies, detailed petrography, bulk in-situ sulfur, and oxygen isotope analysis were perfumed to shed light on the origin of sulfate-rich fluids, pyrite geochemistry, and major mechanisms involved in H_2S generation (Liseroudi, 2021; Liseroudi et al., 2020, 2021).

This project was expanded using additional funds from NRCan's Office of Energy Research and Development (OERD). This extended research, which also included collaboration with provincial geological surveys and industry, allowed for further investigation of geologic factors such as structure, stratigraphy and diagenesis, as well as anthropogenic factors (i.e., hydraulic fracturing fluids) on H_2S distribution and generation in the Montney Formation within WCSB. The current abstract volume presents the collective works of the Geological Survey of Canada, University of Calgary, and the

University of British Columbia undertaken since 2019 on the distribution and origins of H_2S in the Montney Formation of the WCSB.

This open file report presents the proceedings of the online workshop "Hydrogen sulfide (H_2S) in the Montney Formation - investigating a complex issue" on February 9th, 2022 in Calgary Alberta, organized by the Canadian Society for Unconventional Resources (CSUR), Natural Resources Canada (NRCan), and University of Calgary. Sheffer et al. presented the initial results of microbial activity and microbial evolution of hydraulic fracturing, flowback, and produced water from a Montney Formation well in western Alberta. They used DNA sequencing to identify sulfate-reducing microbes in the initial fluids and formation water and their possible role in in-situ H_2S generation during hydraulic fracturing.

Liseroudi, Kingston, and Silva presented the sulfur isotopic composition of H_2S gas, sulfate minerals as well as pyrite to shed light on the sulfur cycle (sulfate – sulfide) in the Montney Formation and the major mechanism of H_2S generation. Cesar and Mort discussed the organic geochemistry of the Montney Formation hydrocarbons as it pertains to H_2S generation, and migration. Kingston and Mackie investigated the H_2S distribution on regional and local scales, respectively.

Mackie further discussed in detail, the stratigraphic controls on the distribution of H_2S on a local scale. Wozniakowska discussed the use of trend surface analysis combined with geophysical imaging in the identification of regional structural corridors in the Montney play. Major structures were found to play a key role in the migration of sulfate-rich fluids, H_2S and hydrocarbon gases.

Finally, in the last section of this proceeding we provide the discussions during Q&A sessions after each talk and session to capture the collective understanding of the workshop participants, and to further elucidate the current knowledge of H_2S in the Montney play, identify new knowledge gaps, and to suggest future research plans that will result in the development of better strategies to avoid areas with risk of high H_2S in the Montney Formation.

Acknowledgements

The authors would like to thank Canadian Society for Unconventional Resources (CSUR) for organizing of this workshop. Natural Resources Canada (NRCan), the Geological Survey of Canada's Geoscience for New Energy Supply Program, NRCan's Office of Energy Research Development (OERD) and the University of Calgary Tight Oil Consortium (TOC) which together, funded the majority of research presented in tis workshop. Moreover, a vast amount of the H_2S data and gas isotope analysis used in this project was obtained from Alberta Geological Survey (AGS) and British Columbia Oil and Gas Commission (BCOGC); their participation in this project is appreciated. Finally, we would like to offer our profound thanks to each of the speakers, and those who actively participated in the discussions.

References

Amrani, A., 2014. Organosulfur Compounds: Molecular and Isotopic Evolution from Biota to Oil and Gas. Annual Review of Earth and Planetary Sciences 42, 733–768. https://doi.org/10.1146/annurev-earth-050212-124126

Cavalazzi, B., Agangi, A., Barbieri, R., Franchi, F., Gasparotto, G., 2014. The formation of low-temperature sedimentary pyrite and its relationship with biologically-induced processes. Geology of Ore Deposits 56, 395–408. https://doi.org/10.1134/S107570151405002X

Chalmers, G.R.L., Bustin, R.M., Bustin, A.A., 2021. Isotopic Fingerprinting of Sulphur Sources for the Hydrogen Sulphide Gas in the Montney Formation, Northeastern British Columbia (NTS 093O, P, 094A, B, G-J, N-P). in: Geoscience BC Summary of Activities 2020:Energy and Water, Geoscience BC, Report 2021-02, p. 103–108.

Chalmers, G.R.L., Bustin, R.M., Bustin, A.A., 2020. Hydrogen Sulphide within the Triassic Montney Formation, Northeastern British Columbia and Northwestern Alberta (NTS 083K–N, 084C–F, 093I, J, O, P, 094A, B, G, H). in: Geoscience BC Summary of Activities 2019:Energy and Water, Geoscience BC, Report 2020-02, p. 41–52.

Chalmers, G.R.L., Bustin, R.M., Bustin, A.A., 2019. Stratigraphic and Lateral Distribution of Hydrogen Sulphide within the Triassic Montney Formation, Northern Regional Play Area, Northeastern British Columbia and Northwestern Alberta. in: Geoscience BC Summary ofActivities 2018: Energy and Water, Geoscience BC, Report 2019-2, p. 43–46.

Cody, J., 1993. Geochemistry of formation fluids in the Mannville Group (Lower Cretaceous), Southern Alberta: Sources, controls and water-rock interaction of carbon dioxide rich fluids. Unpublished M.Sc. thesis, the University of Calgary, 129 p.

Cody, J.D., Hutcheon, I.E., Krouse, H.R., 1999. Fluid flow, mixing and the origin of CO_2 and H_2S by bacterial sulphate reduction in the Mannville Group, southern Alberta, Canada. Marine and Petroleum Geology 16, 495–510. https://doi.org/10.1016/S0264-8172 (99)00012-4

Cooles, G.P., Mackenzie, A.S., Parkes, R.J., 1987. Non-hydrocarbons of significance in petroleum exploration: volatile fatty acids and non-hydrocarbon gases. Mineralogical Magazine 51, 483–493. https://doi.org/10.1180/minmag.1987.051.362.03

Desrocher, S., Hutcheon, I., Kirste, D., Henderson, C.M., 2004. Constraints on the generation of H2S and CO2 in the subsurface Triassic, Alberta Basin, Canada. Chemical Geology 204, 237–254. https://doi.org/10.1016/j.chemgeo.2003.11.012

Edwards, D.W., Barclay, J.E., Gibson, D.W., Kvill, G.E., Halton, E., 1994. Triassic strata of the Western Canada Sedimentary Basin; Chapter, in: Mossop, G.D., Shetsen, I. (Eds.), Geological Atlas of the Western Canada Sedimentary Basin,. Canadian Society of Petroleum Geologists, 257–275.

Fike, D.A., Bradley, A.S., Rose, C. v., 2015. Rethinking the Ancient Sulfur Cycle. Annual Review of Earth and Planetary Sciences 43, 593–622. https://doi.org/10.1146/annurev-earth-060313-054802

Hitchon, B., Gunter, W.D., Gentzis, T., Bailey, R.T., 1999. Sedimentary basins and greenhouse gases: a serendipitous association. Energy Conversion and Management 40, 825–843. https://doi.org/10.1016/S0196-8904(98)00146-0

Hutcheon, I., 1999. Controls on the distribution of non-hydrocarbon gases in the Alberta Basin. Bulletin of Canadian Petroleum Geology 47, 573–593. https://doi.org/10.35767/gscpgbull.47.4.573

Kirste, D., Desrocher, S., Spence, B., Hoyne, B., Tsang, B., Hutcheon, I., 1997. Fluid flow, water chemistry, gas chemistry and diagenesis in the subsurface Triassic in Alberta and British Columbia. Bulletin of Canadian Petroleum Geology 45, 742–764. https://doi.org/gscpgbull.45.4.742

Krouse, H.R., 1983. Stable isotope research in support of more effective utilization of gas fields in Alberta. Final report, Alberta - Canada Energy Resource Research Fund, Agreement U-30

Krouse, H.R., Viau, C.A., Eliuk, L.S., Ueda, A., Halas, S., 1988. Chemical and isotopic evidence of thermochemical sulphate reduction by light hydrocarbon gases in deep carbonate reservoirs. Nature 333, 415–419. https://doi.org/10.1038/333415a0

Liseroudi, M., 2021. Regional Diagenesis and Fluid Flow Study of the Early Triassic Montney Formation as Related to H2S Generation. Unpublished Ph.D. thesis, the University of Calgary, 209 p.

Liseroudi, M.H., Ardakani, O.H., Pedersen, P.K., Stern, R.A., Wood, J.M., Sanei, H., 2021. Microbial and Thermochemical Controlled Sulfur Cycle in the Early Triassic Sediments of the Western Canadian Sedimentary Basin. Journal of the Geological Society 55, jgs2020-175. https://doi.org/10.1144/jgs2020-175

Liseroudi, M.H., Ardakani, O.H., Sanei, H., Pedersen, P.K., Stern, R.A., Wood, J.M., 2020. Origin of sulfate-rich fluids in the Early Triassic Montney Formation, Western Canadian Sedimentary Basin. Marine and Petroleum Geology 114, 104236. https://doi.org/10.1016/j.marpetgeo.2020.104236

Lovley, D.R., Chapelle, F.H., 1995. Deep subsurface microbial processes. Reviews of Geophysics 33, 365. https://doi.org/10.1029/95RG01305

Machel, H.G., 2001. Bacterial and thermochemical sulfate reduction in diagenetic settings - old and new insights. Sedimentary Geology 140, 143–175. https://doi.org/10.1016/S0037-0738(00)00176-7

Machel, H.G., Krouse, H.R., Sassen, R., 1995a. Products and distinguishing criteria of bacterial and thermochemical sulfate reduction. Applied Geochemistry 10, 373–389. https://doi.org/10.1016/0883-2927(95)00008-8

Machel, H. G., Krouse, H. R., Riciputi, L. R., Cole, D. R. 1995b. Devonian Nisku Sour Gas Play, Canada: A Unique Natural Laboratory for Study of Thermochemical Sulfate Reduction. In M. A. Vairavamurthy, M. A. A. Schoonen, T. I. Eglinton, G. W. Luther, & B. Manowitz (Eds.), *Geochemical Transformations of Sedimentary Sulfur* 439–454. American Chemical Society. https://doi.org/10.1021/bk-1995-0612.ch025

Martini, A.M., Walter, L.M., Ku, T.C.W., Budai, J.M., McIntosh, J.C., Schoell, M., 2003. Microbial production and modification of gases in sedimentary basins: A geochemical case study from a Devonian shale gas play, Michigan basin. American Association of Petroleum Geologists Bulletin 87, 1355–1375. https://doi.org/10.1306/031903200184

McIntosh, J.C., Walter, L.M., Martini, A.M., 2004. Extensive microbial modification of formation water geochemistry: Case study from a Midcontinent sedimentary basin, United States. Geological Society of America Bulletin 116, 743. https://doi.org/10.1130/B25371.1

McLellan, S.R., 1995. Fluid flow, gas isotope geochemistry, and diagenesis in the Bow Island Formation (Lower Cretaceous) of southern Alberta. Unpublished M.Sc. thesis, the University of Calgary, 107 p.

National Energy Board, 2013. The Ultimate Potential for Unconventional Petroleum from the Montney Formation of British Columbia and Alberta - Energy Briefing Note - November 2013.

Peters, K.E., Walters, C.C., Moldowan, J.M., 2004. The Biomarker Guide, The Biomarker Guide. Cambridge University Press. https://doi.org/10.1017/CBO9780511524868

Raiswell, R., Berner, R.A., 1986. Pyrite and organic matter in Phanerozoic normal marine shales, Geochimica et Cosmochimica Acta. https://doi.org/10.1016/0016-7037(86)90252-8

Seewald, J.S., 2003. Organic–inorganic interactions in petroleum-producing sedimentary basins. Nature 426, 327–333.

Silva, P.L., Bustin, R.M., 2021. Hydrogen Sulphide within the Triassic Doig Formation, Northeastern British Columbia and Northwestern Alberta (Parts of NTS 083, 084, 093, 094), in: Geoscience BC Summary of Activities 2020: Energy and Water, Geoscience BC, Re-port 2021-02, p. 109–112.

Simpson, G.P., 1999. Sulfate reduction and fluid chemistry of the Devonian Leduc and Nisku formations in south central Alberta. Unpublished Ph.D. thesis, the University of Calgary, 265 p.

Surdam, R.C., Crossey, L.J., Hagen, E.S., Heasler, H.P., 1989. Organic-inorganic interactions and sandstone diagenesis. American Association of Petroleum Geologists Bulletin 73, 1–23. https://doi.org/10.1306/703c9ad7-1707-11d7-8645000102c1865d

Tissot, B.P., Welte, D.H., 1984. Petroleum Formation and Occurrence. Springer Berlin Heidelberg, Berlin, Heidelberg. https://doi.org/10.1007/978-3-642-87813-8

USGS, 2019. Assessment of Continuous Gas Resources in the Montney. https://doi.org/10.3133/fs20183071

Worden, R.H., Smalley, P.C., Oxtoby, N.H., 1996. The effects of thermochemical sulfate reduction upon formation water salinity and oxygen isotopes in carbonate gas reservoirs, Geochimica et Cosmochimica Acta 60, 3925–3931.

Microorganisms from the Montney formation: where are they coming from and what can they do?

Gabrielle Scheffer[1], Carmen Li[1], Andrew Hubley[2] & Casey R.J. Hubert[1]*
[1] Geomicrobiology Group, Department of Biological Sciences, University of Calgary, Calgary, Canada
[2]ARC Resources Ltd., Calgary, Canada

**Gabrielle.scheffe1@ucalgary.ca*

Introduction

Microorganisms have been found within the most unlikely places on Earth including deep-sea sediments, hot springs, acid mines and many others (Kohli et al., 2020). These microorganisms are termed "extremophiles" and can withstand extreme conditions including: very high or very low temperature, high salinity or the presence of radioactive materials (Filippidou et al., 2016; Kohli et al., 2020). It is therefore not a surprise to also find microorganisms within hydraulically fractured shale reservoirs where survival depends on high temperature, high pressure and high salinity. An example in Canada is the Montney shale formation with its well temperature around 90-95ºC (Government of Canada, 2015).

An open question within the field of microbiology is the provenance of microorganisms within the hydraulically fractured shale formation. Some hypothesize that these organisms are native from shale. Others have speculated that microorganisms are introduced to the reservoir with the injection of fluids, can withstand the extreme conditions and proliferate (Lipus et al., 2018). The role of these microorganisms in the production of sulfide (biogenic souring) has been questioned due to the very high temperature of the formation which would allow only for the presence of extremophiles (Gittel et al., 2009; Okpala et al., 2017). The aim of this study was, therefore, to investigate if microorganisms are potentially native from the shale formation or introduced with the input fluids. An additional goal was to identify potential sulfide-producing microorganisms within the shale formation that could lead to biogenic souring.

Methodology

Samples collection and preparation

Drilling muds and shale cuttings were collected in Isojars during the initial drilling of the well at various depths (see Table 1) and kept at 4°C upon delivery to the laboratory. Produced water and fracturing fluid samples were collected in sterile 1L plastic bottles filled in order to limit oxygen within the bottle. Samples were collected during the initial flooding of the well, and each month thereafter.

DNA extraction 16S rRNA gene sequencing

For the shale cuttings and drilling muds, 16g of frozen samples were transferred into a 50 mL plastic tube and processed following the manufacturer's instructions of the PowerMax soil DNA isolation kit (Qiagen, 2022). For produced water and fracturing fluid samples, 400 mL were thawed and filtered through a 0.1 µM filter. This filter was then frozen until DNA extraction using the DNeasy PowerLyzer PowerSoil DNA extraction kit (Qiagen, 2022).

The V6-V8 region of the bacterial and archaeal 16S rRNA gene was amplified using the primers 515F (GTGYCAGCMGCCGCGGTAA) and 806R (GGACTACNVGGGTWTCTAAT), followed by post-PCR cleanup and indexing. Indexed amplicon samples were sequenced using Illumina's v3 600-cycle (paired-end) reagent kit on an Illumina MiSeq benchtop sequencer (Illumina, 2022) after all DNA extraction blanks and PCR reagent blanks were confirmed for negative amplification.

Data processing

Raw sequences were quality controlled and further processed to construct an amplicon sequence variant (ASV) table. ASVs are used in taxonomy to classify identical sequences together. If a sequence has one divergent nucleotide compared to another sequence, it will create two ASVs which will be considered as a part of the same given genus. Analysis and graphing was done using R and GraphPad Prism (GraphPad, 2022; The R Project for Statistical Computing, 2022) . BlastN was used in order to find potential matches to the specie level to provide further information on the ASV results (Nucleotide BLAST, 2022).

Results and Discussion

16S rRNA gene sequencing quality

16S rRNA gene sequencing screens for the microbial community diversity present within the different samples. The number of sequence reads can differ greatly between samples, so relative abundances of microbial groups are compared. Produced water samples generally resulted in a greater amount of 16S rRNA gene sequences, and greater DNA concentrations (data not shown) compared to the cuttings and drilling muds. This is due to the nature of the samples. The presence of bentonite clay within the samples coming from the oil-based drilling muds interferes greatly with DNA isolation abilities (Daly et al., 2018). For this reason, a maximum of 1,810 sequences were retrieved within the cuttings or drillings muds compared to a maximum of 95,434 sequences for one of the produced water samples.

Table 1. Information related to the different types of samples analyzed in this study.

Sample type	Sample name	Depth (m)	Volume flooded (L)	Sampling Month	Number of sequences before quality control	Number of sequences after quality control
Shale cuttings	C4	3450	-	Nov-20	2 332	1 810
Drilling mud	M1	0	-	Nov-20	876	668
Fracturing fluid	FF	0	-	May-21	15 440	13 300
Produced water	PW20	-	20 000	May-21	9 198	7 045
	PW40	-	40 000	May-21	16 809	14 322
	PW60	-	60 000	May-21	22 444	19 332
	PW80	-	80 000	May-21	34 482	30 464
	PW100	-	100 000	May-21	4 741	3 733
	PW200	-	200 000	May-21	11 152	10 178
	PW300	-	300 000	May-21	28 263	26 455
	PW400	-	400 000	May-21	16 596	14 788
	PW500	-	500 000	May-21	17 128	15 138
	PW600	-	600 000	May-21	11 405	10 185
	PW700	-	700 000	May-21	1 588	1 326
	PW800	-	800 000	May-21	6 726	6 004
	PW900	-	900 000	May-21	11 426	9 913
	PWJUNE	-	-	Jun-22	111 477	95 434
	PWJULY	-	-	Jul-22	117 649	10 4827
	PWAUGUST	-	-	Aug-22	36 143	30 826
	PWSEPTEMBER	-	-	Sep-22	36 841	31 634
	PWOCTOBER	-	-	Oct-22	11 309	9 554
	PWNOVEMBER	-	-	Nov-22	26 221	22 151

Input fluid contribution to the produced water microbial community

One of the goals of this study was to understand if microorganisms are native inhabitants of subsurface shales, or rather get introduced with operational input fluid (fracturing fluids, drilling muds). To answer this question, ASVs that were found within only one of the three sample types (shale cuttings, drilling muds or fracturing fluid), and present within the produced water samples were separated in three different plots (Figure 1). This would indicate that the samples are coming either from the shale, the fracturing fluid or the drilling muds and persisting within the well to be retrieved by the produced water samples. As shown, up to ~ 40.3% ASV from the fracturing fluids (Figure 1B) were retrieved within the produced water samples compared to a lower amount for the drilling muds and shale cuttings at ~14.5% and ~6.6% ASV (Figure 1A and C).

As shown in Figure 1A, the ASVs from the shale cuttings that were prevalent in the produced water were ASV22 (*Caminicella*), ASV31 (*Aurantimonas*) and ASV54 (member of the *Rhodobacteraceae* family), with ASV22 being the most abundant. *Caminicella* spp. are anaerobic, thermophilic, endospore-forming bacteria (Chalmers et al., 2018). When using BlastN for a closer identification of ASV22, 4 matches of 100% identity were found, to which one reference sequence came from subseafloor sediments 80 km from the Shimokita peninsula of Japan (265m long core; 1180m water depth) (Imachi et al., 2011).

Within the microorganisms that are potentially introduced by the fracturing fluids (Figure 1B), the most abundant organisms found within the produced water samples and potentially originating from the fracturing fluid were ASV2 (*Malaciobacter*), ASV7 (*Glutaminicibacter*) and ASV8 (*Planococcus*). Members of the genus *Malaciobacter* and *Planococcus* are commonly found within marine environments (Nucleotide BLAST, 2022; Rahman et al., 2020). When looking at potentially introduced microorganisms from the drilling muds, ASV47 (member of the *Rhodobacteraceae* family) is one of the main organisms found within the produced water (700 000L).

Change in signature organisms from the produced water samples over time

At the initial produced water recovery stage, produced water samples were collected at different volume intervals as indicated in Figure 2A. As a general trend, it seems that the microbial diversity decreased as the volume collected increased as more genera were observed in the initial volumes flooded (20 000 to 100 000 L of produced water) compared to samples retrieved between 100 to 800 000 L of produced water. Within those latter samples, *Halanaerobium* is the dominant genus. However, the ASV of *Halanaerobium* increasing in the produced water does not coincide with the ASV104 potentially introduced in the well by the fracturing fluid (Figure 1B). Members of this genus are known as sulfide-producers and potentially endospore-formers (Booker et al., 2017; Jones et al., 2020; Scheffer et al., 2021). Another interesting observation is the increase in member of the *Malaciobacter* genus within the 200 000 to 400 000 L of flooded produced water. The dominant *Malaciobacter* within the Figure 2A matches ASV2 from the fracturing fluid sample (Figure 1B), suggesting that certain organisms within injected fluids can colonize fractured shale reservoirs and even become dominant. *Malaciobacter* is not known to reduce sulfate to sulfide, but possesses genes that are involved in the conversion of thiosulfate to sulfide (Kyoto Encyclopedia of Genes and Genomes, 2022).

Monthly sampling of the produced water enabled tracking the microbial community composition over time. As shown in Figure 2B, there is not a general trend as to which groups are dominant within the samples. As each month shows a high microbial diversity, the September produced water sample appears to be an outlier since *Halanaerobium* was found in very high abundance in the sample.

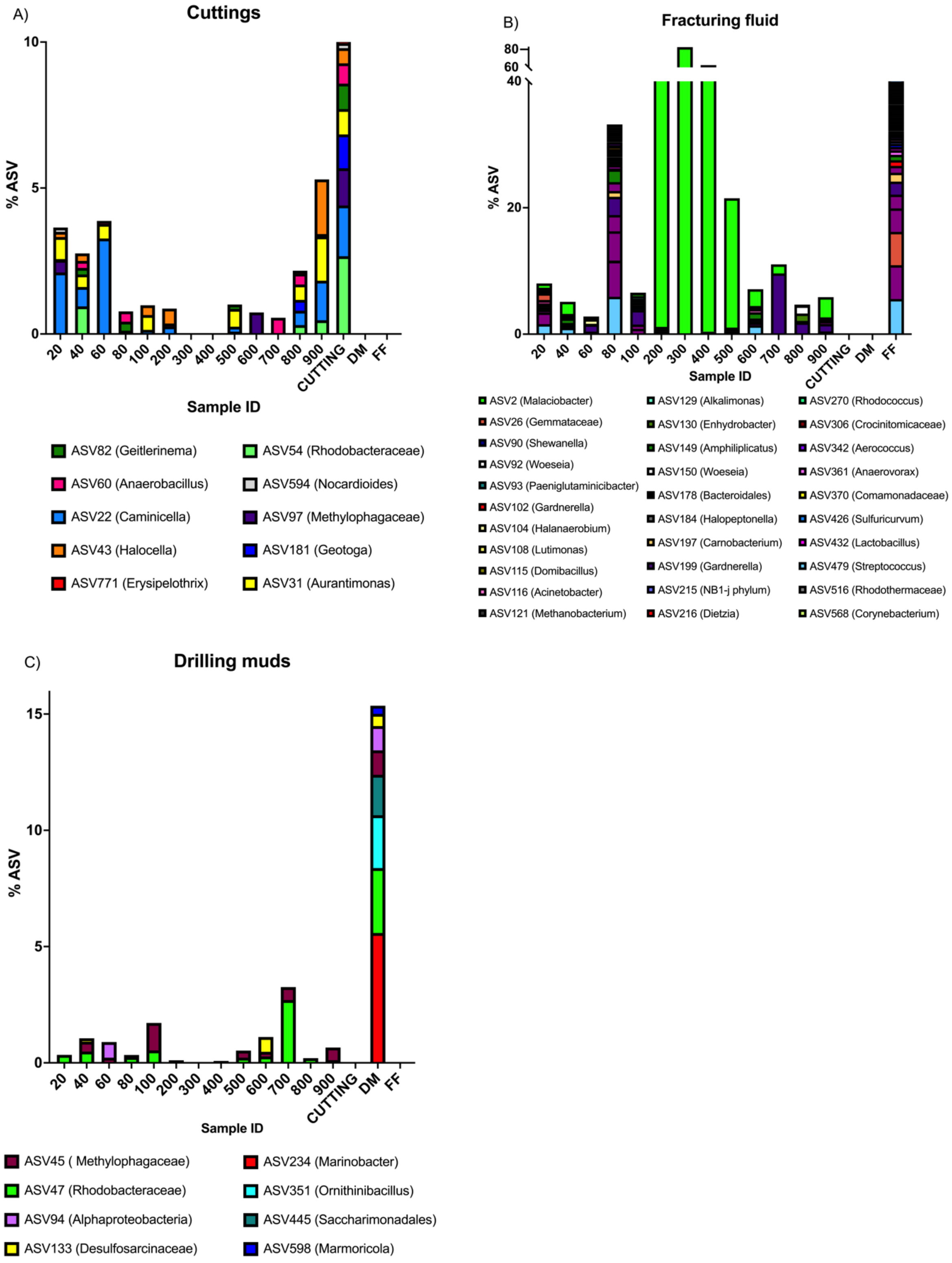

Figure 1. Microbial community composition within A) shale cuttings, B) fracturing fluid and C) drilling muds. These samples were compared at the ASV level in order to identify the potential provenance of microorganisms within each sample. ASV = amplicon sequence variant (of 16S rRNA gene sequence); Cutting = shale cutting sample (C4) ; DM = drilling muds; FF = fracturing fluid.

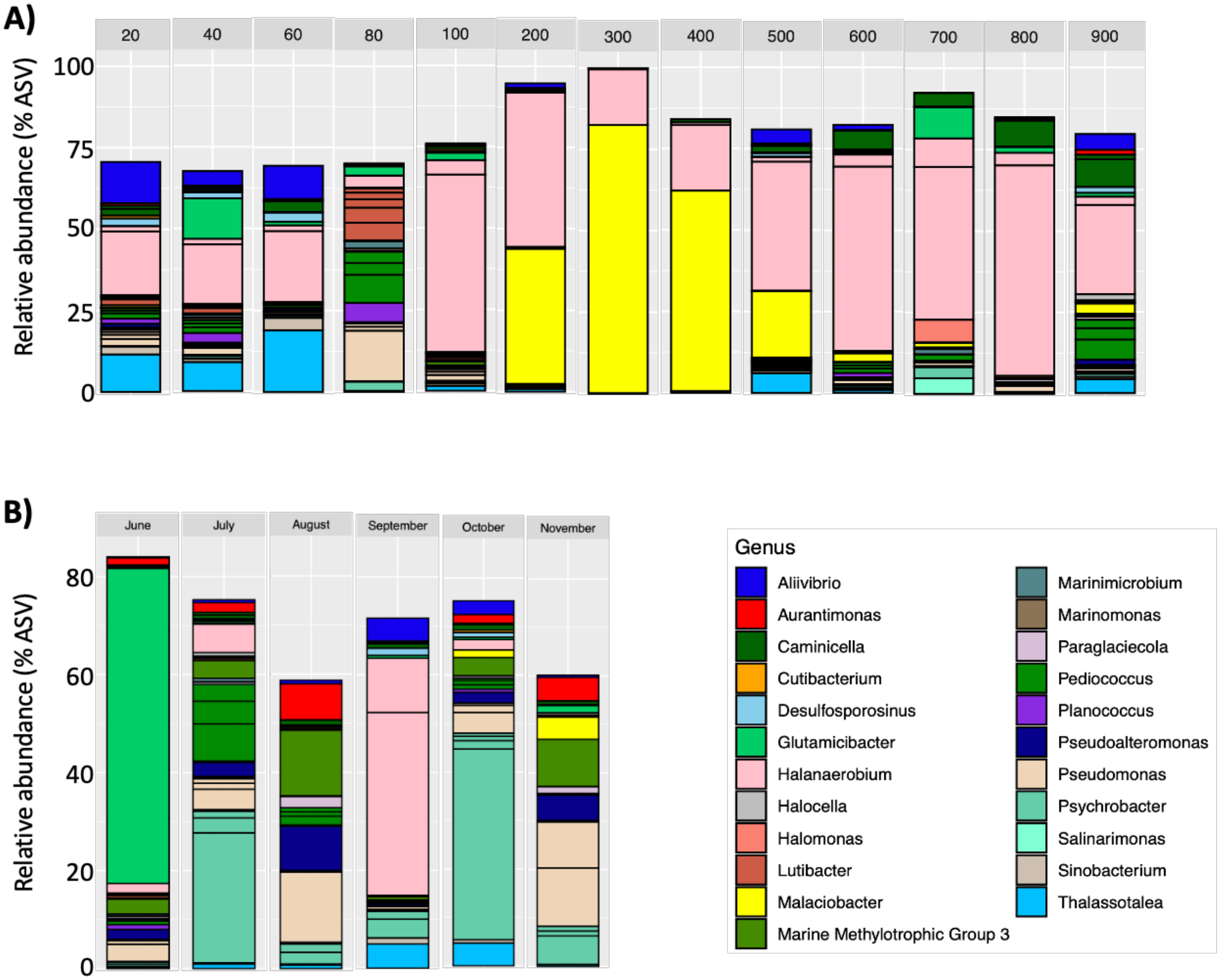

Figure 2. Microbial relative abundance of produced water samples collected A) at different volumes during the initial flooding of the well and B) once a month afterwards. Volumes in (A) above each sample are in thousands of litres.

Overall contribution to biogenic souring within the Montney formation well

Different putative sulfide-producing bacteria were present during the initial produced water flooding of the well (Figure 3). This is especially evident in the samples corresponding to 200 000 L to 800 000L of produced water. The most dominant genus among the putative sulfidogens was *Halanaerobium*, closely followed by *Malaciobacter*. Interestingly, members of the genus *Caminicella* (ASV 22), potentially native from shale (section 2.2) and able to produce sulfide (Alain et al., 2002), were found at the relative abundance of around 5% ASV within the latest samples of the initial flooding (600 000 to 900 000 L samples).

For the monthly sampling, a low abundance of sulfide-producers was retrieved from the samples except for the September sample, where a net increase of the relative abundance of *Halanaerobium* was observed along with a higher proportion of *Desulfosporosinus* (Figure 2B, 3B). This coincides with the blackening of the produced water samples (image not shown). Compared to the usual yellow color of the samples collected from May to July, samples changed color to light grey in August, and then to black in September and for the subsequent months.

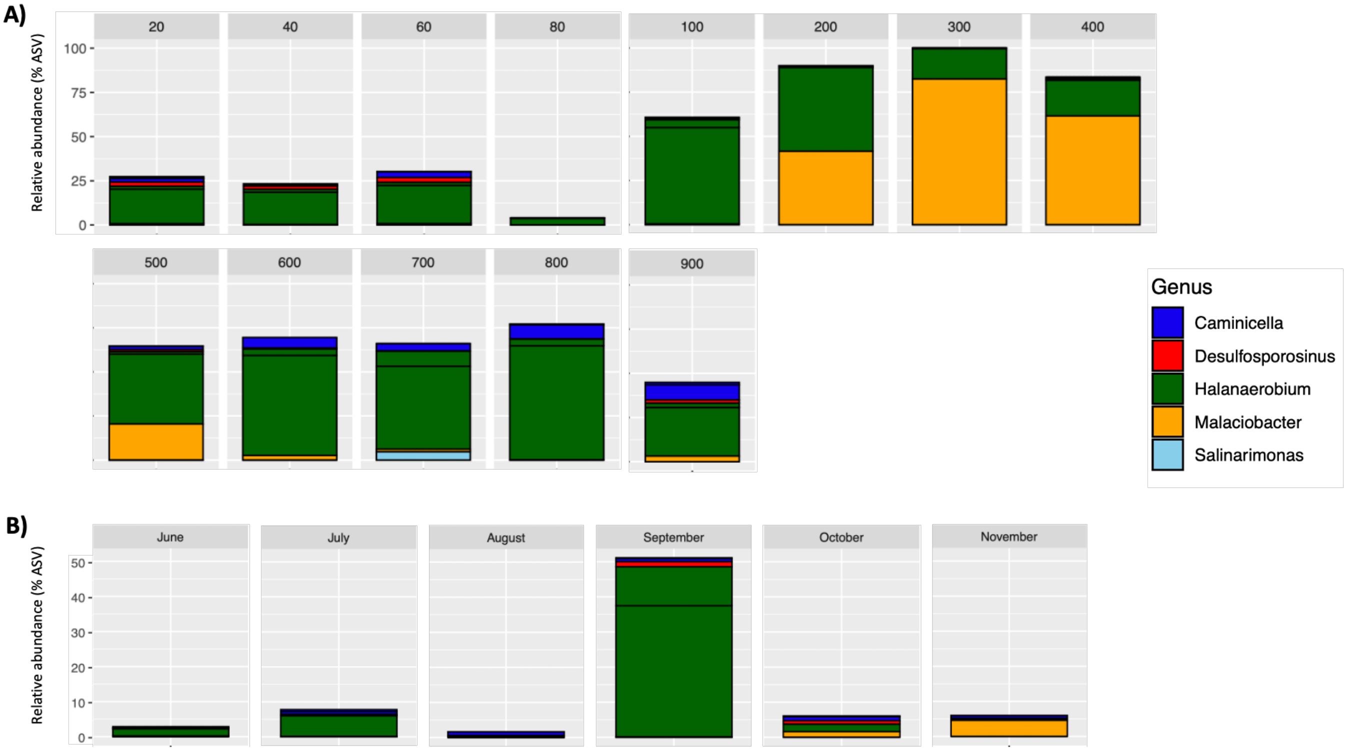

Figure 3. Microbial relative abundance of putative sulfide-producing organisms within produced water samples collected A) at different volumes during the initial flooding of the well and B) once a month afterwards. For A), the volumes should be interpreted as 20 = 20 000L of produced water collected.

Conclusions

While certain organisms are introduced during the hydraulically fracturing process, results presented here show that it is also possible that certain microbes are native to deep shale environments. This has been a debated topic within the field of petroleum microbiology. The extreme pressure and temperature downhole presents conditions that are believed to be challenging for life. Some microorganisms from this formation, introduced or native from it, showed potential for biogenic souring. The continuous monthly sampling of the well will allow to keep track of the microbial dynamic and its potential for biogenic souring.

Acknowledgements

The authors would like to thank AGAT laboratories for the sampling, handling and shipping of samples, Dr. Anirban Chakraborty for scientific expertise, and Dr. Srijak Bhatnagar for bioinformatics expertise. Authors also thank the National Sciences and Engineering Research council of Canada, the Natural Resources Canada's Geoscience for New Energy Supply (GNES) program and University of Calgary's Eyes High program for funding.

References

Alain, K., Pignet, P., Zbinden, M., Quillevere, M., Duchiron, F., Donval, J.-P., Lesongeur, F., Raguenes, G., Crassous, P., Querellou, J., Cambon-Bonavita, M.-A., 2002. *Caminicella sporogenes* gen. nov., sp. nov., a novel thermophilic spore-forming bacterium isolated from an East-Pacific Rise hydrothermal vent. International Journal of Systematic and Evolutionary Microbiology 52, 1621–1628.

Booker, A.E., Borton, M.A., Daly, R.A., Welch, S.A., Nicora, C.D., Hoyt, D.W., Wilson, T., Purvine, S.O., Wolfe, R.A., Sharma, S., Mouser, P.J., Cole, D.R., Lipton, M.S., Wrighton, K.C., Wilkins, M.J., 2017. Sulfide generation by dominant *Halanaerobium* microorganisms in hydraulically fractured shales. mSphere 2, 1-13.

Canada Natural Resources, 2015. British Columbia's Shale and Tight Resources. URL https://www.nrcan.gc.ca/our-natural-resources/energy-sources-distribution/clean-fossil-fuels/natural-gas/shale-and-tight-resources-canada/british-columbias-shale-and-tight-resources (accessed 9.21.20).

Chalmers, A., Gale, A., Birnie, M., Linde, A., Millar, A., 2018. Use of next generation sequencing to identify sources of microbial contamination. Presented at the SPE International Oilfield Corrosion Conference and Exhibition, OnePetro, 190905-MS.

Daly, R.A., Wrighton, K.C., Wilkins, M.J., 2018. Characterizing the deep terrestrial subsurface microbiome. Methods in Molecular Biology. Clifton NJ 1849, 1–15.

Filippidou, S., Wunderlin, T., Junier, T., Jeanneret, N., Dorador, C., Molina, V., Johnson, D.R., Junier, P., 2016. A combination of extreme environmental conditions favor the prevalence of endospore-forming *Firmicutes*. Frontiers in Microbiology 7, 1-11.

Gittel, A., Sørensen, K.B., Skovhus, T.L., Ingvorsen, K., Schramm, A., 2009. Prokaryotic community structure and sulfate reducer activity in water from high-temperature oil reservoirs with and without nitrate treatment. Applied and Environmental Microbiology 9, 1-11.

GraphPad Software, 2022. URL https://www.graphpad.com (accessed 1.12.22).

Illumina - Sequencing and array-based solutions for genetic research. URL https://www.illumina.com/ (accessed 1.12.22).

Imachi, H., Aoi, K., Tasumi, E., Saito, Yumi, Yamanaka, Y., Saito, Yayoi, Yamaguchi, T., Tomaru, H., Takeuchi, R., Morono, Y., Inagaki, F., Takai, K., 2011. Cultivation of methanogenic community from subseafloor sediments using a continuous-flow bioreactor. ISME J. 5, 1913–1925.

Jones, A.A., Pilloni, G., Claypool, J.T., Paiva, A.R., Summers, Z.M., 2020. Evidence of sporulation capability of the ubiquitous oil reservoir microbe *Halanaerobium congolense*. Geomicrobiol. Journal 0, 1–11.

Kyoto Encyclopedia of Genes and Genomes Pathway: Sulfur metabolism - *Malaciobacter canalis*. URL https://www.kegg.jp/kegg-bin/show_pathway?acaa00920 (accessed 1.17.22).

Kohli, I., Joshi, N.C., Mohapatra, S., Varma, A., 2020. Extremophile – an adaptive strategy for extreme conditions and applications. Current Genomics 21, 96–110.

Lipus, D., Roy, D., Khan, E., Ross, D., Vikram, A., Gulliver, D., Hammack, R., Bibby, K., 2018. Microbial communities in Bakken region produced water. FEMS Microbiology Letters 365, 1-15.

Mo Bio'S PowerMax Soil DNA Isolation Kit Handbook - Qiagen. URL https://www.qiagen.com/ca/resources/resourcedetail?id=b72550c8-d622-45f3-b724-5d0ecace84f0&lang=en (accessed 1.11.22).

Nucleotide BLAST. URL https://blast.ncbi.nlm.nih.gov/Blast.cgi?PAGE_TYPE=BlastSearch (accessed 4.20.18).

Okpala, G.N., Chen, C., Fida, T., Voordouw, G., 2017. Effect of thermophilic nitrate reduction on sulfide production in high temperature oil reservoir samples. Frontiers in Microbiology 8, 1-13.

Nucleotide BLAST - *Planococcus plakortidis* strain SLA-340 16S ribosomal RNA gene, partial. URL https://www.ncbi.nlm.nih.gov/nucleotide/MT125778.1?report=genbank&log$=nucltop&blast_rank=4&RID=Y4VC32MM013 (accessed 1.14.22).

R - The R Project for Statistical Computing. URL https://www.r-project.org/ (accessed 1.12.22).

Rahman, F.U., Andree, K.B., Salas-Massó, N., Fernandez-Tejedor, M., Sanjuan, A., Figueras, M.J., Furones, M.D., 2020. Improved culture enrichment broth for isolation of *Arcobacter*-like species from the marine environment. Scientific Reports 10, 14547-14555.

Scheffer, G., Hubert, C.R.J., Enning, D.R., Lahme, S., Mand, J., de Rezende, J.R., 2021. Metagenomic investigation of a low diversity, high salinity offshore oil reservoir. Microorganisms 9, 2266-2287.

Diagenetic and geochemical controls on H_2S distribution in the Montney Formation, Peace River Region, Western Canada

Mastaneh H. Liseroudi[1], Omid H. Ardakani[1, 2], Per K. Pedersen[2], Richard A. Stern[3], James M. Wood[4], Hamed Sanei[5]*

[1] *Natural Resources Canada, Geological Survey of Canada, Calgary, Canada*
[2] *Department of Geoscience, University of Calgary, Calgary, Canada*
[3] *Earth and Atmospheric Sciences, University of Alberta, Earth Sciences Building, Edmonton, Canada*
[4] *Calaber1 Resources, 965 Sierra Morena Court SW, Calgary, Canada*
[5] *Lithospheric Organic Carbon (LOC), Department of Geoscience, Aarhus University, Aarhus, Denmark*

[*]*Presenting Author: mastaneh.liseroudi@nrcan-rncan.gc.ca*

Abstract

The Lower Triassic Montney Formation is a major siltstone dominated unconventional tight gas play in the Western Canadian Sedimentary Basin (WCSB). In the Peace River region, the Montney Formation contains a regionally variable amount of hydrogen sulfide (H_2S) in gas-producing wells with western Alberta's wells having the highest concentrations. Previous studies on the source and distribution of H_2S in the Montney Formation mainly focused on variations of H_2S concentration and its relationship with other hydrocarbon and non-hydrocarbon gases, sulfur isotope composition of H_2S, as well as organo-sulfur compounds in the Montney Formation natural gas. None of those studies, however, focused on the role of diagenetic and geochemical processes in the formation of dissolved sulfate, one of the two major ingredients of H_2S formation mechanisms, and pyrite within the Montney Formation.

According to the results of this study, the Montney Formation consists of two different early and late generations of sulfate minerals (anhydrite and barite), mainly formed by the Montney Formation pore water and incursion of structurally-controlled Devonian-sourced hydrothermal sulfate-rich fluids. In addition, pyrite the dominate sulfide mineral, occurred in two distinct forms as framboidal and crystalline that formed during early to late stages of diagenesis in western Alberta (WAB) and northeast British Columbia (NEBC). The concurrence of the late-stage anhydrite and barite and various types of diagenetic pyrite with high H_2S concentrations, particularly in WAB, their abundance, and spatial distribution, imply a correlation between the presence of these sulfate and sulfide species and the diagenetic evolution of sulfur in the Montney Formation.

The sulfur isotope composition of anhydrite/barite, H_2S, and pyrite demonstrates both microbial and thermochemical sulfate reduction (MSR and TSR) controlled the diagenetic sulfur cycle of the Montney Formation. The relationship between the $\delta^{34}S$ values of the present-day produced gas H_2S and other sulfur-bearing species from the Montney and other neighboring formations verifies a dual native and migrated TSR-derived origin for the H_2S gas with substantial contributions of *in situ* H_2S in the Montney reservoir.

Methodology

A regional Montney Formation core sample set from twelve wells in WAB and NEBC in the Peace River region (Fig.1a) with regionally variable H_2S concentrations (Fig. 1b) was used for petrographic observations and bulk and micro-scale stable sulfur and oxygen isotope geochemistry. Ninety thin sections and nine representative samples were used for petrographic studies and scanning electron microscopy (SEM) and energy dispersive X-ray spectroscopy (EDXS) analyses, respectively. Fifty-nine anhydrite-bearing samples were selected for bulk sulfur ($\delta^{34}S$) and oxygen ($\delta^{18}O$) isotope analysis, using isotope ratio mass spectrometry at the University of Calgary.

Sulfur and oxygen isotope ratios ($^{34}S/^{32}S$; $^{18}O/^{16}O$) of anhydrite (151 spots) and barite (30 spots), and sulfur isotope ratios of pyrite (156 spots) were also determined using secondary ion mass spectrometry (SIMS) method at the University of Alberta. Sulfur isotopic composition of nineteen produced gas H_2S samples from WA and nine samples from NEBC was obtained from Desrocher (1997), the public database of the Alberta Energy Regulator (AER, 2019) and BC Oil and Gas Commission (BCOGC, 2019), and the internal database of Ovintiv Inc.

Results

Petrographic Observations and Isotope Geochemistry

Sulfate Minerals

Anhydrite, formed during early to late stages of diagenesis, is found in various forms, including dissolved residue of anhydrite crystals, blocky (vug-filling, nodule), poikilotopic pore-filling and fracture-filling cement, and replacive crystals (Fig. 2a-d). Barite was observed in trace amounts in WAB as disseminated pore-filling cement enclosing quartz, dolomite, K- and Na-feldspar and framboidal and euhedral pyrite crystals (Fig. 2d).

The bulk $\delta^{34}S$ value of anhydrite in NEBC ranges from 4.9 to 22.9‰ (V-CDT) and its $\delta^{18}O$ value varies from -11.2 to 0.3‰ (V-SMOW) (Fig. 3a). The $\delta^{34}S$ value of anhydrite samples from WAB varies from 2.9 to 24.6‰ (V-CDT) and their $\delta^{18}O$ values show a wider range of variation from -10.5 to 15.7‰ (V-SMOW). The $\delta^{34}S$ and $\delta^{18}O$ values of fracture- and vug-filling anhydrite cement in WAB varies from 23.5 to 24.7‰ (V-CDT) and 13.3 to 14.7‰ (V-SMOW), respectively. The SIMS-analyzed anhydrite is predominantly the pore-filling poikilotopic type with $\delta^{34}S$ and $\delta^{18}O$ values of 18.5 to 37‰ (V-CDT) and 12 to 22‰ (V-SMOW), respectively (Fig. 3a and b). Barite shows $\delta^{34}S$ values mostly ranging from 23.3 to 33.6‰ (V-CDT) and $\delta^{18}O$ values varying from 13.2 to 18.7‰ (V-SMOW) (Fig. 3a and c).

Sulfide Minerals (pyrite)

Pyrite was identified as two main framboidal and crystalline forms with distinct varieties (Fig. 4a-d). Pyrite framboids occur as three varieties (1) single, (2) poly-framboids (Py-F, Fig. 4a-b), and (3) loose aggregates of euhedral microcrystals. Crystalline pyrite shows two main habits: (1) cubic pyrite microcrystals (C-Py), and (2) euhedral to anhedral clusters. Clustered pyrite is present in two main types of recrystallized (Py-R) and coalesced (Py-CO) pyrite formed by partial or complete recrystallization of early framboids and cubic pyrite microcrystals and coalescence of individual pyrite crystals into larger aggregates, respectively (Fig. 4c-d). Figure 5 represents the paragenetic relationships of the main diagenetic phases observed in the Montney Formation in the study area.

The $\delta^{34}S_{pyrite}$ values vary from -34.4 to +57.8‰ V-CDT (Fig. 6a). Based on petrographic observations and the $\delta^{34}S$ values, pyrite is classified into (1) framboidal pyrite that has exclusively depleted $\delta^{34}S$ values (-24.0 to -3.2‰; Fig. 6a-c), (2) recrystallized pyrite with commonly depleted $\delta^{34}S$ values (-34.4 to +3.2‰, Fig. 6a and c,), and (3) coalesced pyrite with exclusively enriched $\delta^{34}S$ values (+1.4 to +57.8‰, Fig. 6a and d).

Produced Gas H_2S $\delta^{34}S$ Values

The $\delta^{34}S$ values of H_2S in WAB and NEBC range from +12.3 to +17.1‰ and +11.9 to +15.8‰, respectively (AER, 2019; BCOGC, 2019).

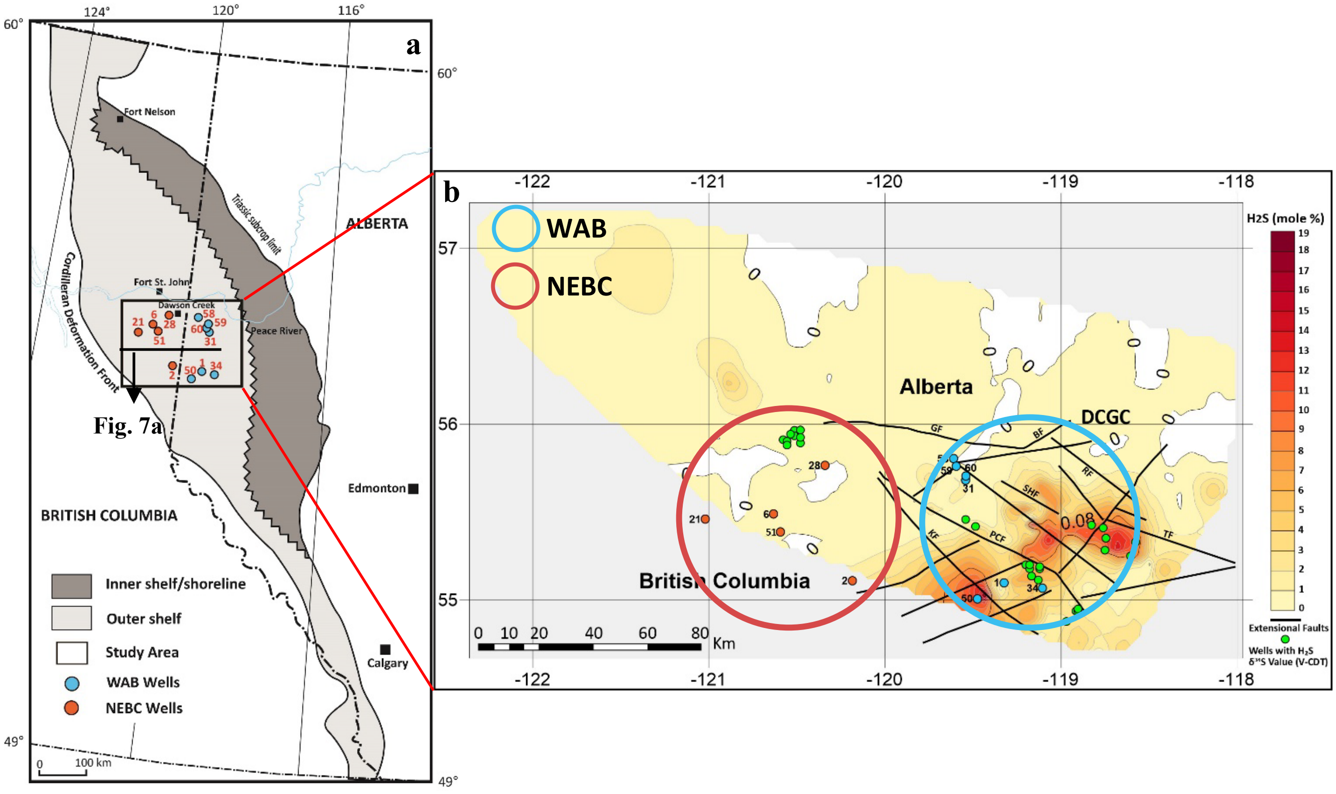

Figure 1. (a) Montney subcrop and outcrop map (modified after Edwards et al., 1994) with the location of the studied wells in NEBC and WAB. (b) H_2S concentration map in WAB (blue circle) and NEBC (red circle; modified after Liseroudi et al., 2020, 2021).

Discussion and Conclusions

Diagenetic and Geochemical Controls on H_2S Concentration in the Montney Formation

Source(s) of Dissolved Sulfate

The results of this study show the occurrence of regionally distributed early and late diagenetic anhydrite and barite cement throughout the study area (Fig. 2a-d). The wide range of $\delta^{34}S$ and $\delta^{18}O$ values of anhydrite and barite suggests that two different sulfate-bearing fluid end-members contributed to sulfate mineral precipitation in the Montney Formation. The early diagenetic anhydrite exhibits less enriched or even depleted sulfur and oxygen isotope composition than the assumed Triassic seawater sulfate (Claypool et al., 1980; Kampschulte and Strauss, 2004).

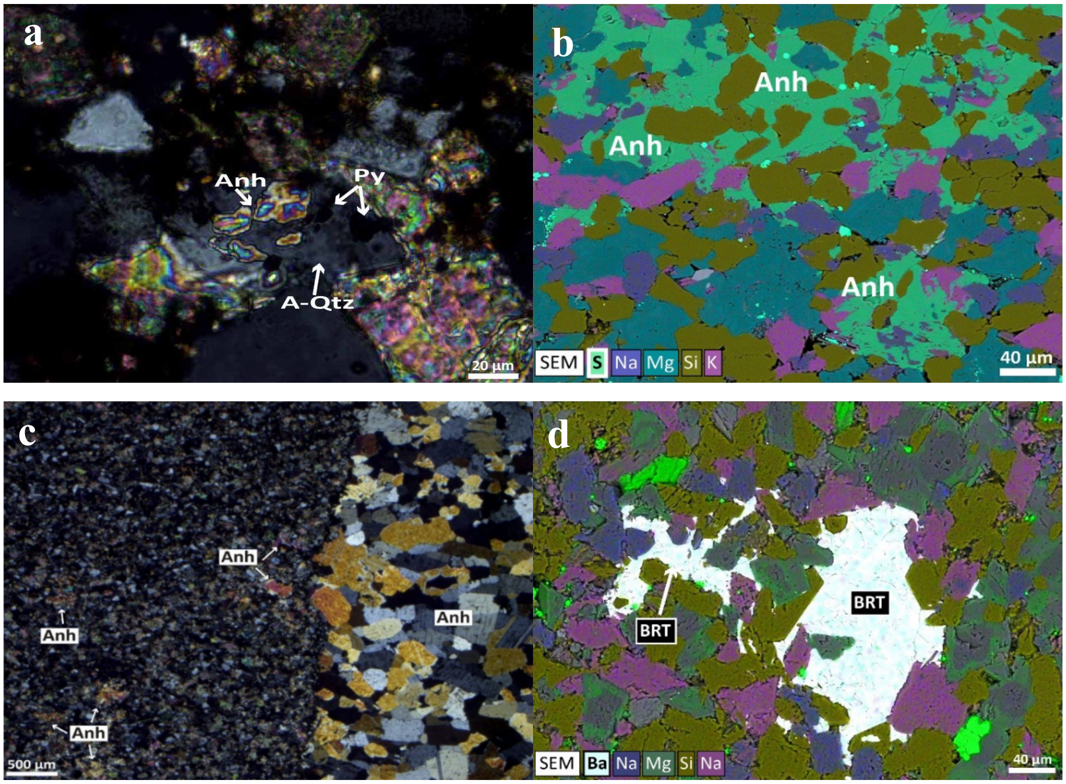

Figure 2. (a) Photomicrograph of authigenic quartz crystals (A-Qtz) enclosing minute remnants of early anhydrite (Anh) and pyrite crystals (Py), (UWI: A-036-G/093-P-01/0, 3753.33 m, XPL. (b) EDXS image of late poikilotopic anhydrite cement (Anh) enclosing quartz, feldspar, and dolomite detrital grains and authigenic cement with superimposed S, Na, K, Si, and Mg X-ray response (UWI: 01-32-070-09W6/0, 2549.03 m). (c) Photomicrograph of late fracture-filling anhydrite and pore-filling poikilotopic anhydrite cement formed in the vicinity of the fracture (UWI: 01-32-070-09W6/0, 2547.33 m, XPL). (d) EDXS image of late pore filling barite (BRT-Ba X-ray response) cement filling available pore spaces and enclosing dolomite, K- and Na-Feldspar, and quartz in this sample. Elements are the same as b (UWI: 04-19-077-10W6/0, 2140.40 m).

This suggests that the early anhydrite precipitated from Triassic formation/pore water, which was modified through interaction with sulfate sourced from sulfide oxidation or formation waters/brines in the basin (Krouse and Mayer, 2000; Bottrell and Newton, 2006). The isotopic signature of the late-stage anhydrite (both poikilotopic and fracture- and vug-filling cement) and barite is similar to the Devonian evaporites isotopic composition (Claypool et al., 1980; Machel, 1985, Fu, 2005), which suggests the dominant involvement of sulfate-rich fluids originated from the dissolution of WCSB Devonian evaporites and mixing with connate water of Triassic seawater origin. The presence of extensive fault systems, with several episodes of reactivation (Hope et al., 1999; Mei, 2009) and extensive hydrothermal activities (Davies and Smith, 2006; Al-Aasm et al., 2019) in the subsurface of the Peace River region is very well documented. Upward movement of saline fluids is basically facilitated by thermal and structural drives (Davies and Smith, 2006). This further confirms that Devonian-sourced sulfate-rich hydrothermal brines migrated upward to the Montney Formation through extensive deep-seated fault/fracture networks in the subsurface of WAB (Fig. 7a).

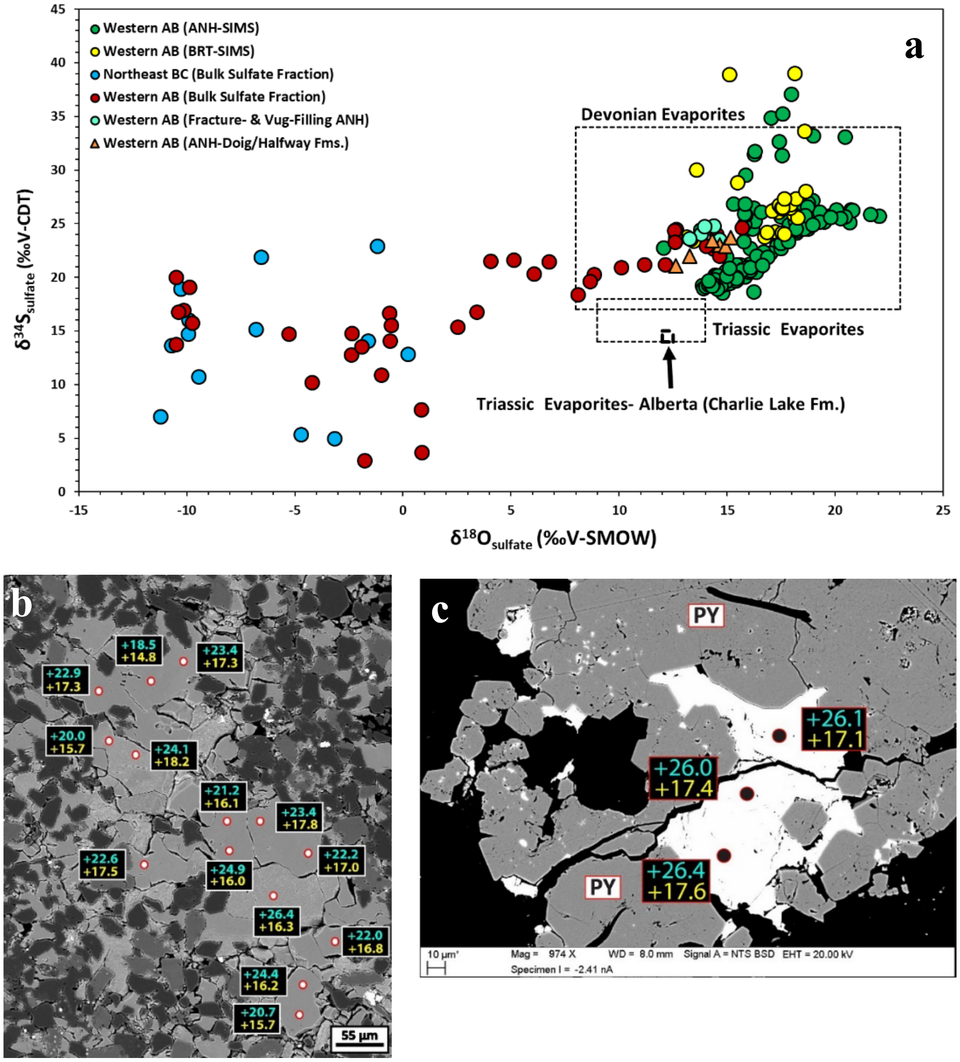

Figure 3. (a) Bulk rock and SIMS $\delta^{34}S$ and $\delta^{18}O$ values of early and late anhydrite and late barite from WAB and NEBC sections of the Montney Formation. Larger box shows estimated $\delta^{34}S$ and $\delta^{18}O$ values of Devonian evaporites in the Alberta Basin (Claypool et al., 1980; Machel, 1985, Fu, 2005). Smaller boxes show the range of $\delta^{34}S$ and $\delta^{18}O$ values of global Triassic evaporites and Triassic evaporites of the Alberta sub-basin (Charlie Lake Formation; Claypool et al., 1980). The $\delta^{34}S$ and $\delta^{18}O$ values of the Middle Triassic Doig and Halfway late fracture- and vug-filling anhydrite samples are shown by orange triangle for comparison. (b-c) Backscattered electron (BSE) image of a representative late anhydrite and barite sample with their SIMS $\delta^{34}S$ and $\delta^{18}O$ values (a: UWI: 01-32-070-09W6/0, 2549.03 m, WAB; b: UWI: 13-22-070-08W6, 2418.41 m, WAB). The $\delta^{34}S$ and $\delta^{18}O$ values are in blue and yellow, respectively. (Abbreviations: Py: pyrite).

Major H_2S/Pyrite-generating Mechanisms

The major mechanisms of H_2S generation in sedimentary basins and hydrocarbon reservoirs are microbial sulfate reduction (MSR), anaerobic oxidation of methane coupled to sulfate reduction (AOM-SR), thermal chemical alteration (TCA) of organosulfur compounds (OSCs), as well as thermochemical sulfate reduction (TSR; e.g., Orr 1977; Worden et al., 1996; Machel 2001; Kelemen et al., 2008; Sim et al., 2011). One of the main destinies of H_2S produced via these mechanisms is its fixation as pyrite (FeS_2) in the presence of Fe(II) (Seal 2006; Bottrell and Newton 2006).

As previously discussed, two major forms of framboidal and crystalline pyrite, with several varieties and habits were identified in the Montney Formation (Fig. 4a-d). The sulfur isotopic signature of framboidal and recrystallized crystalline pyrite is variable and substantially ^{34}S-depleted, with a gradual ^{34}S enrichment in the samples (Fig. 6a-c) confirming a MSR origin for the parent H_2S of these pyrite types in a closed diagenetic system (Fig. 8a; Orr 1977; Machel et al., 1995). The $\delta^{34}S$ values of coalesced pyrite in WAB (Fig. 6a) are representative of H_2S formed *via* TSR (Machel et al., 1995; Olanipekun and Azmy, 2018) in an open diagenetic system (Fig. 7b; Machel et al., 1995; Worden and Smalley 1996) where sulfate-rich fluids were sourced from the dissolution of Montney late anhydrite, as well as underlying hydrothermal sulfate-rich fluids, which originated from the dissolution of Devonian evaporates (Fig. 7a; Liseroudi et al., 2020). The sulfur isotopic composition of coalesced pyrite in NEBC suggests contribution of dissolved early anhydrite to the generation of dominantly TSR-derived H_2S in a localized closed diagenetic environment (Liseroudi et al., 2020; 2021).

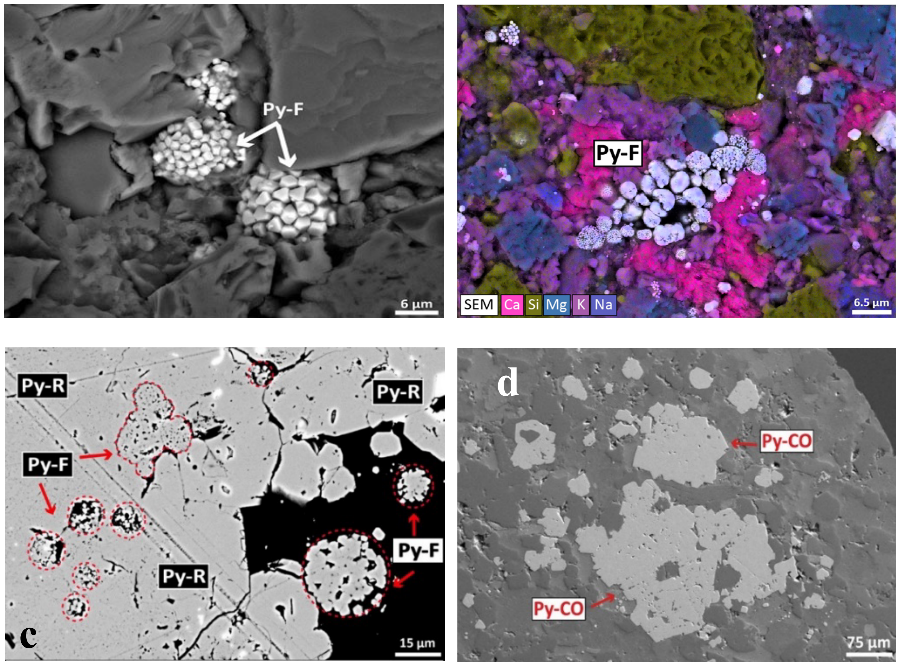

Figure 4. (a-b) SEM image of single and ploy-framboids (Py-F) with superimposed Ca, Si, Mg, K, and Na X-ray response in the sample (a: UWI:13-22-070-08W6, 2418.41 m; b: UWI: B-052-I/093-P-06/2, 4038.36 m). (c) Backscattered image of recrystallized pyrite (Py-R) with some remnants of earlier-formed framboids (red dashed circles; UWI: 13-22-070-08W6, 2418.41 m). (d) SEM image of coalesced pyrite (Py-CO, UWI: 14-13-078-16W6/0, 2887.37 m).

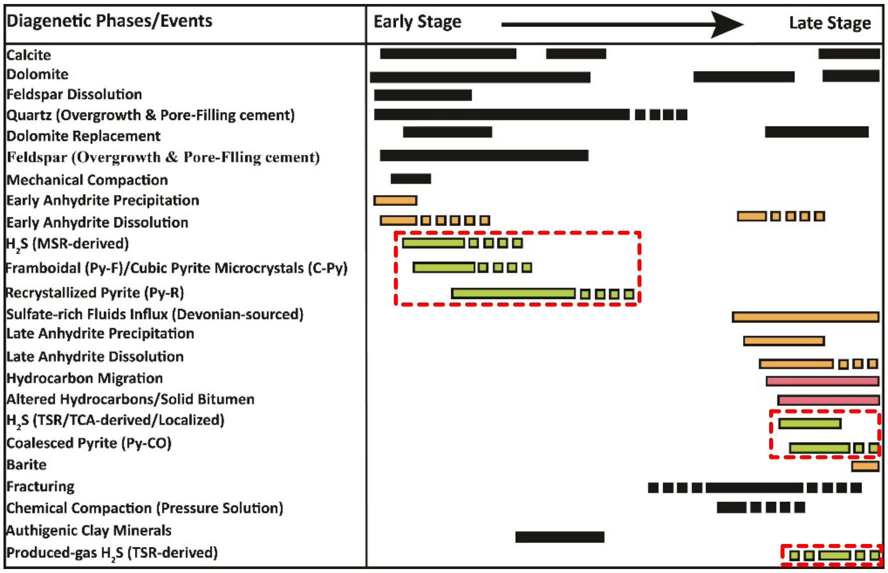

Figure 5. Paragenetic sequence of the main diagenetic phases observed in the Montney Formation in the study area in WAB and NEBC. The main phases of H_2S and pyrite formation are marked by red dashed squares. The major components of H_2S and pyrite formation, including anhydrite and sulfate and hydrocarbon are highlighted in orange and pink. All other diagenetic phases/events are shown in black color (modified after Liseroudi et al., 2021).

Present-day H_2S in the Montney Reservoir: in-situ or migrated?

The $\delta^{34}S_{H2S}$ values of present-day produced gas (+11.9 to + 17.1‰ V-CDT) indicate that H_2S gas in the Montney Formation is of both *in-situ* and migrated nature, with predominate *in-situ* H_2S of TSR origin. *In-situ* generation of H_2S was mainly controlled by the dissolution of early, and late anhydrite, and influx of hydrothermally-driven Devonian-sourced sulfate-rich brines (Fig. 7a: Liseroudi et al., 2020; 2021), facilitated by the late oil migration phase (Wood et al., 2018a,b).

The TSR process commonly has the highest contribution (>10% up to ~90%) to H_2S generation in deeply buried natural gas reservoirs (Orr 1977; Machel 2001). The high H_2S concentrations (overall up to 20%; Fig. 1b) suggests that the produced gas H_2S in WAB is generated *via* TSR process. Present-day cooler temperature at high H_2S depth intervals (2400 to 2600 m) is elevated (110 to 120 °C; Ness 2001), which is at the lower end of the TSR temperature range in hydrocarbon reservoirs (100-220 °C; Jiang et al., 2014).

Replacement of both early anhydrite and late anhydrite by calcite and dolomite provides petrographic evidence of sulfate reduction processes (Worden and Smalley 1996; Machel 2001) and confirms that some TSR-derived H_2S was generated *in situ* from Montney-sourced sulfate. The estimated maximum burial temperature of the Montney Formation (160-170°C; Ness, 2001) demonstrates that a fraction of H_2S may have been generated *via* TSR at the maximum burial condition, and subsequently migrated updip and vertically to the shallower parts of the Montney Formation. The similar $\delta^{34}S_{H2S}$ values of the underlying H_2S-bearing formations such as the Devonian Slave Point Formation and Carboniferous Debolt Formation (+10.9 to +19.3‰ V-CDT) and the Montney Formation in WAB and NEBC (+11.9 to +17.1‰ V-CDT; Fig. 7c) also suggests possible migration of H_2S from underlying Paleozoic strata driven by structurally-controlled hydrothermal fluids (Liseroudi et al., 2020).

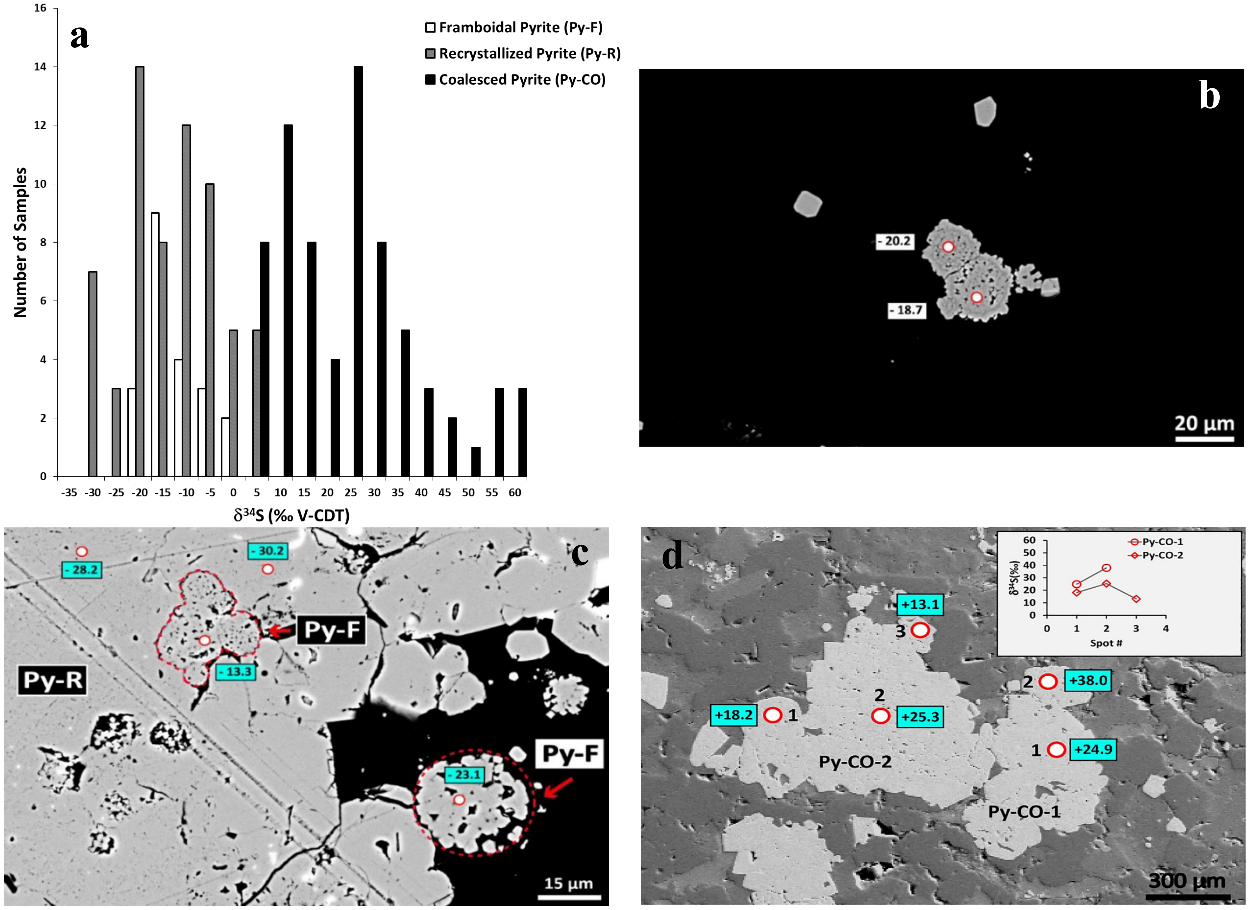

Figure 6. **(a)** Histogram of $\delta^{34}S$ values and distribution of framboidal (Py-F), recrystallized (Py-R), and coalesced (Py-CO) pyrite in different wells. (b) Backscattered electron (BSE) image of framboidal pyrite with SIMS $\delta^{34}S$ values (UWI: 16-29-069-10W6/0, 2877.05 m). (c) SEM-BSE image of recrystallized pyrite and relicts of framboids with their measured SIMS $\delta^{34}S$ values. (c: UWI: 13-22-070-08W6, 2418.41 m). (d) SEM image of coalesced pyrite clusters with their SIMS $\delta^{34}S$ values. The inset shows the large variability of the $\delta^{34}S_{pyrite}$ values within these individual coalesced clusters (UWI: 14-13-078-16W6/0, 2887.37 m).

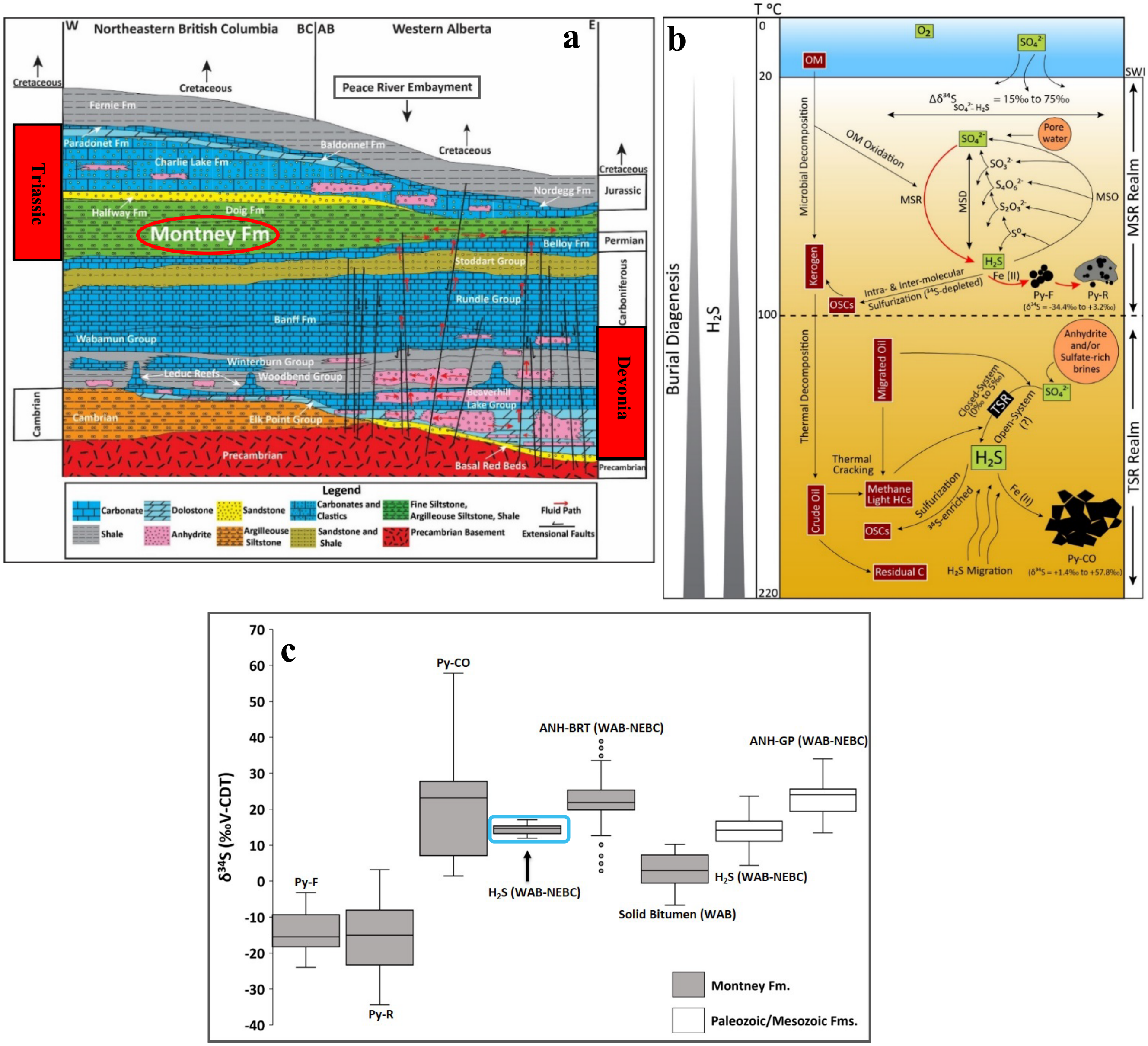

Figure 7. (a) Conceptual cross-section of the study area in WAB and NEBC (located on Fig. 1a) showing the location of the extensional faults and hydrothermal fluid flow path in WAB (modified after Liseroudi et al., 2020). The stratigraphy is compiled from the Geological Atlas of the Western Canadian Sedimentary Basin (Mossop and Shetsen, 1994), and Davies et al., (1997). (b) Schematic illustration of the sulfur cycle during different stages of diagenesis and redox reactions realms (modified after Canfield, 2001; Amrani, 2014; Jiang et al., 2020) with a focus on the Montney Formation. The red arrows in the microbial sulfate reduction (MSR) realm show that MSR process dominantly contributed to the H_2S and framboidal and recrystallized pyrite formation in the Montney Formation. Temperature range for TSR (100 to 220 °C) is from Jiang et al., (2014). (c) Box-plot image showing $\delta^{34}S$ values of various sulfur-bearing species (pyrite, H_2S, anhydrite, barite, solid bitumen) from the Montney and Paleozoic/Mesozoic formations in the WCSB (modified after Liseroudi et al., 2021). Data used in this graph is from current study, Desrocher, (1997), Ovintiv Inc., public database of the AER and BCOGC (2019), Liseroudi et al., (2020), Claypool et al., (1980), Machel, (1985), and Fu, (2005). Abbreviations: MSO: microbial oxidation of sulfide; MSD: microbial disportionation of sulfide; OSCs: organic sulfur compounds; OM: Organic Matter; Py-F: pyrite-framboid; Py-R: recrystallized pyrite; Py-CO: coalesced pyrite. ANH: anhydrite, BRT: barite, GP: gypsum.

The similar $\delta^{34}S$ values of Upper Triassic Charlie Lake Formation anhydrite (+13.7 to +14.8‰ V-CDT; Claypool et al., 1980) and H_2S in WAB and NEBC (+11.9 to +17.1‰ V-CDT) suggest Charlie Lake anhydrite as a potential source of sulfate-rich fluids for produced-gas H_2S in the Montney (Fig. 7c), an interpretation proposed previously by Desrocher et al. (2004) and Kutuzov et al., (2020). However, considering the Montney Formation is an over-pressured basin-centered reservoir (Law 2002; Gibbs and Rakhit, 2019), downward migration of fluids from the overlying lower-pressured Charlie Lake Formation seems unlikely.

Acknowledgements

This work is funded by Natural Resources Canada's Geoscience for New Energy Supply (GNES) program and the Tight Oil Consortium (TOC) industry sponsors. We would like to thank Ovintiv Inc. for providing the core samples, thin sections, and some sulfur isotope values of H_2S gas for this study. Drs. S. Grasby, A. Kingston, and C. Jiang of the Geological Survey of Canada in Calgary are genuinely acknowledged for their constructive discussion, comments, and feedback. The authors also wish to acknowledge Dr. C. Debuhr for SEM/EDXS imaging and Mr. S. Taylor and the staff of the Isotope Science Lab at the University of Calgary for bulk sulfur and oxygen isotope analyses. We also thank Mr. R. Dokken from University of Alberta (CCIM) for SIMS mount preparation and SEM/BSE imaging.

References

Al-Aasm, I.S., Mrad, C., Packard, J., 2019. Fluid compartmentalization of devonian and mississippian dolostones, western canada sedimentary basin: Petrologic and geochemical evidence from fracture mineralization. Canadian Journal of Earth Sciences 56, 265–305. https://doi.org/10.1139/cjes-2018-0226.

[Dataset] Alberta Energy Regulator (AER), 2019. Public Database. https://www.aer.ca/providing-information/data-and-reports/activity-and-data.

Amrani, A., 2014. Organosulfur Compounds: Molecular and Isotopic Evolution from Biota to Oil and Gas. Annual Review of Earth and Planetary Science 42, 733–768. https://doi.org/10.1146/annurev-earth-050212-124126.

[Dataset] BC Oil and Gas Commission (BCOGC), 2019. Public Database. https://www.bcogc.ca/data-reports/data-centre/.

Bottrell, S.H., Newton, R.J., 2006. Reconstruction of changes in global sulfur cycling from marine sulfate isotopes. Earth Science Review 75, 59–83. https://doi.org/10.1016/j.earscirev.2005.10.004.

Canfield, D.E., 2001. Biogeochemistry of sulfur isotopes. In: J.W. Valley and D. Cole, (Eds.), Reviews in Mineralogy and Geochemistry 43. Mineralogical Society of America and Geochemical Society, 607-636.

Claypool, G.E., Holser, W.T., Kaplan, I.R., Sakai, H., Zak, I., 1980. The age curves of sulfur and oxygen isotopes in marine sulfate and their mutual interpretation. Chemical Geology 28, 199–260. https://doi.org/10.1016/0009-2541(80)90047-9.

Davies, G.R., Moslow, T.F., Sherwin, M.D., 1997. The Lower Triassic Montney Formation, west-central Alberta. Bulletin of Canadian Petroleum Geology 45, 474–506.

Davies, G.R., Smith, L.B., 2006. Structurally controlled hydrothermal dolomite reservoir facies: An overview. AAPG Bulletin 90, 1641–1690. https://doi.org/10.1306/05220605164.

Desrocher, S., 1997. Isotopic and Compositional Characterization of Natural Gases in the Lower and Middle Triassic Montney, Halfway, and Doig Formations, Alberta Basin. Unpublished M.Sc. Thesis, The University of Calgary, 218 p.

Desrocher, S., Hutcheon, I., Kirste, D., Henderson, C.M., 2004. Constraints on the generation of H_2S and CO_2 in the subsurface Triassic, Alberta Basin, Canada. Chemical Geology 204, 237–254. https://doi.org/10.1016/j.chemgeo.2003.11.012.

Edwards, D.E., Barclay, J.E., Gibson, D.W., Kvill, G.E., Halton, E., 1994. Triassic strata of the Western Canada sedimentary basin. In: Mossop, G.D., Shetsen, I. (Eds.), Geological Atlas of the Western Canada Sedimentary Basin. Canadian Society of Petroleum Geologists and Alberta Research Council 16, 259–275.

Fu, Q., 2005. Diagenesis of the Middle Devonian Winnipegosis and Ratner Deposits in Southern Saskatchewan, Canada. Unpublished. Ph.D. thesis, The University of Regina, 224 pp.

Gibbs, A., Rakhit, K., 2019. Hydrodynamics, Geothermics and Spatial Variations in Hydrocarbon Fluid Distribution within the Montney Formation, Alberta and British Columbia, Canada. SPE Annual Technical Conference and Exhibition. Alberta, Calgary. Canada, SPE-196101-MS, 12 pp. https://doi.org:10.2118/196101-MS.

Hope, J., Eaton, D.W., Ross, G.M., 1999. Lithoprobe seismic transect of the Alberta Basin: Compilation and overview. Bulletin of Canadian Petroleum Geology 47, 331–345.

Jiang, L., Worden, R.H., Cai, C.F., 2014. Thermochemical sulfate reduction and fluid flow evolution of the Lower Triassic Feixianguan Formation sour gas reservoirs; the Northeast Sichuan Basin, China. AAPG Bulletin 98, 947-973.

Jiang, L., Fakhraee, M., Cai, C.F., Worden, R.H., 2020. Sulfur cycling during progressive burial in sulfate-rich marine carbonates. Geochemistry Geophysics Geosystems 21, e2020GC009383. https://doi. org/10.1029/2020GC009383.

Kampschulte, A. Strauss, H., 2004. The sulfur isotopic evolution of Phanerozoic seawater based on the analysis of structurally substituted sulfate in carbonates, Chemical Geology 204, 255–286. https://doi.org/10.1016/j.chemgeo.2003.11.013.

Kelemen, S.R., Walters, C.C., Kwiatek, P.J., Afeworki, M., Sansone, M., Freund, H., Pottorf, R.J., Machel, H.G., Zhang, T.W., Ellis, G.S., Tang, Y.C., Peters, K.E., 2008. Distinguishing solid bitumens formed by thermochemical sulfate reduction and thermal chemical alteration. Organic Geochemistry 39, 1137-1143. http://dx.doi.org/ 10.1016/j.orggeochem.2008.04.007.

Krouse, H.R., Mayer, B., 2000. Sulphur and oxygen isotopes in sulphate. In: Cook, P. and Herezeg, A.L., (Eds.), Environmental Tracers in Subsurface Hydrology. Kluwer Academic Publisher, 195-231 p.

Kutuzov, I., Said-Ahmad, W., Turich, C., Jiang, C., Luu, N., Jacksier, T., Amrani, A., 2020. The molecular and sulfur isotope distribution of volatile compounds in natural gases and condensates from Alberta, Canada. Organic Geochemistry 104129. https://doi.org/10.1016/j.orggeochem.2020.104129.

Law, B.E., 2002. Basin-centered gas systems. AAPG Bulletin 86, 1891–1919. https://doi.org/10.1306/61eeddb4-173e-11d7-8645000102c1865d.

Liseroudi, M.H., Ardakani, O.H., Sanei, H., Pedersen, P.K., Stern, R.A., Wood, J.M., 2020. Origin of sulfate-rich fluids in the Early Triassic Montney Formation, Western Canadian Sedimentary Basin. Marine and Petroleum Geology 114, 104236. https://doi.org/10.1016/j.marpetgeo.2020.104236.

Liseroudi, M.H., Ardakani, O.H., Pedersen, P.K., Stern, R.A., Wood, J.M., Sanei, H., 2021. Microbial and Thermochemical Controlled Sulfur Cycle in the Early Triassic Sediments of the Western Canadian Sedimentary Basin. Journal of Geological Society https://doi.org/10.1144/jgs2020-175.

Machel, H.G., 1985. Facies and diagenesis of the upper Devonian Nisku Formation in the subsurface of central Alberta. Unpublished. Ph.D. Thesis, McGill University, 392 p.

Machel, H.G., Krouse, H.R., Sassen, R., 1995. Products and Distinguishing Criteria of Bacterial and Thermochemical Sulfate Reduction. Appllied Geochemistry10, 373-389.

Machel, H.G., 2001. Bacterial and thermochemical sulfate reduction in diagenetic settings - old and new insights. Sedimentary Geology 140, 143–175. https://doi.org/10.1016/S0037-0738(00)00176-7.

Mei, S., 2009. New insights on faults in the Peace River Arch region, northwest Alberta, based on existing well-log data and refined trend surface analysis. Canadian Journal of Earth Sciences 46, 41–65. https://doi.org/10.1139/E09-006.

Mossop, G.D., Shetsen, I., compilers, 1994. Geological Atlas of the Western Canadian Sedimentary Basin: Calgary, Alberta, Canadian Society of Petroleum Geologists and Alberta Research Council, 510 p.

Ness, S.M., 2001. The Application of Basin Analysis to the Triassic Succession, Alberta Basin: An Investigation of Burial and Thermal History and Evolution of Hydrocarbons in Triassic Rocks. Unpublished M.Sc. Thesis, University of Calgary, 192 pp.

Olanipekun, B.J., Azmy, K., 2018. In situ geochemical characterization of pyrite crystals in burial dolomites of St. George group carbonates. Canadian Journal of Earth Sciences 55, 536–544. https://doi.org/10.1139/cjes-2016-0152.

Orr, W.L., 1977. Geologic and geochemical controls on the distribution of hydrogen sulfide in natural gas. In: Campos, R., Goni, J., (Eds.), Advances in Organic Geochemistry. Enadimsa, Madrid, 571–597.

Seal, R.R., 2006. Sulfur isotope geochemistry of sulfide minerals. Reviews in Mineralogy and Geochemistry 61, 633–677. https://doi.org/10.2138/rmg.2006.61.12.

Sim, M.S., Bosak, T, Ono, S., 2011. Large sulfur isotope fractionation does not require disproportionation. Science 333, 74 –77. https://doi.org/10.1126/science.1205103.

Wood, J.M., Sanei, C.H., Haeri-Ardakani, O., Curtis, M.E., Akai, T., 2018a. Organic petrography and scanning electron microscopy imaging of a thermal maturity series from the Montney tight-gas and hydrocarbon liquids fairway. Bulletin of Canadian Petroleum Geology 66, 499–515.

Wood, J.M., Sanei, H., Haeri-Ardakani, O., Curtis, M.E., Akai, T., Currie, C., 2018b. Solid bitumen in the Montney Formation: Diagnostic petrographic characteristics and significance for hydrocarbon migration. International Journal of Coal Geology 198, 48–62, https://doi.org/10.1016/j.coal.2018.09.004.

Worden, R.H., Smalley, P.C., 1996. H_2S-producing reactions in deep carbonate gas reservoirs: Khuff Formation, Abu Dhabi. Chemical Geology 133, 157–171. https://doi.org/10.1016/S0009-2541(96)00074-5.

Worden, R.H., Smalley, P.C., Oxtoby, N.H., 1996. The Effects of Thermochemical Sulfate Reduction upon Formation Water Salinity and Oxygen Isotopes in Carbonate Gas Reservoirs. Geochim Cosmochim. Acta 60, 3925-3931.

Organic geochemistry of the Montney Formation. New insights about the source of hydrocarbons, their accumulation history and post accumulation processes

Jaime, R., Cesar[1], Omid, H., Ardakani[1]*
[1]*Natural Resources Canada, Geological Survey of Canada, Calgary, Canada*
[2]*Department of Geoscience, University of Calgary, Calgary, Alberta*

**Jaime.cesarcolmenares@NRCan-RNCan.gc.ca*

Abstract

This study consists of a non-traditional molecular and stable isotope approach to analyze organic matter (soluble bitumen and produced oil/condensate) from the Montney Formation low-permeability reservoirs, with the purpose of identifying source(s) of hydrocarbons, accumulation history and post accumulation processes. The same approach bases on the distribution of compound classes such as aromatic carotenoids, polycyclic aromatic hydrocarbons (PAHs), bicyclic alkanes, and oxygen-polar compounds. The geochemical screening has been enhanced with performing compound specific isotope analysis (CSIA) of *n*-alkanes and selected aromatic hydrocarbons. Widely spread PAHs, the presence of molecular indicators of euxinia, and hydrocarbon mixtures identified using CSIA profiles, are some of the key findings from this research, which will improve our understanding of the Montney petroleum system(s).

Methodology

Rock samples from the Montney Formation were extracted using soxhlet apparatus for 24 hours. The extracted bitumen was further divided into saturate, aromatic, and polar fractions. Saturate and aromatic hydrocarbons were analyzed using gas chromatography – mass spectrometry (GC-MS). For low amounts of extracted bitumen (<2 mg), the total extract was analyzed using high resolution gas chromatography with time-of-flight mass spectrometry (GC–QTOF-MS). The polar fractions were derivatized using a trimethylsilyl agent and subsequently analyzed using GC–QTOF-MS. Selected saturate and aromatic fractions were analyzed via gas chromatography – isotope ratio mass spectrometry (GC-irMS) for compound specific carbon isotope analysis. Additional analyses to support our interpretations included HAWK pyrolysis and organic petrography, the later using an incident light Zeiss Axioimager II microscope system equipped with an ultraviolet (UV) light source and the Diskus-Fossil system. Legacy data containing molecular composition of oils and condensates were generated using GC-MS and GC with flame ionization detection (GC-FID).

Results and discussion

Studying compound classes that are different to traditional biomarkers (i.e. hopanes and steranes) has revealed intriguing features of the organic matter accumulated within the Montney Formation. For example, green sulfur bacteria (GSB) derived biomarkers, including aryl-isoprenoids and isorenieratane, are widely spread in the Montney Formation. GSB can only survive in photic zone euxinia (PZE; Grice et al., 2005). However, it is difficult to conceive that euxinia was favored during deposition of Montney since conditions such as basin restriction and water stratification were unlikely (Davies et al., 2018; Zonneveld and Moslow, 2018). The closest modern analogue seems to be the Namibian Shelf where upwelling of H_2S facilitates the occurrence of GSB for short periods in an open marine setting (Ma et al., 2021).

Another compound class that is gaining relevance is the polycyclic aromatic hydrocarbons or PAHs. Although typical combustion derived PAHs such as corenane and benzoanthracene have not been detected in Montney samples, a large variety of other PAHs is widely spread in the strata. These include molecules such as chrysene, perylene, methylchrysenes, methylpyrenes, methylanthracenes, among others. Although in some occasions they seem to be associated to terrestrial macerals such as inertinite, this is not always the case. They may represent thermal alteration residues from migrated hydrocarbons or aromatized products from other compound classes such as hopanes and steranes (which are present in low amounts in Montney, especially in the British Columbia section).

When samples discrimination is rather weak using a traditional biomarker approach, the distinction improves when we use molecular parameters based on bicyclic alkanes or drimane-type compounds. The distribution of drimane and rearranged drimanes in a set of samples from the Doig and Montney Formations was found to be unique.

With respect to polar compounds, a variety of oxygen-containing molecules was identified, which includes carboxylic acids, aliphatic and aromatic ketones, and alcohols. The length of the alkyl chain in these compounds was found to be generally shorter with increasing thermal maturity of the samples. The distribution of aromatic ketones and diols in particular do not show correlation with other known molecular parameters thus deserve further investigation of their applicability for the identification of hydrocarbon source and/or depositional environment.

The stable carbon isotope composition of individual compounds (e.g. *n*-alkanes and selected aromatic hydrocarbons) was key to identified mixtures of hydrocarbon charges of different origin. In some cases, the main difference between the charges was thermal maturity while sometimes the accumulated charges differed in the generation process (e.g. phase fractionation versus thermal alteration). The carbon isotope composition of PAHs in particular is suggesting a marine source rather than terrestrial and/or combustion origin for the poly-aromatic structures. Organic petrography was also key for the identification of hydrocarbon mixtures.

Acknowledgements

The authors acknowledge funding for this study provided by Natural Resources Canada (NRCan) Geoscience for New Energy Supply (GNES) program (331403). Rachel Robinson and Marina Milovic are acknowledged for technical support. The authors also thank industry partners for their guidance on sampling and technical support.

References

Davies, G.R., Watson, N., Moslow, T.F., Maceachern, J.A., 2018. Regional subdivisions, sequences, correlations and facies relationships of the lower Triassic Montney Formation, west-central Alberta to northeastern British Columbia, Canada — with emphasis on role of paleostructure. Bulletin of Canadian Petroleum Geology 66, 23–92.

Grice, K., Cao, C., Love, G.D., Bottcher, M.E., Twitchett, R.J., Grosjean, E., Summons, R.E., Turgeon, S.C., Dunning, W., Jin, Y., 2005. Photic zone euxinia during the Permian-Triassic superanoxic event. Science 307, 706–709. https://doi.org/10.1126/science.1106911

Ma, J., French, K.L., Cui, X., Bryant, D.A., Summons, R.E., 2021. Carotenoid biomarkers in Namibian shelf sediments: anoxygenic photosynthesis during sulfide eruptions in the Benguela upwelling system. PNAS 118, e2106040118. https://doi.org/10.1073/pnas.2106040118

Zonneveld, J.P., Moslow, T.F., 2018. Palaeogeographic setting, lithostratigraphy, and sedimentary framework of the lower Triassic Montney Formation of western Alberta and northeastern British Columbia. Bulletin of Canadian Petroleum Geology 66, 93–127.

Tracing the subsurface sulfur cycle using isotopic and elemental fingerprinting: From the micro to the macro scale

Andrew, W, Kingston[1], Omid, H, Ardakani[1,2], Richard A. Stern[3]*
[1] Natural Resources Canada, Geological Survey of Canada, Calgary, Canada
[2]Department of Geoscience, University of Calgary, Calgary, Alberta
[3]Earth and Atmospheric Sciences, University of Alberta, Earth Sciences Building, Edmonton, Canada
[*]andrew.kingston@NRCan-RNCan.gc.ca

Abstract

Hydrogen sulfide (H_2S) is a toxic and corrosive gas that commonly occurs in deeply buried sedimentary systems. Understanding its distribution is paramount to creating safe and effective models of H_2S occurrence aiding in the identification of high-risk areas. Characterizing subsurface sulfur sources and H_2S formation pathways would enhance these models leading to more accurate predictions of potential high H_2S regions. However, gaps remain in our understanding of the dominant formation processes and migration pathways of key ingredients for H_2S production in the Lower Triassic Montney Formation of the Western Canada Sedimentary Basin (WCSB). Essential to this is assessing the reactants necessary for H_2S production, potential pathways for fluid migration, diagenetic history, and changes in redox conditions through time.

The Montney Formation has undergone several phases of diagenesis related to post-depositional alteration and multiple cycles of tectonic burial and uplift. Early chemical alteration includes dolomitization and, in some cases, microbial reduction of porewater sulfate to sulfide that occurred prior to significant burial (Davies et al., 1997; Vaisblat et al., 2021; Liseroudi et al., 2020, 2021). The most recent tectonic-related burial during the Laramide Orogeny resulted in burial depths in excess of 3-5 km (Ness, 2001; Ducros et al., 2017) leading to significant thermal and barometric alteration. Associated with this orogenic activity was the reactivation of underlying faults (O'Connell et al., 1990) and development of fractures especially near the deformation front. These fractures provide conduits for fluid migration into the Montney that combined with heat and pressure resulting in hydrocarbon generation, migration, and development of overpressure, notably in the western margin of the basin. In addition, high temperatures resulted in thermochemical sulfate reduction (TSR) leading to the formation of H_2S and subsequently pyrite.

We present an interpretation of the Montney subsurface sulfur cycle through the use of petrography, micro- and macro-scale geochemical analysis (isotopic and elemental) to illustrate the complexity of this system. This work relies heavily on previous studies within and outside our research group and incorporates new analytical techniques to expand the toolbox. We aim to guide future research directions and activities by addressing issues related to sampling and data quality issues, analytical approaches, and highlight knowledge gaps.

Methodology

A series of full-length Montney cores were selected for sampling in order to assess both regional and stratigraphic variability within the Montney Formation in the WCSB. From these cores a suite of samples was acquired stretching from the underlying Belloy Formation to the overlying Doig Formation. Sample material was washed to remove drilling muds and contamination before submission for geochemical and petrographic analysis detailed below.

For bulk rock analysis (trace and major elemental analysis, bulk stable isotope) samples were powdered and then split for various geochemical analyses. Trace and major element chemistry (60 elements) was performed via ICP-MS by Bureau Veritas Labs Vancouver. Bulk rock sulfur isotope analysis was performed via elemental analysis isotope ratio mass spectrometry by the Isotope Science Lab at the University of Calgary.

Petrographic analysis of thin sections was used to identify variability in the abundances of the different sulfur-bearing species such as pyrite, anhydrite, and barite. Different mineral phases were characterized via textural context and paragenetic sequencing, and then flagged for *in situ* stable isotope analysis. Secondary ion mass spectrometry at the University of Alberta was used to target individual mineral phases for *in situ* stable isotope analysis.

In our research, we performed a combination of bulk rock and *in situ* sulfur isotope analysis because they provide different but complimentary information. Bulk sampling is used to evaluate broad-scale contributions of the various sulfur-species to the overall variability in sulfur chemistry stratigraphically. However, the indiscriminate nature of bulk sampling limits its usefulness in accurately characterizing multi-dimensional nature of the subsurface sulfur cycle. For example, the various pyrite textures (e.g., framboidal, euhedral, etc.) form via different processes/sulfur sources/times and therefore can have differing isotopic geochemistry, which will affect bulk sulfur isotope composition. The presence of different redox states (sulfides and sulfates) also affects bulk chemistry and even chemical processing to extract sulfates can oxidize sulfides thereby altering $\delta^{34}S$ values (e.g., Balci et al. 2007). *In situ* sulfur isotope analysis allows us to differentiate the isotope geochemistry of different pyrite and sulfate texture/mineralogies, which provides a more detailed record of sulfur cycling in the subsurface.

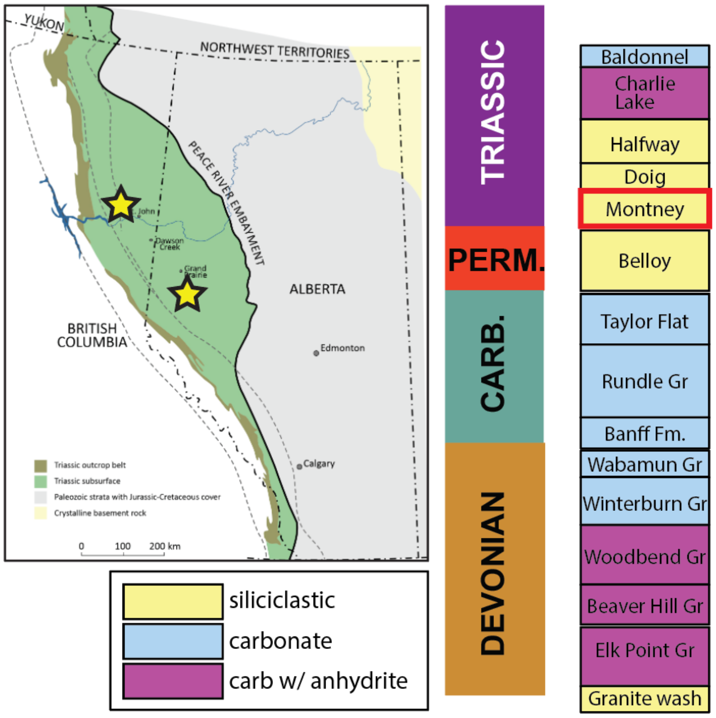

Figure 1. Study sites and regional stratigraphy of the Western Canadian Sedimentary Basin. Potential sources of sulfate for H_2S production shown as purple in stratigraphic column.

Results and Discussion

Petrographic analysis of thin sections indicates a complex array of sulfur-bearing species, which vary both stratigraphically and regionally and can be environmental or diagenetically controlled. Major sulfur-bearing species include pyrite, anhydrite, and barite with pyrite being dominant throughout the studied sections.

Sulfates

In general, sulfates are rare in studied material north of the Peace Rive Arch (PRA) in BC and abundant in material from south of the PRA in AB. This may be related to the higher thermal maturity of these samples leading to near total TSR of anhydrite in studied BC sections. Indeed, the sulfur isotope composition of pyrite in the studied BC sections are generally higher than those in AB suggesting TSR played a major role in sulfate reduction within samples from BC. In AB early and late anhydrite phases are observed, however, cement-forming late anhydrite is dominant and typically occurs within coarser grain beds (e.g., sediment gravity flows) often in the Middle to Upper Montney (Fig. 2a). Previous studies suggest that late anhydrite cements can be associated with fracture and vug-filling anhydrite, potentially implicating hydrothermal fluid flow from underlying strata through inter-formational faulting as a source for late anhydrite cements (Liseroudi et al., 2020). Barite is less abundant than anhydrite and originates from either diagenetic fluid (Fig. 2b) with elevated δ^{34}S values (>40 ‰ VCDT); or potentially ancient relicts precipitated from original seawater (Fig. 2c) with δ^{34}S values of 21 ‰ VCDT.

Two proposed sources of Montney anhydrite are the overlying Triassic Charlie Lake Formation and/or one of several underlying Devonian sources (Fig. 1) (Liseroudi et al., 2020; Chalmers et al., 2021). Charlie Lake anhydrite is generally around 16.5 ‰ (±1.0 ‰ VCDT), which is lower then measured Montney anhydrite values, which are generally >19 ‰ VCDT, closer to Devonian sulfates values. However, the regional extent of sampling is still quite low and the likelihood of Montney sulfate comprising a mixture of both Triassic and Devonian sulfate sources is likely.

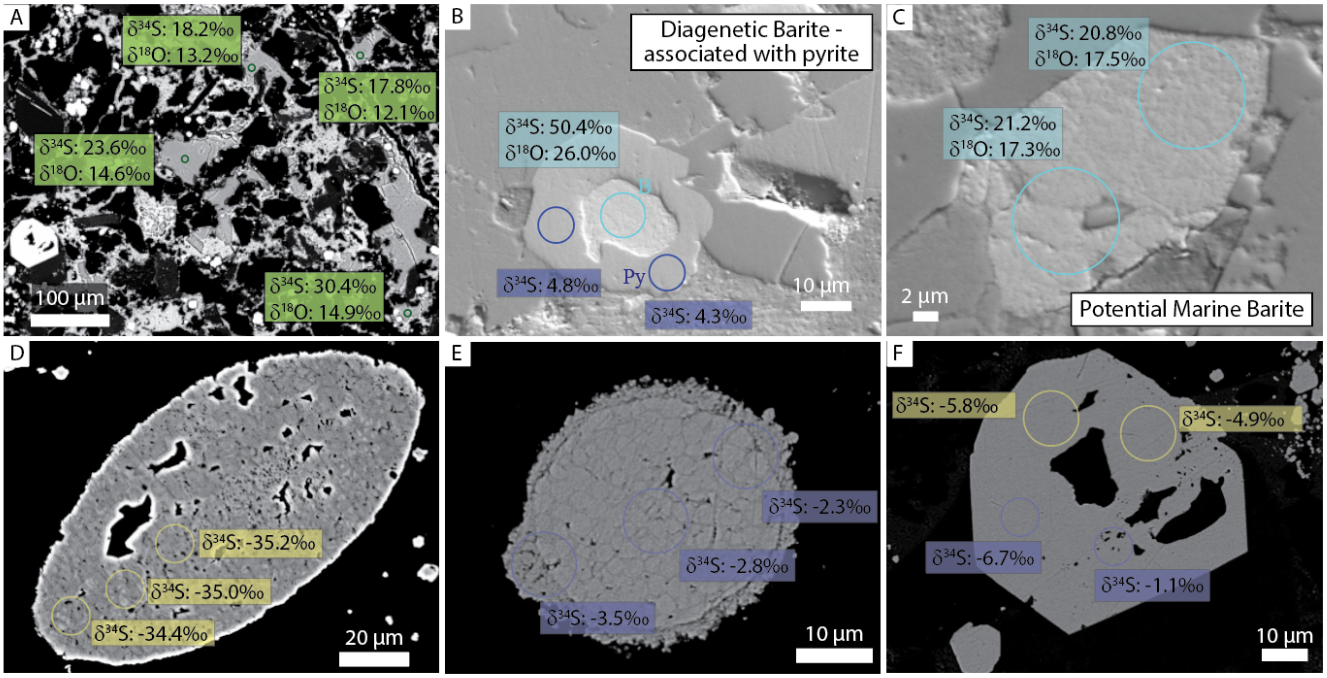

Figure 2. Main types of sulfate and pyrite textures. A) Anhydrite cement common in the Upper Montney in AB core. Note large range in δ^{34}S values. B) Diagenetic barite with pyritized margin. Light blue spot is barite analysis, purple is pyrite analysis. C) Potential marine barite grain with δ^{34}S values near seawater value. D) Pyritized microfossils. Ostracod skeletal material replaced by pyrite, note core is composed of framboidal pyrite. Lowest δ^{34}S values. E) Large framboidal pyrite with later precipitated pyrite cement. Note higher δ^{34}S values compared with pyritized microfossil. F) Euhedral pyrite grain. Larger intra-grain δ^{34}S variability, similar in composition to recrystallized framboids.

Sulfides

Sulfides are ubiquitous throughout all the studied sections and represent the dominant sulfur species observed, mainly in the form of pyrite. Different phases of pyrite are easily recognizable via their textures with euhedral/crystalline and framboidal forms being the most abundant base structures that can undergo alteration to coalesced arrangements during ongoing diagenesis. Framboidal pyrite grains (Fig. 2d) are typically associated with microbial sulfate reduction (MSR), occur at various sizes, and can be either disseminated throughout host rock or concentrated in pore space where they are closely associated with pore-filling bitumen. Framboidal grains can form the core from which pyritic growth occurs (Fig. 2e) or individual grains within framboids can be cemented together with secondary pyrite (Fig. 2f). Euhedral pyrite occurs as disseminated grains, and as centimeter-scale lenses and layers. In addition, there are isolated occurrences of pyrite nodules typically in the form of pyritic rims on anhydrite cores often associated with fossilized organic and/or skeletal material. Diagenetic barite can also have pyritic rims resulting from late thermochemical sulfate reduction of barite.

In situ sulfur isotope analysis of individual pyrite grains results in values ranging from –37 to +21 ‰ VCDT indicating that both MSR and TSR processes are responsible for authigenic H_2S formation in the Montney. However, our understanding of the contribution that each of these authigenic processes make in concert with contributions from migrated H_2S is poorly understood and may vary regionally and stratigraphically. Key to evaluating these contributions is *in situ* micro-sampling as different phases of pyrite can occur in close proximity (Fig. 3) obfuscating bulk sampling techniques.

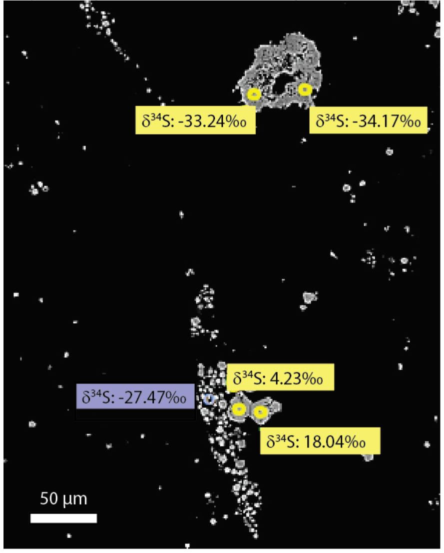

Figure 3. Microscale variations in sulfur isotope values. Note the 45.5‰ difference in values over a distance of approximately 25 µm. This difference is associated with two different pyrite textures (e.g., framboidal vs. euhedral) highlighting the advantage of *in situ* techniques for discriminating various pyrite forming processes.

Sulfurized organic matter

Sulfur is also associated with organic matter including gases such as thiols, carbonyl sulfide, and carbon sulfide; and a diverse group of liquid and solid sulfurized organic matter (SOM) compounds. Currently, our knowledge of the distribution and role that SOM compounds play in H_2S occurrence is lacking and an area for future research. However, the Montney Fm. generally has low TOC content in the studied samples (~2%) with sulfur contents within this organic matter ranging from 3–29%, with the higher-end associated with H_2S-rich strata. Because SOM represents a minor fraction of the total sulfur in the Montney we acknowledge it exists but have excluded it from further discussion in this study.

Hydrogen Sulfide (H_2S)

Finally, H_2S gas, H_2S is heterogeneously distributed in the Montney (Kingston et al., 2021) with the causes of this confounded by the complex diagenetic history of the Montney. Sulfur isotope values of Montney H_2S range from 8.6–19.5 ‰ VCDT (Fig. 4), which is broadly consistent with the H_2S values from all other formations within the WCSB. This suggests H_2S in the WCSB is either well mixed, singly sourced, or similar processes are responsible for its formation; but clearly indicates that $\delta^{34}S$ values of H_2S cannot be used to discriminate H_2S sources at a regional scale.

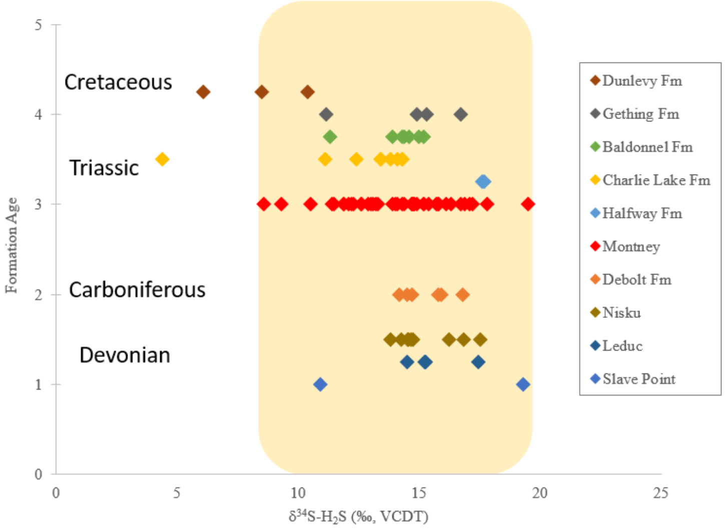

Figure 4. Compilation of $\delta^{34}S$ values of H_2S in various formations from the Western Canadian Sedimentary Basin. Note broad overlap of values.

Ongoing and Future Work

There are several notable knowledge gaps that our research group is currently investigating and/or have identified for future work, including: a) the role of fluid migration, b) mapping H_2S distribution in under- and overlying strata, and c) characterization of sulfurized organic matter. Evaluating the role that H_2S migration plays throughout the WCSB is essential to characterizing authigenic versus allogenic contributions to Montney H_2S. Inter-formational fluid migration through tectonic-related features such as faults and intra-formation fluid migration through high permeability beds are both likely important conduits for sulfur-bearing species (including H_2S) in the Montney. However, more work is needed to understand their role in H_2S migration. Mapping H_2S in under- and overlying strata will help identify regions with high concentrations of H_2S in the WCSB better constraining the main sources and reservoirs of sulfur-bearing compounds and potential sources of migrated H_2S. This includes attempting to map the distribution of anhydrite within the Montney, as a key ingredient for H_2S production. Finally, looking at the role organic matter plays in the subsurface sulfur cycle is being investigated to better constrain its role and contributions to H_2S distribution in the Montney including the timing of organic matter migration and its thermal history.

Acknowledgements

The authors acknowledge funding for this study provided by Natural Resources Canada (NRCan) Geoscience for New Energy Supply (GNES) program (331403). Steve Taylor and Veith Becker (University of Calgary) for assistance with bulk stable isotope work. Aloma Braganza (Geological Survey of Canada) for assistance with petrology. Patricia Webster and Carlo Gallotta (Geological Survey of Canada) for assistance in sample preparation.

References

Balci, N., Shanks III, W.C., Mayer, B. and Mandernack, K.W., 2007. Oxygen and sulfur isotope systematics of sulfate produced by bacterial and abiotic oxidation of pyrite. Geochimica et Cosmochimica Acta 71(15), 3796-3811.

Chalmers, G.R.L., Bustin, R.M. and Bustin, A.A., 2021. Isotopic fingerprinting of sulphur sources for the hydrogen sulphide gas in the Montney Formation, northeastern British Columbia (NTS 093O, P, 094A, B, G–J, N–P); in Geoscience BC Summary of Activities 2020: Energy and Water, Geoscience BC, Report 2021-02, p. 103–108.

Davies, G. R., Moslow, T. F., & Sherwin, M. D. (1997). The Lower Triassic Montney Formation, west-central Alberta. Bulletin of Canadian Petroleum Geology 45(4), 474–505. https://doi.org/10.35767/gscpgbull.45.4.474

Ducros, M., W. Sassi, R. Vially, T. Euzen, and V. Crombez, 2017, 2-D Basin Modeling of the Western Canada Sedimentary Basin across the Montney-Doig System: Implications for Hydrocarbon Migration Pathways and Unconventional Resources Potential, in Mahdi A. Abu Ali, Isabelle Moretti, and Hege M. Nordgård Bolås, eds., Petroleum Systems Analysis—Case Studies: AAPG Memoir 114, 117–134.

Kingston, A.W., Mort, A., Deblonde, C., and Ardakani, O.H., 2021. Hydrogen sulfide (H2S) distribution in the Triassic Montney Formation of the Western Canadian Sedimentary Basin; Geological Survey of Canada, Open File 8849, 21 p. https://doi.org/10.4095/329266

Liseroudi, M.H., Ardakani, O.H., Sanei, H., Pedersen, P.K., Stern, R.A. and Wood, J.M., 2020. Origin of sulfate-rich fluids in the Early Triassic Montney Formation, Western Canadian Sedimentary Basin. Marine and Petroleum Geology, 114, 104236.

Liseroudi, M. H., Ardakani, O. H., Pedersen, P. K., Stern, R. A., Wood, J. M., & Sanei, H. (2021). Microbial and Thermochemical Controlled Sulfur Cycle in the Early Triassic Sediments of the Western Canadian Sedimentary Basin. Journal of the Geological Society, *55*(1), jgs2020-175. https://doi.org/10.1144/jgs2020-175

Ness, S.M., 2001. The Application of Basin Analysis to the Triassic Succession, Alberta Basin: an Investigation of Burial and Thermal History and Evolution of Hydrocarbons in Triassic Rocks (M.Sc. thesis), University of Calgary, Canada, 192 p.

O'Connell, S.C., Dixon, G.R., Barclay, J.E., 1990. The origin, history, and regional structural development of the Peace River Arch, Western Canada. Bulletin of Canadian Petroleum Geology 38A, 4–24.

Vaisblat, N., Harris, N. B., Ayranci, K., Power, M., DeBhur, C., Bish, D. L., Chalaturnyk, R., Krause, F., Crombez, V., Euzen, T., & Rohais, S. (2021). Compositional and diagenetic evolution of a siltstone, with implications for reservoir quality; an example from the Lower Triassic Montney Formation in western Canada. Marine and Petroleum Geology, 129, 105066. https://doi.org/10.1016/J.MARPETGEO.2021.105066

Controls on the distribution and composition of gas and condensate in the Montney resource play

*Andy Mort[1]**
Natural Resources Canada, Geological Survey of Canada, Calgary, Canada
**andy.mort@nrcan-rncan.gc.ca*

Abstract

The Montney resource play has evolved from a peripheral conventional play to one of the most important hydrocarbon-producing unconventional resource plays in North America and has remained resilient throughout the economic challenges of recent years. Despite maturing as a resource play as a result of more than 15 years of unconventional development and research there are still aspects of the play that are not fully de-risked and prediction of fluid quality remains haphazard due to the complex interplay of geological and engineering factors. Among these are the delineation of structural and stratigraphic barriers and conduits, identification of enigmatic source rocks, which defy traditional methods, evaluating effects of fluid migration and the difficulty in predicting phase behavior in a tight, but open system. This study uses a combined approach leveraging geochemical tools combined with spatial and stratigraphic analysis in an attempt to improve current understanding of these issues.

Methodology

Energy regulators in Western Canada have been instrumental in making an unprecedented vast volume of subsurface data readily available including routine oil, gas and water analysis. The British Columbia Oil and Gas Commission's (OGC) data center also includes one of the largest publically available subsurface gas isotope datasets, which has been integrated with stratigraphic analyses, reported in hundreds of off-confidential wells. Geochemical analysis of core extract data obtained from the Alberta Energy Regulator (AER) and OGC have also been compiled at the Geological Survey of Canada and filtered, standardized, and loaded into the GSCs corporate Sample Management System (SAMS) according to a rigorous QAQC procedure, formalized (for spatial data) in the FME data integration platform. This has enabled a rudimentary 3D geospatial model to be constructed across the Montney play fairway straddling the 120°W meridian. The model extends selected horizons taken from the Alberta Geological Survey's Geological Framework into NE BC (Lyster et al., 2020), allowing spatially resolved data of any kind to be projected into this subsurface model. The model divides the Montney into Upper, Middle and Lower informal members described and defined in several publications (Davies et al., 2018).

Conventional petroleum systems analysis includes the use of molecular organic geochemistry to analyses biological and process-specific markers for source identification and fluid correlation purposes. However, in many tight unconventional plays the produced fluids are often volatile liquids and gas in which these geochemical tracers are in low abundance or absent. Some of the tools used in reservoir geochemistry such as light hydrocarbon fingerprinting and gas compositional and isotopic analysis can potentially be adapted to great effect in discriminating unconventional reservoir fluids and helping to explain their formation and evolution. These tools are most powerful when integrated with other subsurface data as has been performed in this study.

Results and Discussion

Previous research indicates that the gas and light oil produced from the Montney could have more than one origin, including self-sourcing from autochthonous organic matter from basinal shales in the Middle and Lower Montney. An example of the utility and shortcoming of molecular organic geochemistry is illustrated in Figure 1 (Ejezie et al., 2007), where the Upper Montney fluids can be correlated with a high degree of confidence with core extract m/z 191 extracted ion chromatogram fingerprints showing a highly diagnostic series of extended tricyclic terpanes. However, this forensic evidence is missing in the Lower Montney fluid from the same well (Figure 1, below right), despite having experienced only 250m of extra burial equivalent to a few °C.

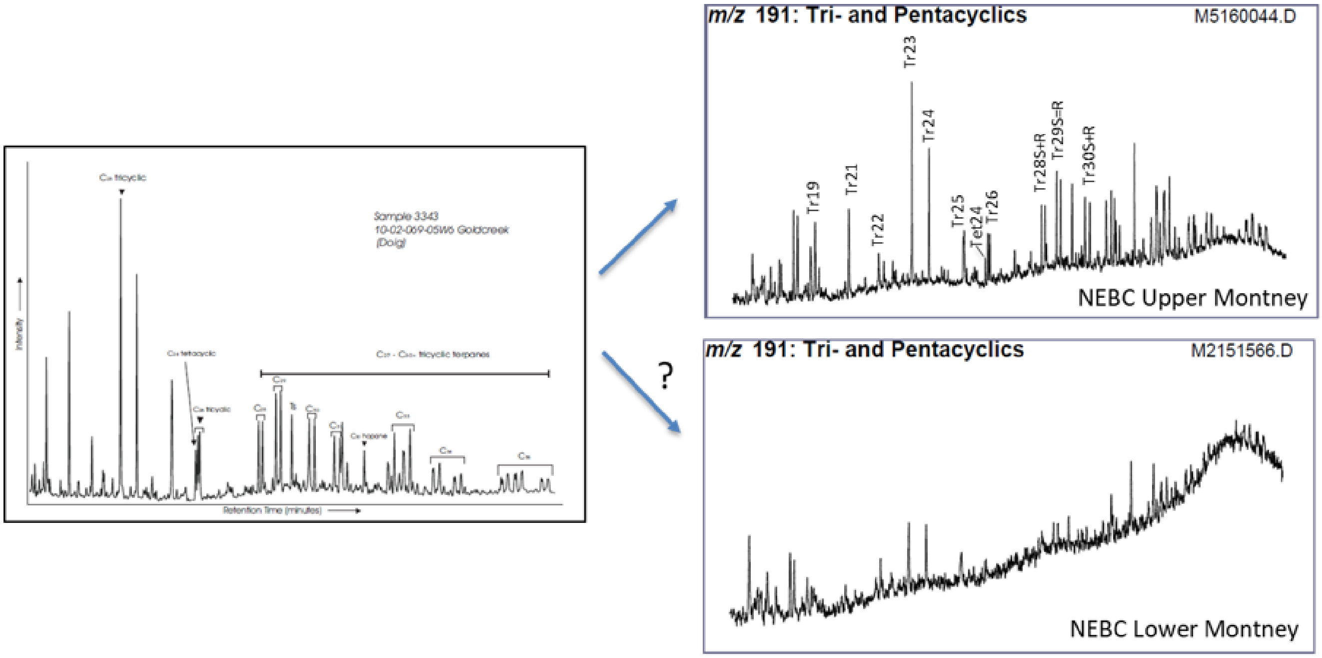

Figure 1. GCMS ion chromatograms of the m/z 191 fragment diagnostics for hopanes. The Doig Phosphate core extract (left) shows excellent correlation with Upper Montney reservoir fluids (above right) evidenced by a homologous series of tricyclic terpanes (cheilanthanes) which are below the limits of detection in the equivalent trace of a fluid produced from the Lower Montney.

The overlying Doig Phosphate, although relatively thin is extremely organically rich and when juxtaposed above higher permeability zones of the Upper Montney, excess pressure will allow the expulsion of hydrocarbons stratigraphically downwards. This is demonstrated the burial history model of a Blueberry area well for which extensive calibration data are available. The 1D model constructed to test hydrocarbon generation and overpressure in the Montney is shown in Figure 2. Although Jurassic burial and exhumation are difficult to constrain, thermal calibration is regionally robust and indicates maximum burial during subsidence of the Laramide foreland basin. Pressure test data have been used to calibrate overpressure modelling of the well as the excursion of the black line in Figure 2B to the right of the hydrostatic pressure line shows. This overpressure is a relic of the regime during peak burial when a combination of rapid burial and hydrocarbon generation and expulsion resulted in pressures sufficient to permit migration of hydrocarbons from the Doig stratigraphically deeper into the Upper Montney, as the purple shading in Figure 2D demonstrates.

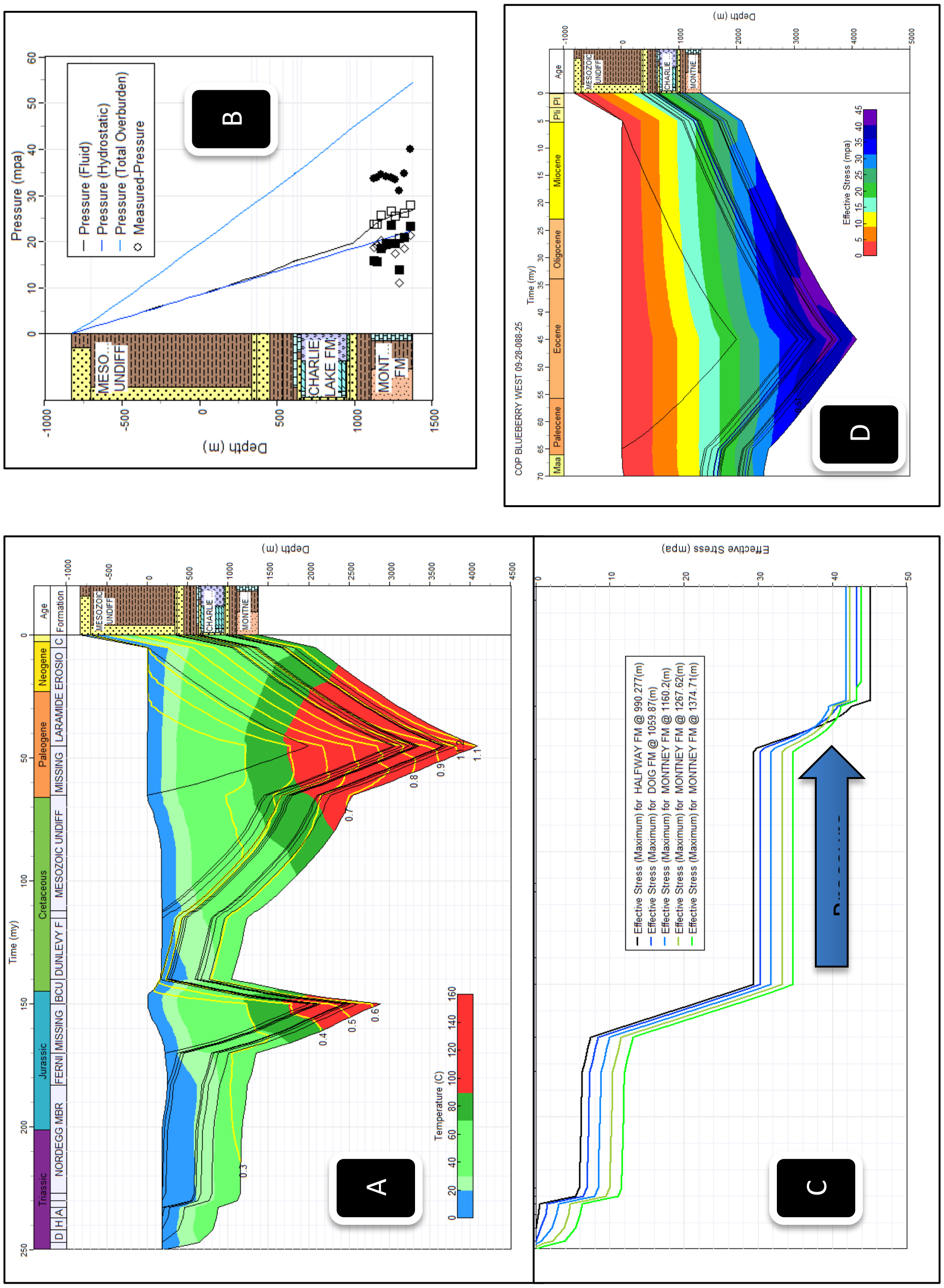

Figure 2. Burial History for NEBC Blueberry well (A) showing the maximum temperatures attained and peak hydrocarbon generation and expulsion. The well is also calibrated to demonstrate excess pressure in the Montney and Doig (B). The relative increase in pore pressure in the Doig, relative to the Montney is demonstrated by the crossover in effective stress as a result of hydrocarbon generation at maximum burial (C). This pressure inversion in the Doig relative to Upper Montney is shown on the burial history with colour indicating excess pressure (D).

Having established a genetic link between the Upper Montney reservoir fluids and overlying Doig Phosphate, and demonstrating the physics for this causative link through modelling, the origin of the fluids in the deeper part of the Montney remains in question. In the absence of molecular biomarkers in the liquid phase, the gas phase components and their stable isotope ratios represent a potentially useful tool to investigate these fluids. Figure 3 demonstrates why many industry geologists are increasingly using gas isotopes to evaluate fluid segregation and maturity in preference to traditional methods like Rock-Eval T_{max}, which is unreliable in low yield samples; and reflectance analysis of vitrinite, a maceral absent or masked by bitumen in high maturity shale plays. The natural gas plot (Figure 3, left) demonstrates the excellent separation of fluids by mud gas isotope analysis in the Blueberry well previously use for modelling. Regional calibration of a large suite of samples by GeoMark Research (Euzen et al., 2021) has furthermore permitted an empirical estimate of the maturity differential between the Lower Montney with a clear gap evident between the basal reservoir and further up the section in the plot of ethane versus propane isotopes (Figure 3, right).

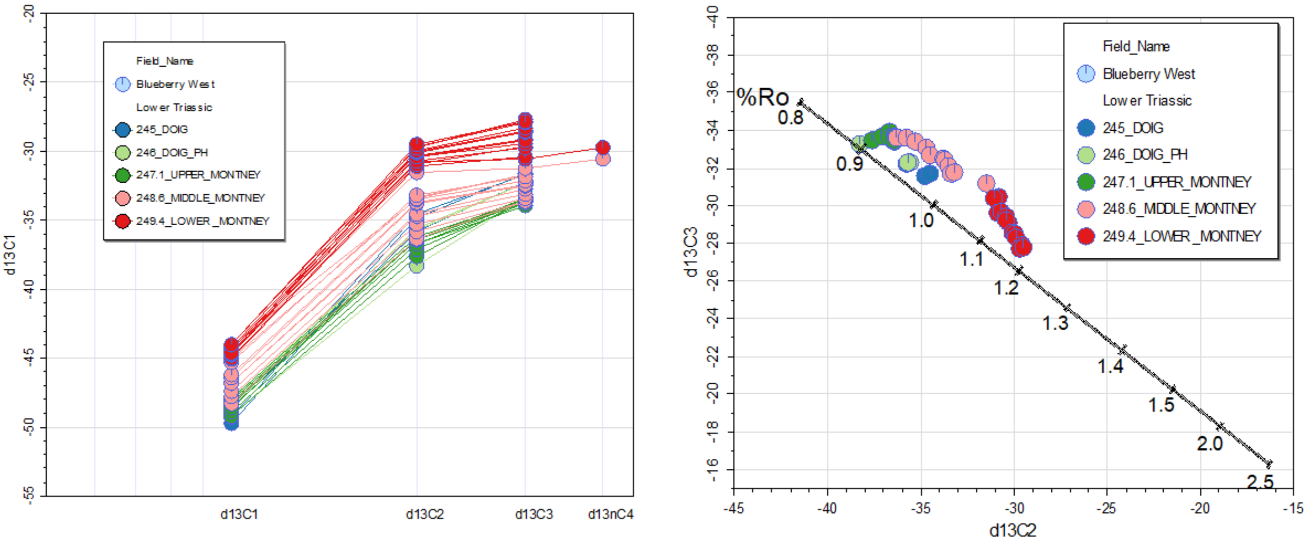

Figure 3. Mud gas isotope data for the Doig-Montney section of a well in the Blueberry area of the Montney play fairway in NEBC. The natural gas plot (left) shows excellent separation of fluids by internal stratigraphic boundaries. Local calibration of propane and ethane isotopes (right).

The maturity gap demonstrated by the use of gas isotopes suggests that the Lower Montney fluids in this area have migrated in from kitchens either down dip or stratigraphically deeper. Further work will attempt to build on this observation to place constraints on the origin of these fluids and elucidate the plumbing system that controls fluids movement in the WCSB.

Acknowledgements

This study would not have been possible without the help of the AER and BCOGC staff who have facilitated access to data for GSC research scientists. The help of Christine DeBlonde and Richard Nairn in the Geoinformatics section at GSC Calgary has been invaluable in processing these data to make them accessible for interpretation. This work has been supported by NRCan's Geoscience for New Energy Supply (GNES) research program

References

Davies G. R., Watson N., Moslow T. F. and Maceachern J. A. (2018) Regional subdivisions, sequences, correlations and facies relationships of the Lower Triassic Montney Formation, west-central Alberta to northeastern British Columbia, Canada — With emphasis on role of paleostructure. Bulletin of Canadian Petroleum Geology 66, 23–92.

Ejezie N., Riediger C. L. and Fowler M. (2007) Triassic Oil Families and Possible Source Rocks, Peace River Embayment Area, Alberta, Canada. Unpublished M.Sc. thesis, The University of Calgary.

Euzen T., Watson N., Fowler M., Mort A. and Moslow T. F. (2021) Petroleum distribution in the Montney hybrid play: Source, carrier bed, and structural controls. AAPG Bulletin 105, 1867–1892.

Lyster S., Brown L. and Playter T. L. (2020) AER/AGS Model 2020-03: 3D Property Model of the Montney Formation in Alberta, Version 2: Methodology., Edmonton, AB. Available at: https://ags.aer.ca/publication/model-2020-03.

Gas Geochemistry and the Origins of H_2S in the Montney Formation

Pablo, Lacerda Silva[1], Gareth, R., Chalmers[2], Amanda, M. M.., Bustin[3], R., Marc, Bustin[3]*
[1]MTI Energy Inc., Edmonton, Canada
[2]University of the Sunshine Coast, Queensland, Australia
[3]The University of British Columbia, British Columbia, Canada
[*]pablols@alum.ubc.ca

Abstract

The geology of the Montney Formation and the geochemistry of its produced fluids, including non-hydrocarbon gases such as hydrogen sulfide were investigated for both Alberta and BC play areas. Key parameters for understanding a complex petroleum system like the Montney play include changes in thickness, depth of burial, mass balance calculations, timing and magnitudes of paleotemperature exposure, as well as kerogen concentration and types to determine the distribution of hydrocarbon composition, H_2S concentrations and CO_2 concentrations. Results show that there is first-, second- and third- order variations in the maturation patterns that impact the hydrocarbon composition. Isomer ratio calculations for butane and propane, in combination with excess methane estimation from produced fluids, are powerful tools to highlight effects of migration in the hydrocarbon distribution. The present-day distribution of hydrocarbons is a result of fluid mixing between hydrocarbons generated in-situ with shorter-chained hydrocarbons (i.e., methane) migrated from deeper, more mature areas proximal to the deformation front, along structural elements like the Fort St. John Graben, as well as through areas of lithology with higher permeability.

The BC Montney play appears to have hydrocarbon composition that reflects a larger contribution from in-situ generation, while the Montney play in Alberta has a higher proportion of its hydrocarbon volumes from migrated hydrocarbons. Hydrogen sulphide is observed to be laterally discontinuous and found in discrete zones or pockets. The locations of higher concentrations of hydrogen sulphide do not align with the sulphate-rich facies of the Charlie Lake Formation but can be seen to underlie areas of higher sulphate ion concentrations in the formation water. There is some alignment between CO_2 and H_2S, particularly south of Dawson Creek; however, the cross-plot of CO_2 and H_2S illustrates some deviation away from any correlation and there must be other processes at play (i.e., decomposition of kerogen or carbonate dissolution). The sources of sulphur in the produced H_2S were investigated through isotopic analyses coupled with scanning electron microscopy, energy dispersive spectroscopy, and mineralogy by X-ray diffraction.

The Montney Formation in BC can contain small discrete amounts of sulphur in the form of anhydrite as shown by XRD and SEM-EDX results. Sulphur isotopic analyses indicate that the most likely source of sulphur is from Triassic rocks, in particular, the Charlie Lake Formation, due to its close proximity, its high concentration of anhydrite (18-42%), and the evidence that dissolved sulphate ions migrated within the groundwater in fractures and transported anhydrite into the Halfway Formation and into the Montney Formation. The isotopic signature shows the sulphur isotopic ratio of the anhydrite in the Montney Formation is in the same range as the sulphur within the H_2S gas and is a lighter ratio than what is found in Devonian anhydrite and H_2S gas. This integrated study contributes to a better understanding of the hydrocarbon system for enhancing the efficiency of and optimizing the planning of drilling and production operations. Operators in BC should include mapping of the Charlie Lake evaporites and structural elements, three-dimensional seismic and sulphate ion concentrations in the connate water, when planning wells, in order to reduce the risk of encountering unexpected souring.

Methodology

This study is based largely on data collected, analysed and interpreted for the study with the support of industry partners. Some data we utilise is public data submitted by oil and gas companies to the Oil and Gas Commission in British Columbia (OGC) or the Alberta Energy Regulator in Alberta (AER). The regional distribution of fluid analyses used in the study is almost entirely derived from the public data and was accessed either directly from this source or through use of geoLOGIC’s Geoscout program, a third-party aggregator and provider. A total of 11,331 gas compositional samples were analysed from the Montney Formation in both BC and Alberta. Gas fractions and ratios, particularly of nC4/iC4 isomers and gas dryness (ratio between the methane fraction and the sum of all gas and natural gas liquids) were mapped and their spatial distribution analysed. The regional maturation polynomial regression line from Euzen et al. (2021) was used to determine the gas dryness percentage for each well based on its maturation level determined by the butane isomer ratio. The deviation from the calculated gas dryness based on the regression was determined as an excess methane percentage and subdivided into nine categories of excess methane (< 1%; 1-2%; 2-3%; 4-5%; 6-7%; 8-10%; 11-12%; and 12%+).

A total of 59 drill cuttings samples were analysed for mineralogical composition using XRD analyses and Rietveld analysis, and the mineral composition was quantified (Munson et al., 2016) by Rietveld analysis (Rietveld, 1967). Sulfur isotopic analysis in anhydrite was performed on chemically separated anhydrite from a total of 37 samples from 4 wells. To test if sulphur could be sourced from organic matter or pyrite, a selection of Montney Formation samples was processed to concentrate kerogen (n = 5) and pyrite (n = 3). The hydrogen sulphide sampling for this study was performed by Stratum Reservoir, LLC (Calgary, AB) at the request of operators, and sent to Stratum Reservoir’s Isotech Laboratory in Champaign, Illinois, USA.

A total of 29 drill cutting samples were cut and polished and analysed by back-scattered electron microscopy (BSEM). Elemental identification was obtained using an energy-dispersive spectrometer (EDX). The potential for thermochemical sulphate reduction (TSR) H_2S generation in the Montney Formation was assessed through basin modeling. A sulphate (SO_4) content of the average seawater for the Montney pore water, and 1% sulphate by weight of sulphur in petroleum were assumed.

Results and Discussion

The regional trend of thermal maturity of the Montney is subparallel to the basin axis, increasing to the southwest towards the eastern limit of the deformation front. The gas dryness also generally increases towards the deformation front, corresponding to increasing thermal maturity on a broad scale. However, significant deflections from the overall trend, caused by second and third-order controls, such as variable amounts of eroded section, variations in the heat flow patterns, impact the hydrocarbon composition of the Montney Formation and the ability for generation of hydrogen sulphide through thermochemical reactions.

The hydrocarbon composition of the Montney Formation is complex due to interplay between in-situ generation and migration of shorter-chain hydrocarbons like methane, from more mature zones in the west and moving updip towards the eastern portion of the Montney play areas. This is illustrated by the higher excess methane percentages in the Alberta play areas (Figure 1). Migration updip is also controlled by lineaments and lithologic changes in the Montney Formation. Changes into higher permeability lithologies are also highlighted by Wood and Sanei (2016).

Distribution of carbon dioxide is distinct from hydrogen sulfide, and higher concentrations of CO_2 (>2%) are restricted to the deeper parts of the basin, where it reaches up to 18%. The origin of carbon dioxide in sedimentary basins without metamorphic or volcanic episodes could be related to dissolution of carbonate minerals during diagenesis, a by-product from hydrogen sulphide generation or breakdown of Type III kerogen. When comparing the distribution of H_2S and CO_2 in the Montney Formation, there is a log-linear correlation for regions with a high ratio (>5) of H_2S to CO_2 (Figure 2). These regions are located around the Grande Prairie area, where the H_2S concentrations are more elevated. This area is also flanked to the northwest and southeast by areas of elevated CO_2 and low H_2S. Considering the cogeneration of CO_2 and H_2S through reduction of sulphate in anhydrite, there may have been either updip migration of the H_2S generated in the high CO_2 southwest and northwest areas; or the CO_2 in those areas is not associated with thermal sulphate reduction, but instead due to decomposition of kerogen or limestone dissolution.

The central western and southwestern portions of the Montney Formation are at higher risk of H_2S generation by thermochemical sulfate reduction from generated petroleum (Figure 3). Based on a lower temperature threshold for TSR of 120 °C (Goldstein & Aizenshtat, 1994; Mougin et al., 2007), the lower Montney Formation entered the TSR phase in its central western portion (located at the centre of the PRE) by approximately 100 M, although it did not start generating significant quantities of H_2S until 72 Ma. The entirety of the lower Montney Formation was within the TSR zone by 60 Ma. As Paleogene sediments were eroded and the basin uplifted, the eastern half of the Montney Formation area remained in the TSR for less than 40 Ma. Exhumation rates were lower in the southwest, where the Montney Formation had entered the TSR between 75 and 95 Ma, and so the Montney Formation did not exit the TSR zone in this region until at least 20 Ma.

The isotopic signatures of the H_2S gas in the Montney Formation in BC range between 9.3 and 17.4‰, with one outlier of 20.9‰. This range is similar to the sulphur isotopic ratios for Triassic anhydrite, which range between 8.9 and 20.98‰ (Figure 4). The sulphur isotopic ratio for anhydrite in Devonian rocks ranges between 17.1 and 34‰, and when plotted with oxygen isotopic ratio show a distinct signature from that of anhydrite in Triassic rocks (Figure 4). The similarity in the sulphur isotopic ratio between H_2S and anhydrite in the Triassic rocks indicates that anhydrite-rich Triassic rocks, such as the Charlie Lake Formation, are the likely sources of sulphur, instead of Devonian rocks, as expected by some operators. The isotopic ratio for sulphur is also too heavy to have been generated by bacterial sulfate reduction.

SEM and EDX analyses have shown that the anhydrite texture is massive in the Montney Formation. The texture appears to be part of fracture fill cement (secondary texture) and did not form from transportation or evaporative processes (primary textures). As this analysis is performed on drill cuttings, this observation may be due to contamination of drill cuttings from the Charlie Lake Formation above; however, the texture seen in the anhydrite in the Montney Formation (secondary texture) is not the same as the anhydrite in the Charlie Lake Formation (primary, evaporite textures). The anhydrite that is found within the Montney Formation is likely sourced from another formation through solution and redeposition as a cement from a sulphate-rich solution prior to hydrocarbon generation. Hydrogen sulphide gas then is generated locally at the anhydrite-cemented fractures, as it reacts with the hydrocarbons being generated in the Montney Formation. This would explain the localised souring of horizontal wells adjacent to sweet horizontal wells on the same multi-well pad, and fits a structurally controlled model, in which anhydrite or sulphate ions derived from sulphate minerals with the Charlie Lake Formation migrate through local fracture/fault systems into the Montney Formation.

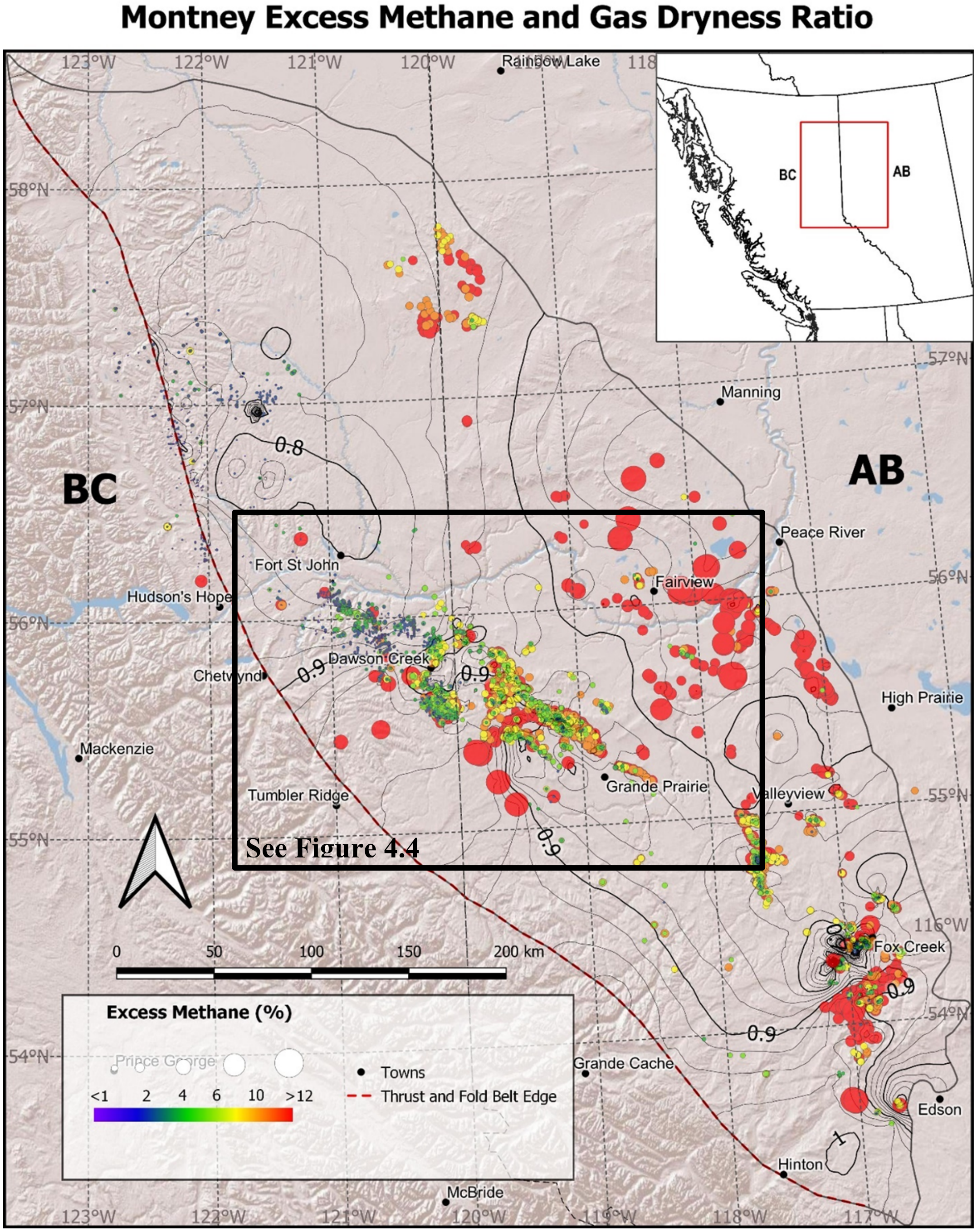

Figure 1. The excess methane percentage (symbols) for Montney Producers in BC and Alberta. The excess methane percentage is the calculated increase percentage of methane based on the iC4/nC4 ratio regional maturation trend of Euzen et al. (2021). The methane gas dryness percentage is also shown as contour lines. Contour interval is 0.025 (i.e., 2.5%). Darker colors are indicative of hydrocarbon compositions that are aligned with the regional maturation trends across the basin and probably self-sourced hydrocarbons or very limited migration distances. The larger orange and red symbols indicate locations that have the hydrocarbon composition is not aligned with regional maturation trends and there is a larger component of migrated hydrocarbons in the reservoir. This is well illustrated by the Montney in eastern Alberta that is a more conventional petroleum system.

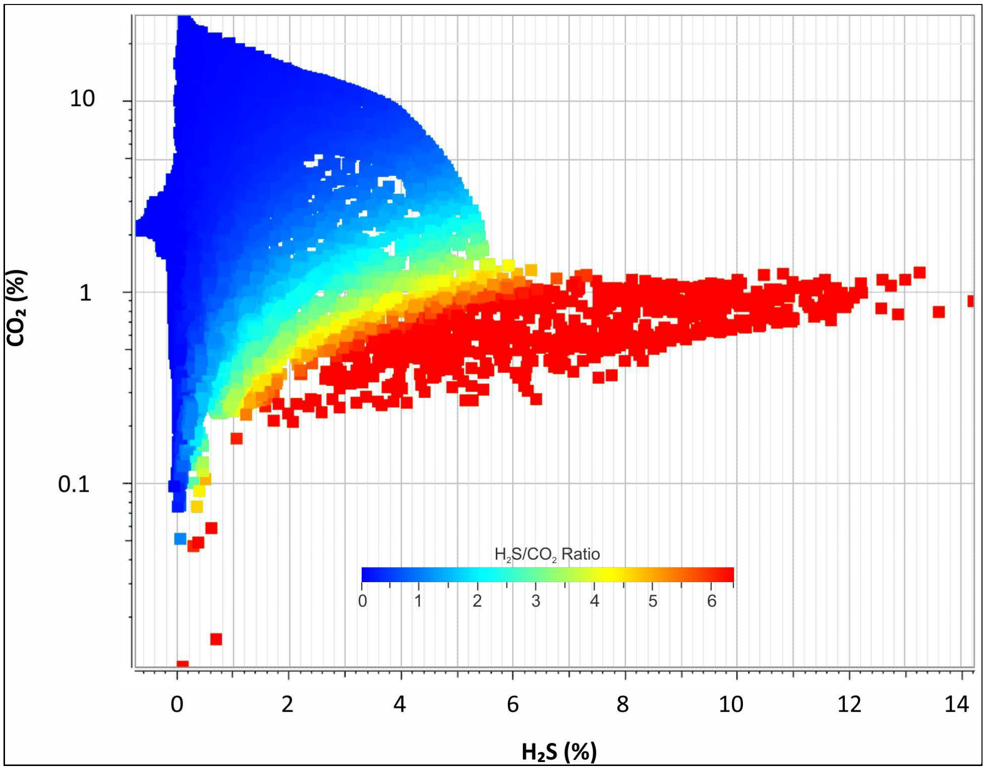

Figure 2. Cross-plot of the spatial distribution of CO2 versus H2S in the Montney Formation, colored by the ratio between H2S and CO2, highlighting the correlation that exists only in the high H2S area (> 5%).

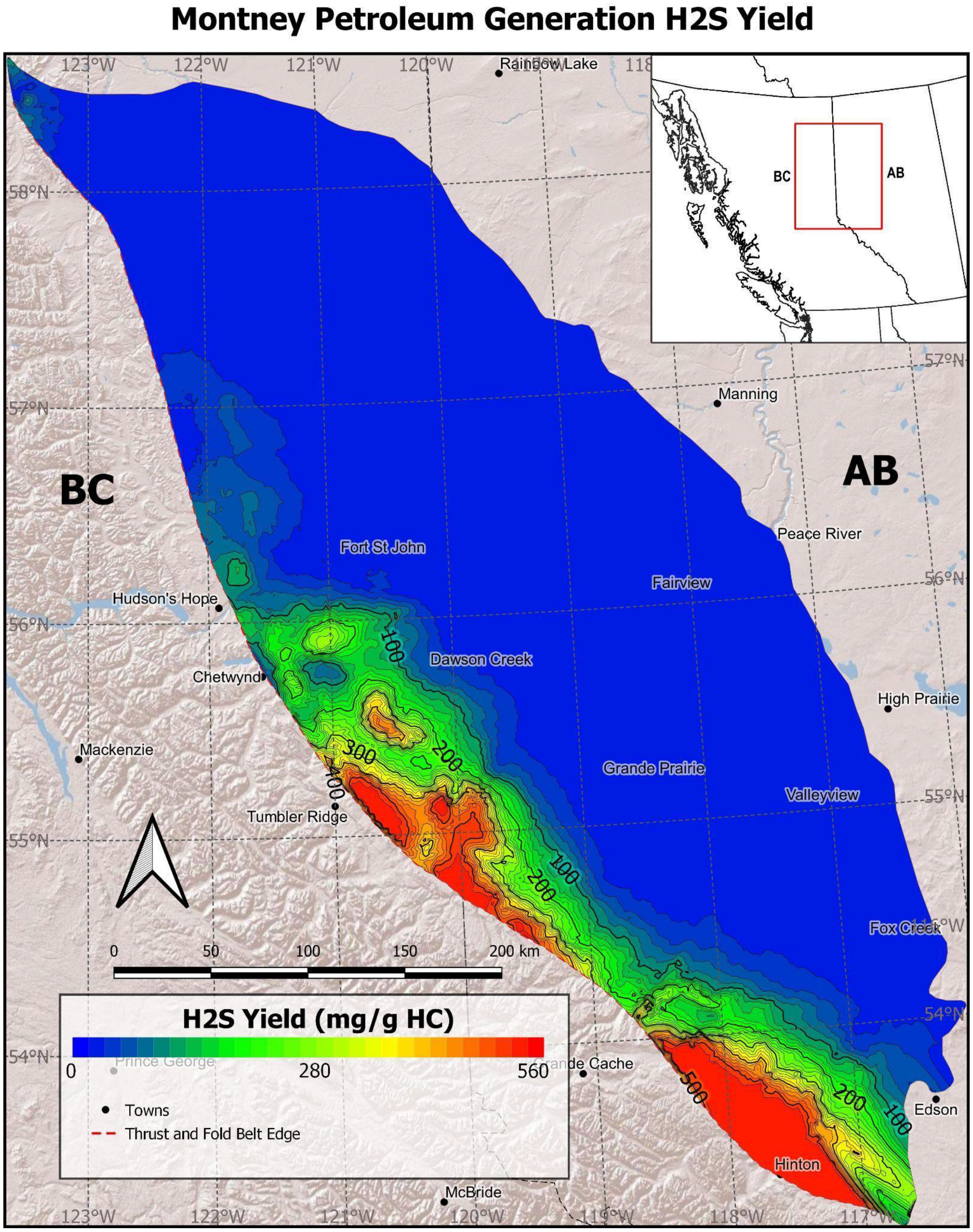

Figure 3. Distribution of H2S yield from thermochemical sulphate reduction during petroleum generation in the Montney Formation.

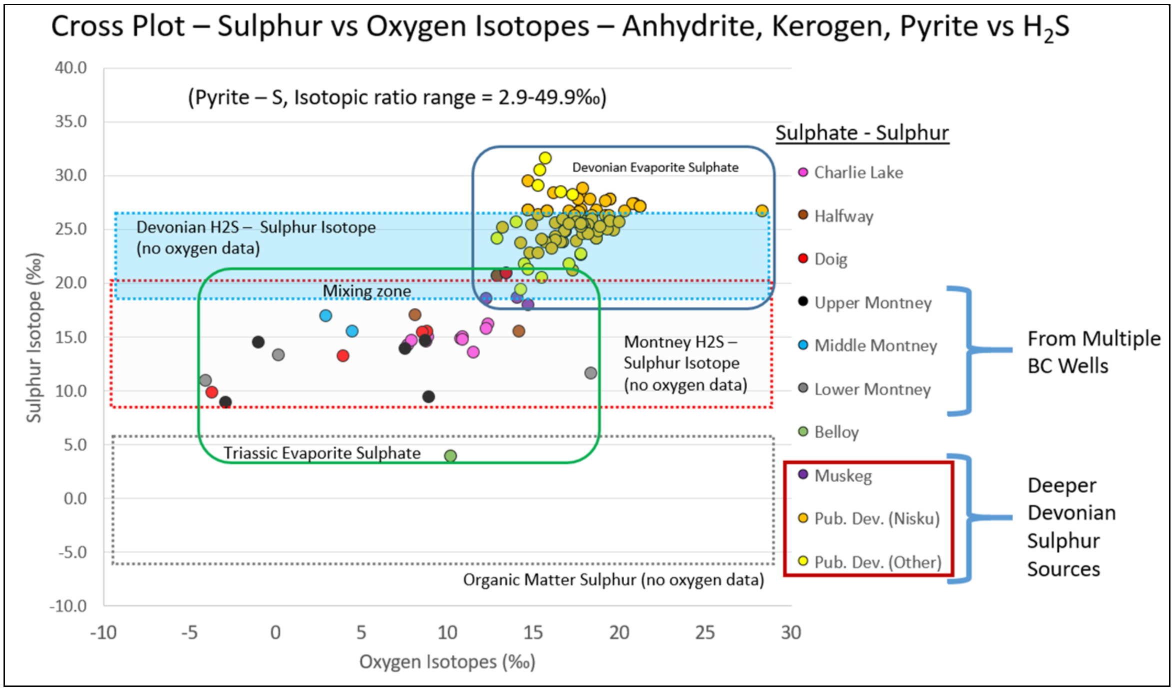

Figure 4. Cross plot of Sulphur and oxygen isotopes from anhydrite, pyrite, kerogen and H_2S gas from both Triassic and Devonian sources. Point data is the oxygen and Sulphur isotopic data for anhydrite minerals for both Triassic and Devonian samples. Triassic sourced Sulphur from anhydrite minerals all plot within the green box and are isotopically lighter compared to the Devonian sourced Sulphur from anhydrite (blue box). Samples from the Muskeg Formation in this project (purple circles) have isotopically lightest Devonian sulphur/oxygen anhydrite and with the two samples from the Doig and Halfway formations have created a transitional zone between the two data sets (i.e., 18-20 ‰). Yellow points are from published data for the Devonian sulphate minerals. Concentrated pyrite samples (n = 3) have been separated from Montney Formation and are not plotted on this graph as the range of sulphur isotopic results is too broad. Concentrated kerogen samples (n = 6) are from the Montney Formation and are represented by grey dashed box as the oxygen data is not necessarily associated with the organic sulphur and therefore not included in the plot. The isotopic sulphur data from the H_2S gas are also represented by dashed boxes (red = Montney H_2S gas; Blue and blue shaded = Devonian H_2S gas) as the H_2S gas has no oxygen data associated with the sulphur. Montney H_2S gas is isotopically lighter compared to Devonian H_2S and each data set divided by geological age reflecting a similar isotopic range as the anhydrite mineral from each geological age. These results indicate the sulphur of the Montney H_2S is sourced from Triassic anhydrite or from a mixture of Triassic and Devonian anhydrite sources if isotopically heavier (i.e., 17-21 ‰).

Acknowledgements

The results of this study and the associated training of students and other high qualified people involved in the study would not have been possible without the financial support of Geoscience BC, NSERC and our industry partners Chevron Canada, Ovitniv (EnCana), AGAT Laboratories, Crew Energy, and Canbriam (Pacific Canbriam Energy), and Saguaro Resources (Tourmaline Oil). We also thank Progress Energy (Petronas Canada) and particularly Mathew Adams for logistic support and access to data and sharing of ideas. We are indebted to Travis Hobbs of Ovitniv for access to data that would not have been otherwise accessible. This study would not have been possible without software donations to UBC by Geologic (Geoscout) and Schlumberger, for which we thank them.

References

Euzen, T., Watson, N., Fowler, M., Mort, A., Moslow, T., 2021. Petroleum distribution in the Montney hybrid play: Source, carrier bed, and structural controls. AAPG Bulletin, 105, 1867-1892. https://doi.org/10.1306/12222020088.

Goldstein, T.P., Aizenshtat, Z., 1994. Thermochemical sulfate reduction: A review. Journal of Thermal Analysis, 42(1), 241–290. https://doi.org/10.1007/BF02547004.

Mougin, P., Lamoureux-Var, V., Bariteau, A., Huc, A.Y., 2007. Thermodynamic of thermochemical sulphate reduction. Journal of Petroleum Science and Engineering, 58(3–4), 413–427. https://doi.org/10.1016/j.petrol.2007.01.005.

Wood, J., Sanei, H., 2016. Secondary migration and leakage of methane from a major tight-gas system. Nature Communications, 7(13614). https://doi.org/10.1038/ncomms13614.

Identification of regional structural corridors in the Montney play using trend surface analysis combined with geophysical imaging

Paulina Wozniakowska[1], David W. Eaton[1], C. Deblonde[2], A. Mort[2], O. Haeri Ardakani[2,1]*
[1]Department of Geoscience, University of Calgary, Canada
[2]Natural Resources Canada, Geological Survey of Canada, Calgary, Canada
[*]paulina.wozniakowska@ucalgary.ca

Abstract

Induced (anthropogenic) earthquakes are caused by reactivation of pre-existing faults due to human activities, including hydraulic fracturing and saltwater disposal. The Montney play, the pre-eminent shale gas play in Canada, contains localized regions with relatively high geological susceptibility to induced seismicity. Identification of potential seismogenic structures is hindered because published fault maps in the Montney play are often focused on small areas, leading to inconsistencies when these are compiled across the region. We have developed a regional framework based on structural corridors: complex, multi-strand faults systems. A three-step structural interpretation workflow was used, including seismic and structural interpretation along with trend surface analysis (TSA). This approach was used to identify 34 structural corridors in NE BC and NW Alberta.

Introduction

The presence of pre-existing, critically stressed faults is one of the key conditions of injection-induced seismicity, which can potentially be reactivated during hydraulic fracturing operations or saltwater disposal (Eaton, 2018). Faults also play a major role in the transport of deep-crustal-fluids, resulting in diagenetic processes, including dolomitization, or formation of hydrothermal fluids and gases, such as H_2S (Liseroudi et al., 2020). However, published information about the distribution of faults is often limited, due to limited spatial extent of geophysical surveys. Figure 1 shows an example of a published seismic line showing structural deformation within the Montney play, which is limited to a small portion of the area.

In general, previous structural studies, including field mapping and analog models, show that activation of basement faults beneath mechanically layered sedimentary rocks produces complex multi-strand fault systems characterized by power-law scaling relationships with respect to fault length and displacement. Therefore, rather than map-ping individual faults, we have developed a regional framework that employs a structural-corridor paradigm, which is well suited to probabilistic induced-seismicity risk analysis. Here, we define a *structural corridor* as a spatially coherent trend of co-genetic structural features comprising folds and faults. The aim of this study is to perform a comprehensive, regional-scale interpretation of potential seismogenic structures throughout the Montney play in NE BC and NW Alberta, to provide quality-controlled inputs for further geoscientific analyses. This area is known to have relatively high susceptibility to induced seismicity (Wozniakowska and Eaton, 2020). Applications that could benefit from detailed information about the presence of faults include analysis of induced seismicity, geological modelling, and various geomechanical and geochemical studies.

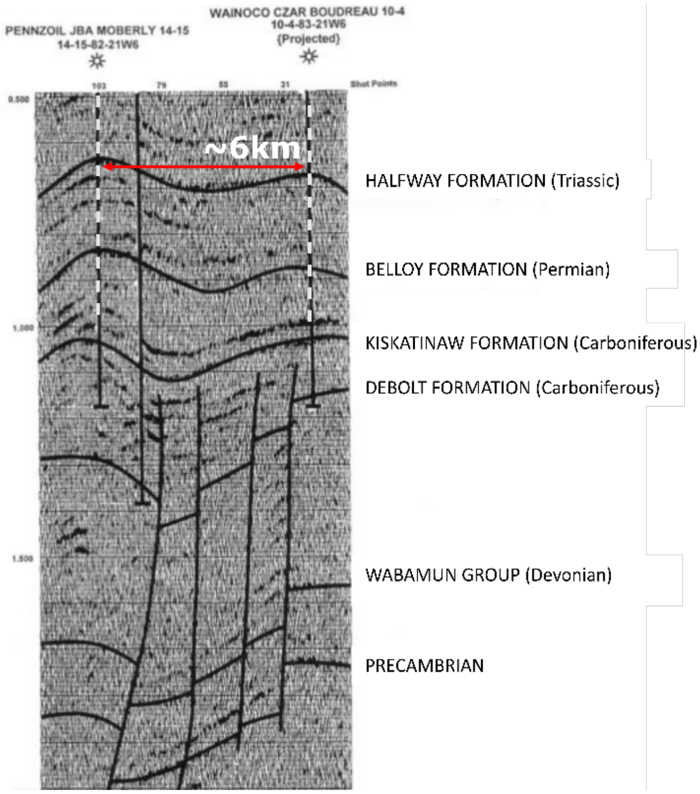

Figure 1. Seismic expression of the Monias structural corridor (modified from Norgard, 1997).

Methodology

The main steps in our workflow are summarized in the Fig. 2. The first step of the study involves trend surface analysis applied to well log data, to identify major structural corridors using the residual mapping obtained from the geostatistical analysis of the formation-top picks. We analyzed 7 different geological formations from the period between Devonian to Cretaceous (Basal Fish Scale Zone, Bluesky, Halfway, Upper Montney, Belloy, Debolt and Wabamun) to capture the evolution of the geological surfaces and allow for broader analysis of the tectonic activity and development of fault structures in time. Trend surface analysis consists of preprocessing, regional trend surface and residual calculations as well as the interpolation of residuals. The next step of the workflow was focused on the interpretation of seismic data within the area of study. In addition to publicly available LITHOPROBE seismic profiles, we have analyzed one seismic line located within the KSMMA region near Fort St. John, BC.

In the last step, spatially limited information about subsurface structures from the trend surface analysis was complemented by seismic interpretation results to perform complex structural interpretation. Specifically, seismic interpretation provided information regarding the location of faults corresponding to the approximate horizontal boundaries of structural corridors intersected by the seismic line which were crucial in determination of geometry of structural corridors. Fault interpretation is facilitated in this study by constructing a residual surface, obtained by interpolating the observed picks and subtraction it from a trend surface that provides a smooth fit to the formation-top surface. The method is based on a previously developed workflow that uses a geostatistical approach f(Mei, 2009). The concept is simple: an abrupt lateral change in surface elevation due to vertical fault offset will produce a paired anomaly, with a negative residual in the hanging wall and a positive residual in the footwall. Folds are also considered in our interpretation of structural corridors. In the case of a fold with wavelength that is small compared with the spatial smoothing, the residual anomaly is not necessarily a positive-negative pair; in general, an antiform will produce a negative residual and a synform will produce a positive residual. Where a significant paired residual anomaly is evident, the location of the corresponding fault is approximated by the zero crossing of the residual surface, while the apparent local vertical fault throw is given by the elevation difference between the positive and negative residual anomalies, measured perpendicular to the anomaly strike direction.

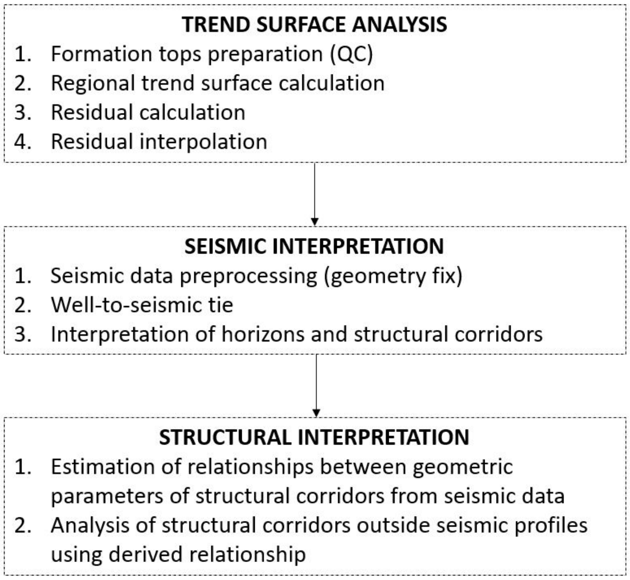

Figure 2. Flow chart of the workflow used to process formation top data to identify faults using trend surface analysis and validate/characterize the results using regional reflection seismic data.

Results and Discussion

Figure 3 shows grayscale images of residual maps for four of the formations with the major structural features highlighted. The spatial resolution, and therefore the ability to resolve short-wavelength structure, depends on the number of picks available. The best spatial resolution is provided by the Basal Fish Scale Zone (BSFZ), for which 104,073 wells were available to construct the residual map, compared with about 20,000 wells for the other formations. The spatial extent for each map is limited to the region of available well data, and the extreme values of the grayscale depend on the minimum and maximum residual values. In the case of the oldest units shown in Figure 3 (Wabamun and Debolt), the east-west trending Dawson Creek Graben Complex (DCGC) is conspicuous, near 56 ° N. This structural belt has a total length of approximately 250 km and consists of a series of grabens, the largest of which is the Fort St. John graben (FSJG).

To the north and east, this complex contains major, oblique-trending satellite grabens including the Hines Creek, Dunvegan, Tangent and Boundary Lake grabens. The DCGC formed in late Carboniferous time due to collapse of the underlying Peace River Arch (Barclay et al., 1990; Hope et al., 1999). Although the residual maps indicate a maximum apparent throw of just over 76m, this value significantly underestimates the actual vertical throw since, as noted above, part of the structural relief is taken up by the trend surface. To the west, the DCGC extends into the disturbed belt, although in these maps its western limit is obscure due to lack of well control at the Debolt and Wabamun levels. In the case of the Wabamun residual map, several isolated high features are well constrained by drilling and lie above major reefs (atolls) within the underlying Leduc and Swan Hills formations. These residual highs may represent the effects of differential compaction, as underlying off-reef strata (e.g., Ireton shale) are more compacted than the Leduc reefs (O'Connor & Gretener, 1974). In general, structural corridors correlate with anomalies that exhibit a coherent trend. In the case of the Upper Montney residual map (Fig. 3), some features in the DCGC can be discerned, although it is clear that only some parts of the DCGC were active during and/or after deposition of the Upper Montney.

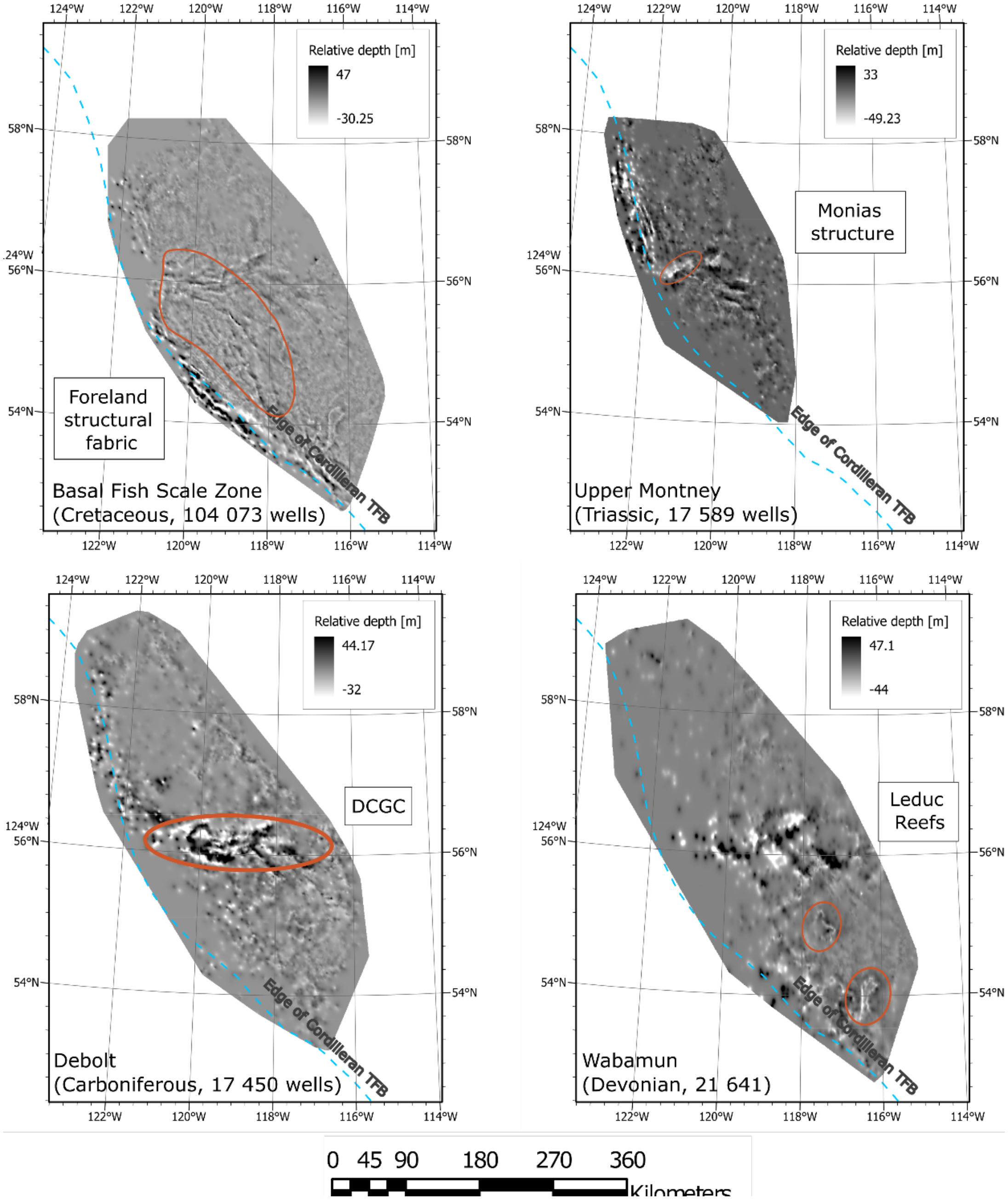

Figure 3. Residual maps of Basal Fish Scale Zone, Upper Montney, Debolt and Wabamun tops. Coherent trends in the maps are indicative of structural corridors (faults and folds). For reference, the eastern edge of the Cordilleran thrust and fold belt (TFB) is indicated by the dashed blue line. Major structural trends expressed on the residual maps are outlined in red. For each unit, the age and number of wells used for residual calculation are indicated in the lower left of the map. Data provided by geoLOGIC systems ltd. ©2021.

Structural corridors identified using described, multi-step approach overlaid on Debolt residuals are presented in the Fig. 4. The approach integrates all the available data including trend surface analysis, seismic profiles and published structural corridors based on the literature, addressing the issues spatial limitations of available seismic information within Montney Formation. We have identified three main structural corridor complexes corresponding to the most distinct features in the area: Bovie Fault, Hay River Fault Zone and Dawson Creek Graben Complex.

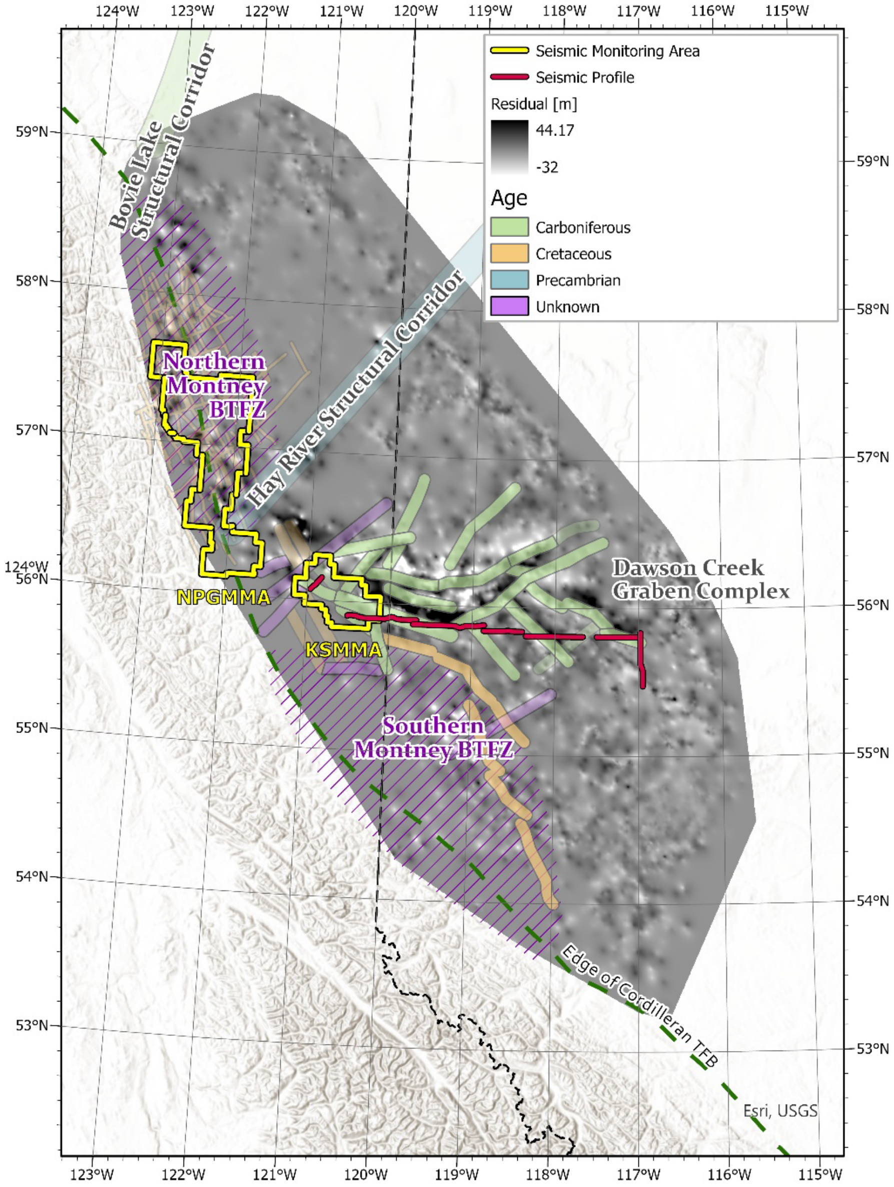

Figure 4. Regional map of the main structural corridors within study area overlaid on the Debolt residual map. Yellow and right lines indicate the seismic monitoring areas and reflection seismic lines, respectively. The eastern surface limit of the Late Cretaceous - Paleocene Cordilleran thrust and fold belt (TFB) is shown, for reference. Dashed line polygons indicate the extent of the Northern and Southern Montney buried TFB zones. Colors of the structural corridors correspond to the geological age when the corridors were formed. More transparent polygons correspond to structural corridors identified in literature examples, while less transparent polygons indicate corridors interpreted on residual maps through Trend Surface Analysis (TSA). Data provided by geoLOGIC systems ltd. ©2021.

Figure 5 shows an enlargement of structural corridors in the vicinity of the DCGC and the southern Montney, including the main fault zones. The corridors have been numbered and color-coded depending on the source of information. Within DCGC, we have identified 34 structural corridors. While most of the corridors are characterized by the strong residual contrasts on the residual maps for the Debolt Formation, in the areas outside of DCGC, where the formation top data was insufficient, some structural features were identified on the BFSZ residual map or identified using examples from the literature. The corridors have been numbered and named according to the previous structural interpretations and maps where possible. Remaining corridors were named according to the geographical elements.

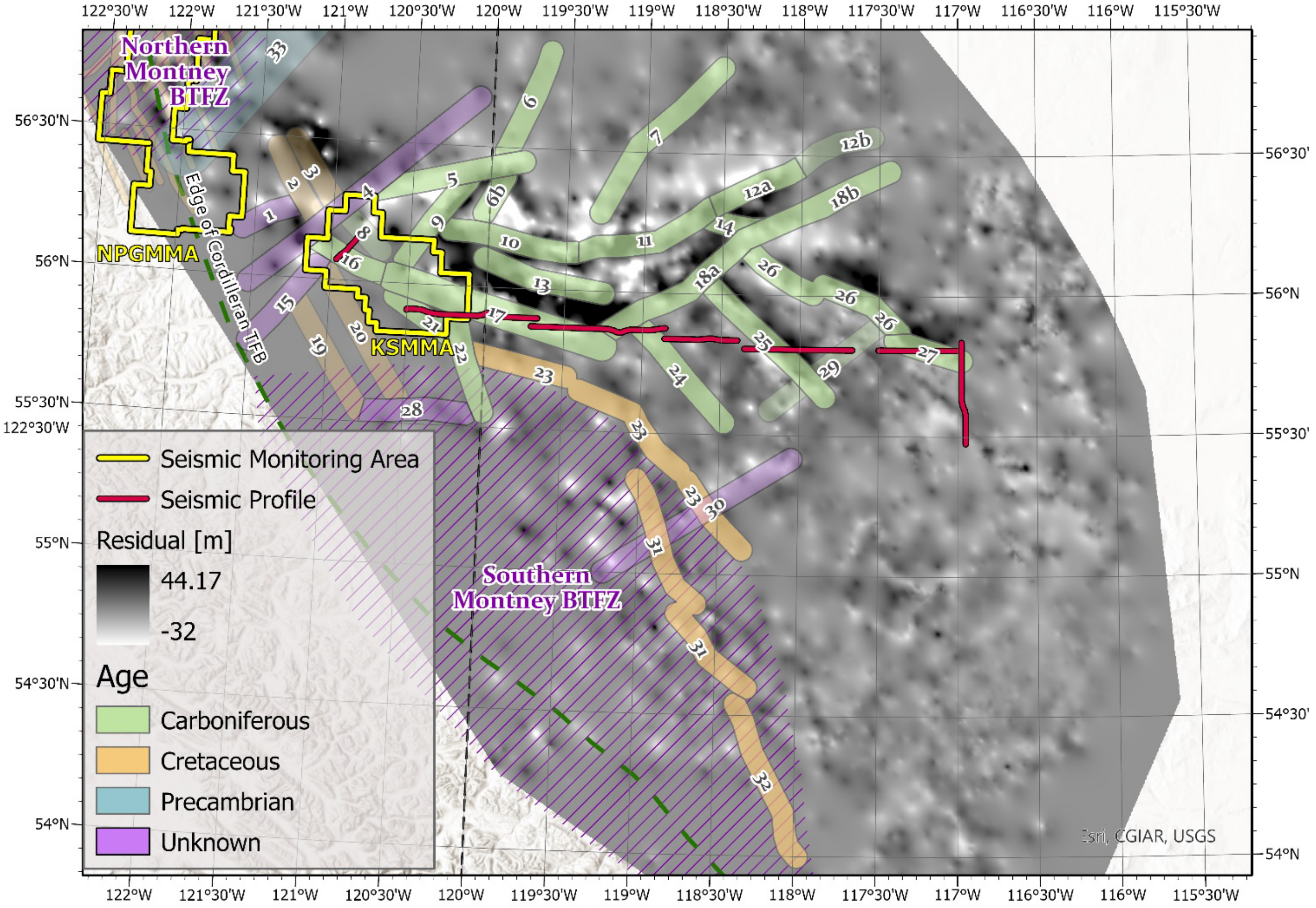

Figure 5. Map of Debolt Residual within Dawson Creek Graben Complex and southern Montney with overlayed structural corridors and main fault zones. Yellow and right lines indicate the seismic monitoring areas and reflection seismic lines, respectively. The eastern surface limit of the Late Cretaceous - Paleocene Cordilleran TFB is shown, for reference. Dashed line polygons indicate the extent of the Northern and Southern Montney buried thrust and fold zones (BTFZ). Colors of the structural corridors correspond to the geological age when the corridors were formed. More transparent polygons correspond to structural corridors identified in literature examples, while less transparent polygons indicate corridors interpreted on residual maps through Trend Surface Analysis (TSA). Data provided by geoLOGIC systems ltd. ©2021.

We have developed a new, comprehensive fault framework based on seismic data and trend surface analysis which captures the commonly observed, multi-strand character of fault structures and allows for more regional-scale analysis of fault networks. The approach enabled identification of 34 structural corridors in NE BC and NW Alberta, the majority of which are concentrated within Dawson Creek Graben Complex. Several structural corridors characterized by similar orientations were identified in the foreland of the Rocky Mountain Thrust and Fold Belt. Names of interpreted structural corridors are presented in the Table 1.

Table 1. The names and horizontal extent assigned to structural corridors are based primarily on past publications and geographical references. Numbers in superscript indicate the original source of the corridor name and/or extent.

Farrell Creek[9]	1	Southern FSJG (a)[8]	18a
North Cache Creek[9]	2	Southern FSJG (b)[10]	18b
Charlie Lake[10]	3	Groundbirch[9]	19
Monias[5]	4	Sunset Creek[9]	20
Pineview[10]	5	Farmington[11]	21
Boundary Lake (a)[8]	6a	Dawson Creek	22
Boundary Lake (b)[10]	6b	Clear River - Pouce Coupe[8]	23
South Whitemud River[9]	7	Rycroft[4]	24
Old Fort[11]	8	Dunvegan[1] / Belloy[2]	25
Flatrock[11]	9	Fairview-Bluesky[8]	26
Bear Canyon[8]	10	Tangent[4]	27
Peace River[10]	11	Brassey Creek[9]	28
Hines Creek (a)[3]	12a	Watino[10]	29
Hines Creek (b)[8]	12b	Grande Prairie[10]	30
Josephine Creek[8]	13	Bear Lake - Smoky River[11]	31
Whitemud[8]	14	Simonette River[11]	32
Pine River[10]	15	HRFZ[9]	33
Septimus[11]	16	Bovie Lake[7]	34
Gordondale[4]	17		

Superscript codes explanations: [1]Lavoie (1958), [2]Sikabonyi and Rodgers (1959), [3]Leckie and Hayes (1990), [4]Richards et al. (1990), [5]Norgard, G. T. (1997), [6]Eaton et al. (1999), [7]MacLean and Morrow (2004), [8]Mei (2009), [9]Davies et al. (2018), [10]Geological Atlas of the Western Canada Sedimentary Basin,[11]Geographic reference (Trend Surface Analysis).

There are several important assumptions and limitations of our analysis that must be considered. Both the trend surface residual method (using formation tops) and interpretation of seismic profiles are best suited to characterize faults with vertical offset. Thus, it is likely that strike-slip structures have been missed. In addition, trend surface residual analysis and seismic interpretation suffer from other resolution constraints. The trend surface analysis is limited by the spatial resolution afforded by well control; for example, it is clear that the Basal Fish Scale Zone residual map has both better spatial resolution and more uniform coverage than the deeper horizons. Similarly, seismic interpretations are constrained by both the limited availability of seismic data as well as its inherent low vertical resolution limit (minimum resolvable fault offset of approximately 25m, in the case of the LITHOPROBE profiles considered here). This implies that many "subseismic" faults may exist that could be incorporated in the analysis within the context of fault scaling relationships and structural corridors (e.g., Gauthier et al., 1993). Ultimately, our analysis provides a structural model that can be further examined and tested with new data as it becomes available.

Acknowledgments

The authors would like to thank Pulse Seismic Inc. for allowing the publication of seismic profile A in this report. Mark Cooper, Mark Hayes and Taylor Mennis are thanked for valuable discussions regarding formation tops catalogues. Authors would like to also thank Michelle Gaucher and Stu Venables for their valuable insights. Authors would like to acknowledge the Natural Resources Canada Geoscience for New Energy Supply (GNES) program, Geoscience BC and NSERC Discovery Grant (grant number RGPIN/03823-2017) for providing the financial support for this research. The authors thank geoLOGIC systems ltd. for their contribution of data and software used in this study. All geoLOGIC systems ltd. data and software is ©2021.

References

Barclay, J. E., Krause, F. F., Campbell, R. I., Utting, J., 1990. Dynamic casting of a graben complex: basin infill and differential subsidence during the Permo–Carboniferous, Peace River Embayment, western Canada. Bulletin of Canadian Petroleum Geology 38, 115–145.

Eaton, D. W., 2018. Passive seismic monitoring of induced seismicity: Fundamental principles and application to energy technologies. Cambridge University Press.

Gauthier, B. D. M., Lake, S. D., 1993. Probabilistic modeling of faults below the limit of seismic resolution in Pelican Field, North Sea, offshore United Kingdom. AAPG Bulletin 77, 761–777.

Hope, J., Eaton, D. W., Ross, G. M., 1999. Lithoprobe seismic transect of the Alberta Basin: Compilation and overview. Bulletin of Canadian Petroleum Geology 47, 331–345.

Liseroudi, M. H., Ardakani, O. H., Sanei, H., Pedersen, P. K., Stern, R. A., Wood, J. M., 2020. Origin of sulfate-rich fluids in the Early Triassic Montney Formation, Western Canadian Sedimentary Basin. Marine and Petroleum Geology 114, 104236.

Mei, S., 2009. New insights on faults in the Peace River Arch region, northwest Alberta, based on existing well-log data and refined trend surface analysis. Canadian Journal of Earth Sciences 46, 41–65.

O'Connor, M. J., Gretener, P. E., 1974. Differential compaction within the Woodbend Group of central Alberta. Bulletin of Canadian Petroleum Geology 22, 269–304.

Wozniakowska, P., Eaton, D. W., 2020. Machine Learning-Based Analysis of Geological Susceptibility to Induced Seismicity in the Montney Formation, Canada. Geophysical Research Letters, 47, e2020GL089651.

Stratigraphy, facies heterogeneities, and structure in the Montney Formation of northeastern British Columbia: Relation to H_2S distribution

Samantha J. Mackie [1], Carolyn M. Furlong[1], Per K. Pedersen[1], and Omid H. Ardakani[2,1]*
[1]Department of Geoscience, University of Calgary, Calgary, Alberta
[2] Natural Resources Canada, Geological Survey of Canada, Calgary, Canada
[*] samantha.mackie@ucalgary.ca

Abstract

In the last decade, the Lower Triassic Montney Formation of the Western Canada Sedimentary Basin (WCSB) has undergone significant development, providing a rich dataset to study structural, stratigraphic, and facies control on the variations in hydrogen sulphide (H_2S) gas content. Splitting the siltstone dominated Montney into the three regional members (i.e., Lower Montney, Middle Montney, and Upper Montney) allows for detailed analysis on the enrichment of H_2S within a local-scale study area in northeastern British Columbia (BC). Within this study area, Upper Montney H_2S content increases within individual parasequences both up-dip and towards the east. In addition to potential up-dip migration, there may be greater sulphur-bearing components in the east, allowing for the sulphate reduction required to generate H_2S. The overlying Middle Triassic thins eastward, providing proximity to the overlying anhydrite-rich beds of the Upper Triassic Charlie Lake Formation. Further, the overlying Middle Triassic Sunset Prairie Formation has an erosional edge that corresponds with eastern elevated H_2S concentrations within the Upper Montney unit. Mapped structures are syn-depositional to the Middle Triassic, potentially providing conduits for early sulphate-rich fluid migration.

In the Middle and Lower Montney, elevated H_2S generally occurs with proximity to the top of the Permian Belloy Formation. Within this study area, limited Lower Montney data is available and thus needs to be further corroborated with regional data. Both the Middle and Lower Montney display elevated H_2S in trends that generally align with mapped faults. The faults may have acted as conduits for sulphate-rich fluids to migrate during early burial then migrate laterally through facies that may have been permeable during early burial, such as the carbonate-rich facies at the boundary between the Middle and Lower Montney. Further core and isotope analyses are required to fully understand this relationship.

Methodology

The study area in northeastern BC is located within the Peace River Block and spans from Township 79 to 81, Range 14 to 18 West of the 6th meridian (Figures 1 and 2). The area selected for this study has a relatively dense dataset of horizontal and vertical wells that penetrate the Montney Formation. Additionally, there is a well-established structural history (Barclay et al., 1990; Davies, 1997, Davies et al., 2018; Furlong et al., 2018; Wozniakowska et al., 2021), mapped hydrocarbon migration fairways (Wood and Sanei, 2016; Sereda and Fur, 2017; Euzen et al., 2021), and various levels of H_2S enrichment within different Montney Members. Within this area, the Montney Formation unconformably overlies the Permian Belloy Formation and unconformably underlies the Sunset Prairie Formation (Furlong et al., 2018; Figure 1).

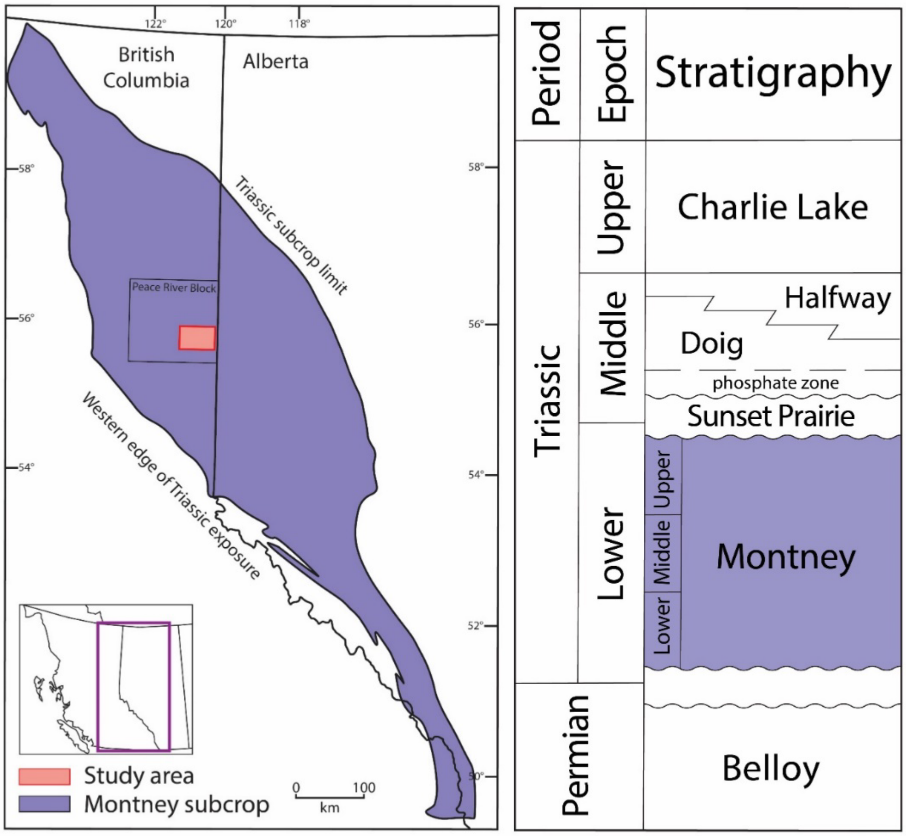

Figure 1. Montney study area located in northeastern British Columbia, Canada (modified from Ghanizadeh et al., 2018). Stratigraphic column of the Montney Formation and surrounding formations in northeastern British Columbia (modified from Furlong et al., 2018).

Within the study area, 865 vertical wells penetrate the Montney Formation, and 1,656 lateral wells produce from the Montney Formation (Figure 2). Using the petrophysical logs from the vertical wells, a regional stratigraphic framework was established comprised of the Lower Montney, Middle Montney (subdivided further into the lower and upper Middle Montney), and Upper Montney members by picking tops, guided by previous work by Davies et al. (2018), Euzen et al. (2018), Proverbs et al. (2018), Zonneveld and Moslow (2018) and Furlong et al. (2021). Next, parasequences within individual Montney members were identified based on coarsening-upward trends within the core and were tied to wireline-log signatures, then correlated throughout the study area. Facies were identified within the core and correlated through the established parasequences. The facies scheme of Furlong et al. (2021) was used to log core and includes fifteen detailed facies that can be binned into three categories: fine-grained silt, coarse-grained silt and carbonate-rich intervals. The binned facies categories were correlated to wireline-log signatures and were correlated through the study area's vertical wells.

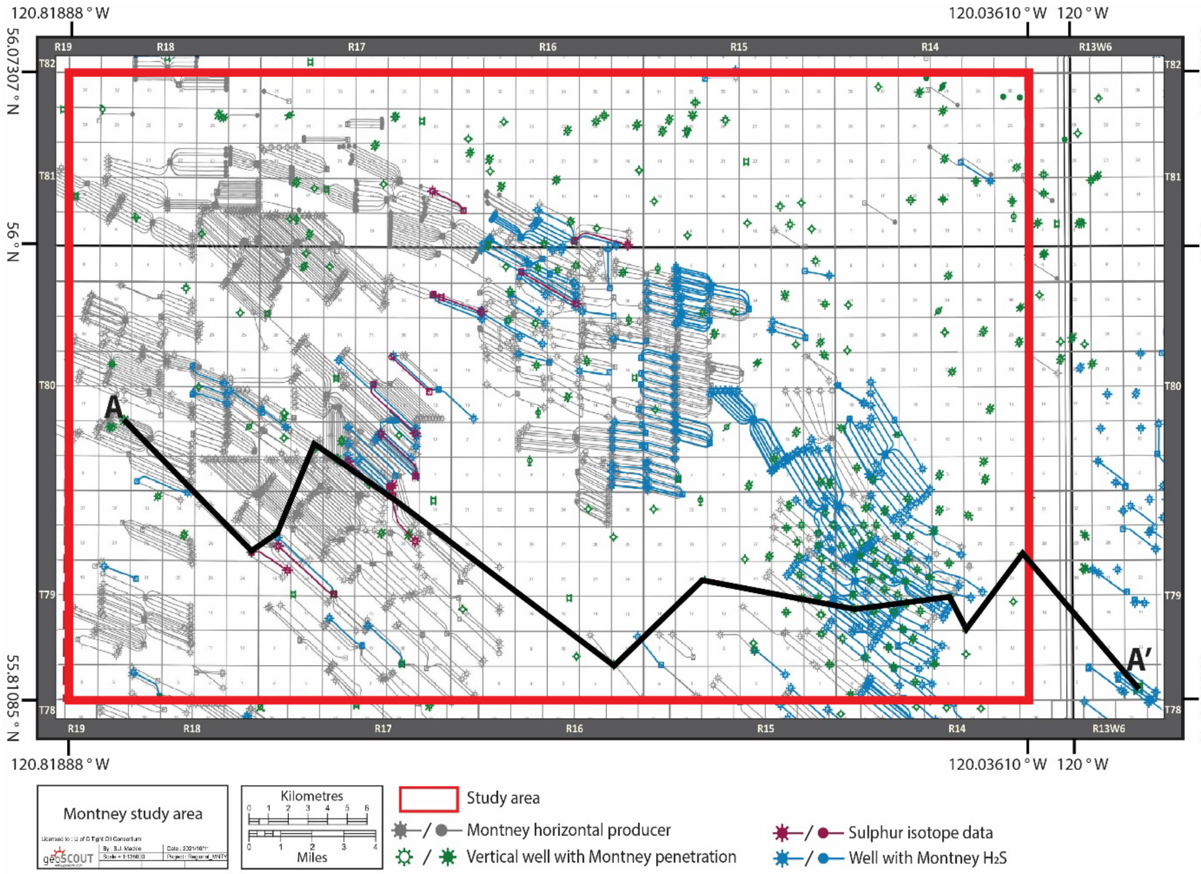

Figure 2. Northeastern British Columbia study area, showing the Montney Formation horizontal producers, vertical wells used for mapping, wells with H_2S, and wells with stable isotope data. The cross-section (A–A') in the southern portion of the study area can be viewed in Figure 3. Map from GeoSCOUT provided by geoLOGIC systems ltd. © 2021.

Publicly available gas-analysis data was accessed through geoSCOUT and the maximum recorded H_2S value for each well was obtained (geoLOGIC systems ltd., 2021). The gas analysis data is highly variable due to sample container, sample-point location, and well-production time. Due to this variability, a single maximum H_2S value per well was used as the research goal of this study is to improve risk mitigation. Of the Montney wells within the study area, ~ 20% (334 wells) have H_2S gas concentrations greater than 0.01%, which is the minimum threshold recorded. Wells were categorized visually based on the stratigraphic unit within the Montney Formation from which the well was landed and are producing hydrocarbons. Maximum H_2S values from the gas analysis data were plotted for wells within each landing zone. The H_2S concentration data was then contoured logarithmically for individual Montney units due to the high variations in values (0.01–1%).

A recent compilation of major structural corridors was then overlaid onto the maps to incorporate the regional structural events (Wozniakowska et al., 2021). Once the structural corridors were located, detailed local faults associated with the Montney Formation were then identified using a wireline log-based structure map of a regional flooding surface in the Doig Formation. The local faults identified were used when hand contouring isopach maps of the Middle Triassic including the Sunset Prairie, Doig, and Halfway formations. The wells form a linear SW – NE trend across the central portion of the study area.

Results and Discussion

The regional cross-section (Figure 3) and the H_2S-production distribution maps for each Montney unit (Figure 4) allow for visualization of trends and correlations between produced H_2S concentration, lithology, stratigraphic intervals, and structural features. In the Upper Montney, wells that were landed within the same parasequence targeting similar coarse-grained siltstone facies can have no, low or high H_2S contents, highlighting the lateral variability. Upper Montney H_2S concentrations increase eastward and up-dip, likely migrating through permeability pathways. In addition to structurally influenced H_2S migration, there may be higher concentrations of sulphur-bearing components needed for sulphate reduction. A recent study by Liseroudi et al. (2021), based on the relationship between the $\delta^{34}S$ values of the present-day produced-gas H_2S and other sulphur-bearing species from the Montney and neighbouring formations, proposed a dual in situ and migrated TSR-derived origin for the H_2S gas, with substantial contributions of in situ H_2S in the Montney Formation. To generate in situ H_2S via TSR, early anhydrite and/or sulphate-rich brines are required (Liseroudi et al., 2021).

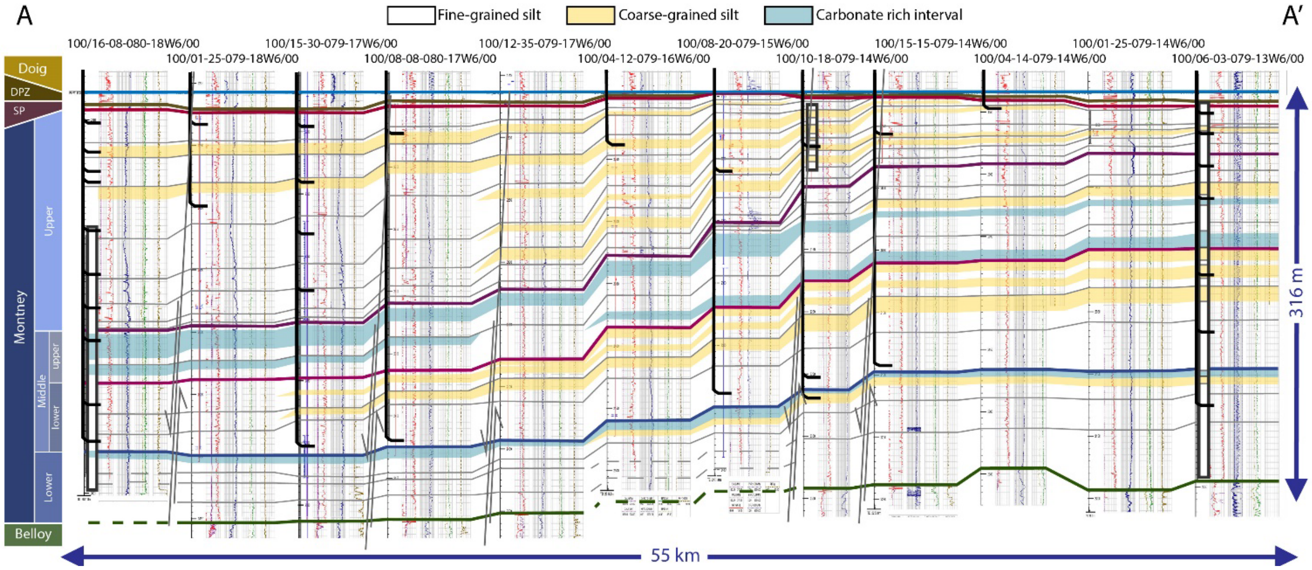

Figure 3. Stratigraphic cross-section highlighting the Montney Formation units and the parasequences within individual Montney units in northeastern British Columbia. The Montney facies, based on a scheme developed by Furlong et al., (2021) were mapped across the study area and constrained laterally within individual parasequences. The variability in vertical and lateral facies heterogeneities highlights the complexity of the Montney Formation. Montney lateral facies are schematically projected onto cross-section A–A’ (location shown in Figure 2), highlighting various operational target zones. Well logs are accessed through GeoSCOUT provided by geoLOGIC systems ltd. © 2021. Abbreviations: DPZ, Doig phosphate zone; SP, Sunset Prairie.

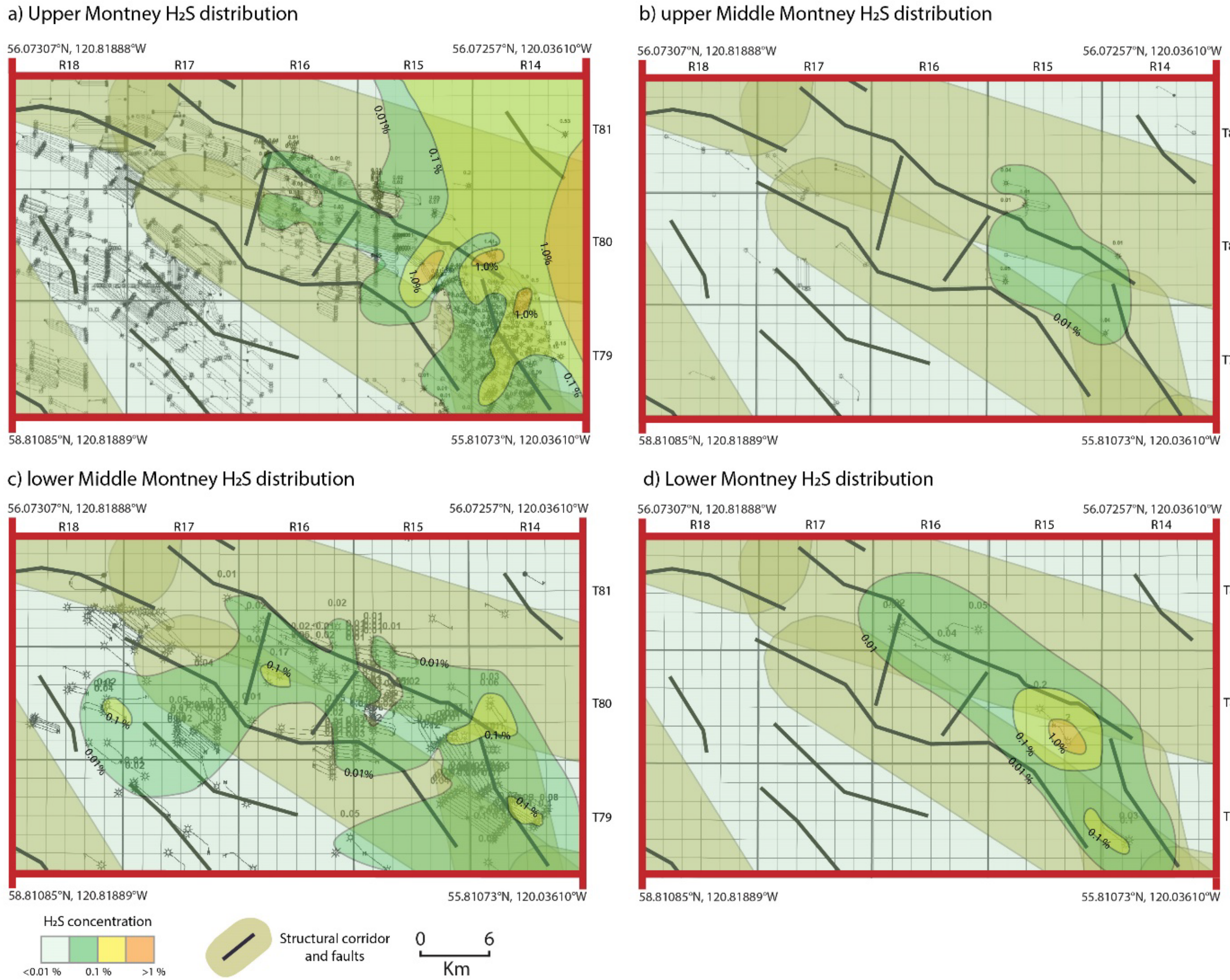

Figure 4. Montney Formation H_2S distribution within the northeastern British Columbia study area, split according to individual Montney units and contoured logarithmically with an overlay of structural corridors after Wozniakowska et al. (2021): **a)** Upper Montney H_2S map, showing a drastic increase in H_2S concentration toward the east of the study area; **b)** upper Middle Montney H_2S map, showing a small dataset primarily with H_2S in the eastern portion of the study area; **c)** lower Middle Montney H_2S map, displaying an arc shape across the study area, which may change as more wells are drilled in the northern portion; **d)** Lower Montney H_2S map, using a very limited dataset that shows a high concentration of H_2S in the eastern portion of the study area. Map data from GeoSCOUT provided by geoLOGIC systems ltd. © 2021

In this study area, the overlying Middle Triassic Doig, Halfway, and Sunset Prairie formations thin toward the east. This thinning in combination with faulting may have allowed sulphate-rich fluids sourced from anhydrite beds in the Charlie Lake Formation to diffuse downward into the Montney Formation (Desrocher et al., 2004). The Charlie Lake Formation sourcing sulphur is supported by Chalmers et al. (2021), who demonstrated that Upper Montney samples in northeastern BC have a solely Triassic or mixed Triassic and Devonian signature through anhydrite sulphur-isotope analysis. In addition to the overall Middle Triassic thinning, the overlying Sunset Prairie Formation has an erosive edge within the study area that corresponds to regions of elevated H_2S in the Upper Montney. As the Sunset Prairie Formation directly overlays the Montney Formation in this area, it is a potential sulphate contributor that is in closer stratigraphic proximity to the Montney Formation than the Charlie Lake Formation.

In the eastern part of the study area, the upper part of the Montney Formation was likely subaerially exposed landward of marine deposits of the Sunset Prairie Formation. With the seasonally arid climate of the WCSB in the Triassic (Davies, 1997; Zonneveld and Moslow, 2018), this may have lead to migration of hypersaline meteoric water into the upper part of the Montney Formation in this eastern area. The Sunset Prairie Formation was deposited during a tectonically active time as the base has structural downfaulting preserved, evident by syn-depositional faulting (Furlong et al., 2018). These faults may have acted as fluid conduits for early sulphate-rich brines to enter the Montney Formation. Both potential sulphate sources are associated with a combination of the overlying thinning Middle Triassic and faults acting as fluid conduits. However, further research, potentially studying hypersaline meteoric brines through $\delta^{18}O$ data would allow for a better understanding of the relationship between the Sunset Prairie erosional edge, thinning Triassic, and elevated H_2S occurrence in the Upper Montney Formation.

Within the Middle Montney, most wells are landed in fine-grained siltstone, near the base of the lower Middle Montney (Figure 3). The distribution of lower Middle Montney H_2S is relatively consistent across the study area and does not display the same increase with up-dip direction as seen in the Upper Montney (Figure 4). The Lower Montney H_2S data is limited in this study, thus no distinct Lower Montney trends are observable. Isopachs of Lower Montney in this study area show a westward thinning by approximately 100 m. However, due to the limited number of Lower Montney producing wells in this study and marginal variations in the lower Middle Montney H_2S concentrations (0.01 – 0.1 %), there is no distinct trend between Lower Montney thickness and H_2S concentration. Both the lower Middle Montney and Lower Montney have elevated H_2S zones that trend along mapped faults, which potentially implies early fluid migration through faults. Early fluids migrating through faults may have permeated laterally through the once porous carbonate shell beds found at the top of the Lower Montney or through other previously permeable facies within the Lower Montney.

These hypersaline fluids may have precipitated as sulphate-rich cement (i.e., anhydrite or barite) contributing to the established *in situ* H_2S generation within the Montney Formation (Liseroudi et al., 2021). Although the dataset from the Lower Montney is limited, comparing the Middle and Lower Montney members, H_2S content increases approaching the anhydrite-rich Permian Belloy Formation. Future studies focused on the detailed relationship between faulting and isotopic signatures would improve the understanding of structural controls on elevated H_2S occurrences in northeastern BC. Isotopic studies using $\delta^{18}O$ data focused on the distinct signatures of hypersaline meteoric brines may further this understanding. Detailed core isotope analysis on the carbonate-rich and Lower Montney barite-rich beds may provide additional insights into the early burial fluid migration history of the Montney Formation.

Acknowledgements

Natural Resources Canada, Geoscience BC, and the sponsors of the Tight Oil Consortium at the University of Calgary are thanked for their financial support of this research. The authors would also like to thank geoLOGIC systems ltd. for access to the geoSCOUT GIS program used to search and analyze the well data for this study.

References

Barclay, J.E., Krause, F.F., Campbell, R.I. and Utting, J., 1990. Dynamic casting and growth faulting of the Dawson Creek Graben Complex: Carboniferous-Permian Peace River Embayment, Western Canada. Bull. Can. Pet. Geol. 38, 115–145.

BC Oil and Gas Commission., 2021. Well lookup and reports; BC Oil and Gas Commission, http://www.bcogc.ca/online-services. [November 2021].

Chalmers, G.R.L., Bustin, R.M. Bustin, A.A., 2021. Isotopic fingerprinting of sulphur sources for the hydrogen sulphide gas in the Montney Formation, northeastern British Columbia (NTS 093O, P, 094A, B, G–J, N–P). Geoscience BC Summary of Activities 2020: Energy and Water, Geoscience BC, Report 2021-02, 103–108, http://www.geosciencebc.com/summary-of-activities-2021-energy-and-water/ [November 2021].

Coplen, T.B and Krouse, H.R., 1998. Sulphur isotope data consistency improved. Nature 392, 32. https://doi.org/10.1038/32080.

Davies, G.R., 1997. The Triassic of the Western Canada Sedimentary Basin: tectonic and stratigraphic framework, paleogeography, paleoclimate, and biota. Bulletin of Canadian Petroleum Geology 45, 434–460.

Davies, G., Watson, N., Moslow, T.F., MacEachern, J., 2018. Regional subdivision, sequences, correlation and facies relationships of the Lower Triassic Montney Formation, west-central Alberta to northeastern British Columbia, Canada–with emphasis on the role of paleostructure. Bulletin of Canadian Petroleum Geology 66, 23–92.

Desrocher, S., Hutcheon, I., Kirste, D., Henderson, C.M., 2004. Constraints on the generation of H_2S and CO_2 in the subsurface Triassic, Alberta Basin, Canada. Chemical Geology 204, 237–257. https://doi.org/10.1016/j.geochem.2003.11.012.

Euzen, T., Moslow, T.F., Crombez, V., Rohais, S., 2018. Regional stratigraphic architecture of the Spathian depositions in Western Canada–implications for the Montney resource play. Bulletin of Canadian Petroleum Geology 66, 175–192.

Euzen, T., Watson, N., Fowler, M., Mort, A., 2021. Petroleum distribution in the Montney hybrid play: source, carrier bed, and structural controls. AAPG Bulletin 105, 1867–1892. https://doi.org/10.1306/12222020088.

Furlong, C.M., Gingras, M.K., Moslow, T.F., Zonneveld, J-P., 2018. The Sunset Prairie Formation: designation of a new Middle Triassic formation between the Lower Triassic Montney Formation and Middle Triassic Doig Formation in the Western Canada Sedimentary Basin, northeast British Columbia. Bulletin of Canadian Petroleum Geology 66, 193–214.

Furlong, C.M., Pedersen, P.K., Eaton, D.W., 2021. Sedimentological heterogeneities of the Montney Formation: case study from the

Greater Pouce Coupe area. Canadian Society of Petroleum Geologists, 2021 Online Core Conference, June 17–18, 2021, Calgary, Alberta, Program with Abstracts, 34–38.

geoLOGIC systems ltd., 2021. geoSCOUT version 8.8; geoLOGIC systems ltd., mapping, data management and analysis software, https://www.geologic.com/products/geoscout [August 2021].

Ghanizahed, A., Clarkson, C.R., Vahedian, A., Ardakani. O.H., Wood, J.M., Sanei, H., 2018. Laboratory-based characterization of pore network and matrix permeability in the Montney formation: Insights from methodology comparisons. Bulletin of Canadian Petroleum Geology 66, 472-498.

Liseroudi, M.H., Ardakani, O.H., Pedersen, P.K., Stern, R.A., Wood, J.M., Sanei, H., 2021. Microbial and thermochemical controlled sulfur cycle in the Early Triassic sediments of the Western Canadian Sedimentary Basin. Journal of Geological Society 178, 1–20.

Proverbs, I.P., Bann, K.L., Fratton, C.M., Frostad, C.J., Juska, A., 2018. Facies architecture and sequence stratigraphy of the Lower Triassic Montney Formation, NE British Columbia: fundamental controls on the distribution of 'sweet spots' in a world-class unconventional reservoir. Bull. Can. Pet. Geol. 66, 237–258.

Sereda, R. and Fur, J., 2017 The Lower Montney turbidite complex of northwest Alberta and northeast British Columbia: evolution of an oil and gas play from conventional to unconventional. Proceedings of the 5th Society of Petroleum Engineers, American Association of Petroleum Geologists and Society of Exploration Geophysicists Unconventional Resources Technology Conference, July 24–26, 2017, Austin, Texas, URTeC-2674327-MS, 8 p., https://doi.org/10.15530/urtec-2017-2674327.

Wood, J.M. and Sanei, H., 2016. Secondary migration and leakage of methane from a major tight-gas system. Nat. Commun. 7, art.13614, 9 p.

Wozniakowska, P., Eaton, D.W., Deblonde, C., Mort, A., Ardakani, O.H., 2021. Identification of regional structural corridors in the Montney play using trend surface analysis combined with geophysical imaging. GSC Open File Report 8814; Geological Survey of Canada, Open File 8814, 59 p. https://doi.org/10.4095/328850.

Zonneveld, J-P. and Moslow, T.F., 2018. Paleogeographic setting, lithostratigraphy, and sedimentary framework of the Lower Triassic Montney Formation of western Alberta and northeastern British Columbia. Bulletin of Canadian Petroleum Geology 66, 93–127.

Hydrogen Sulfide (H_2S) Distribution in the Triassic Montney Formation of the Western Canadian Sedimentary Basin

Andrew, W, Kingston[1], Andy, Mort[1], Christine[1], Deblonde, Omid, H, Ardakani[1,2]*
[1]Natural Resources Canada, Geological Survey of Canada, Calgary, Canada
[2]Department of Geoscience, University of Calgary, Calgary, Alberta

[*]andrew.kingston@NRCan-RNCan.gc.ca

Abstract

The Montney Formation is a highly productive hydrocarbon reservoir with significant reserves of hydrocarbon gases and liquids making it of great economic importance to Canada. However, high concentrations of hydrogen sulfide (H_2S) have been encountered during exploration and development that have detrimental effects on environmental, health, and economics of production. H_2S is a highly toxic and corrosive gas and therefore it is essential to understand the distribution of H_2S within the basin in order to enhance identification of areas with a high risk of encountering elevated H_2S concentrations in order to mitigate against potential negative impacts.

Gas composition data from Montney wells is routinely collected by operators for submission to provincial regulators and is publicly available. We have combined data from Alberta (AB) and British Columbia (BC) to create a basin-wide database of Montney H_2S concentrations. We then used an iterative quality control and quality assurance process to produce a dataset that best represents gas composition in reservoir fluids. This included: 1) designating gas source formation based on directional surveys using a newly developed basin-wide 3D model incorporating AGS's Montney model of Alberta with a model in BC, which removes errors associated with reported formations; 2) removed injection and disposal wells; 3) assessed wells with the 50 highest H_2S concentrations to determine if gas composition data is accurate and reflective of reservoir fluid chemistry; and 4) evaluated spatially isolated extreme values to ensure data accuracy and prevent isolated highs from negatively impacting data interpolation. The resulting dataset was then used to calculate statistics for each x, y location to input into the interpolation process. Three interpolations were constructed based on the associated phase classification: H_2S in gas, H_2S in liquid (C7+), and aqueous H_2S. We used Empirical Bayesian Kriging interpolation to generate H_2S distribution maps along with a series of model uncertainty maps.

These interpolations illustrate that H_2S is heterogeneously distributed across the Montney basin. In general, higher concentrations are found in AB compared with BC with the highest concentrations in the Grande Prairie region along with several other isolated region in the southeastern portion of the basin. The interpolations of H_2S associated with different phases show broad similarities. Future mapping research will focus on subdividing intra-Montney sub-members plus under- and overlying strata to further our understanding of the role migration plays in H_2S distribution within the Montney basin.

Methodology

H_2S concentration values were derived from the Alberta Energy Regulator (AER) and British Columbia Oil and Gas Commission (BCOGC) data archives. Operators are required to submit fluid composition analysis to their respective provincial regulator and this data is publicly available for both Alberta and British Columbia. Data used in these models was current as of December 2020.

A 3D model was constructed by implementing AGS's 3D model of Alberta, which was extended into northeast BC resulting in a coherent depth structure for the whole Montney basin. Well data were corrected for true location using directional survey data forming a cloud data points in 3D space. Using this method, we are able to avoid errors associated with inaccuracies in reported formations and permits to use of data without a reported target formation thus greatly increasing the size of the database.

For quality assurance purposes a workflow was developed using FME™ (Safe Software) which employs data transformation capabilities to enable an iterative approach to the QA/QC process. This allowed us filter out Montney-specific data, remove spurious data, and finally conduct statistical analysis. Using this approach we removed outliers, different data types (e.g. binary vs. continuous), injection and disposal well data (not reflective of connate formation chemistry), and checked spatially isolated extreme values. Finally, in order to evaluate the role phase partitioning plays in H_2S distribution we classified data based on hydrocarbon composition defined as: gas-phase (heptane and heavier components <0.1 mol%), liquid-phase (C7+ >0.1 mol%), and aqueous phase. For quality control purposes we evaluated data quality and removed data that was inaccurate and/or not indicative of formation fluids. This generally consisted of removing data with anomalous stratigraphic provenance, sampling location (e.g. "bottom of storage tank"), commingling fluids from multiple depth in a well, and spot-checking the 50 highest values for each geochemical species.

Data interpolation was performed using Empirical Bayesian Kriging within the Geostatistical Analyst toolbox in ArcGIS Pro 2.8. Model quality was assessed via cross-validation with a series of prediction error statistics and using model uncertainty maps

Results and Discussion

Maps of H_2S distribution in the gas-phase, liquid-phase, and aqueous-phase are shown in Figures 1, 2, and 3 respectively. These maps illustrate the heterogeneous distribution of H_2S within the Montney basin and highlight the need to increase our understanding of the cause(s) and processes responsible for H_2S occurrence. Regions with elevated H_2S concentrations (e.g. region around Grande Prairie) tend to have high concentrations in all three phases (gas, liquid, aqueous). Maps of model uncertainty and the standard deviation of values within the interpolation illustrate that regions with elevated H_2S concentrations are also associated with a large range in measured values.

We suggest future research should address intra-Montney variations in H_2S concentrations across the basin and assess the role that major sulfur sources (e.g. Charlie Lake and Leduc Formations) play in the distribution of H_2S in the Montney. Including mapping H_2S distribution in the under- and overlying strata in order to evaluate the role migration plays in the distribution of H_2S within the Western Canadian Sedimentary Basin.

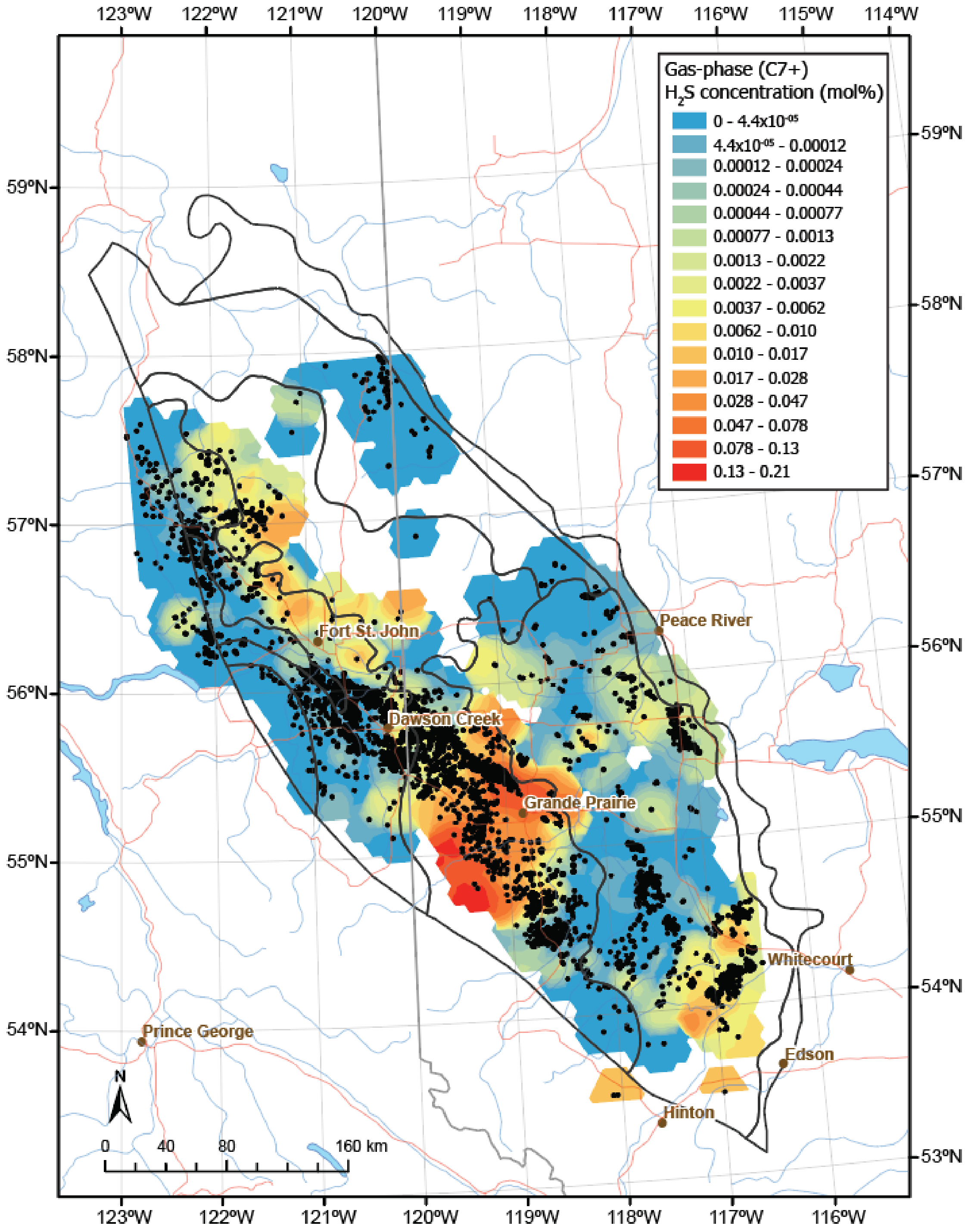

Figure 1. Hydrogen sulfide (H_2S) concentration in the gas-phase. Gas-phase samples are defined as those with a C7+ value lower than 0.1 mol%. Maximum H_2S concentrations were calculated for each surface X-Y location for interpolation.

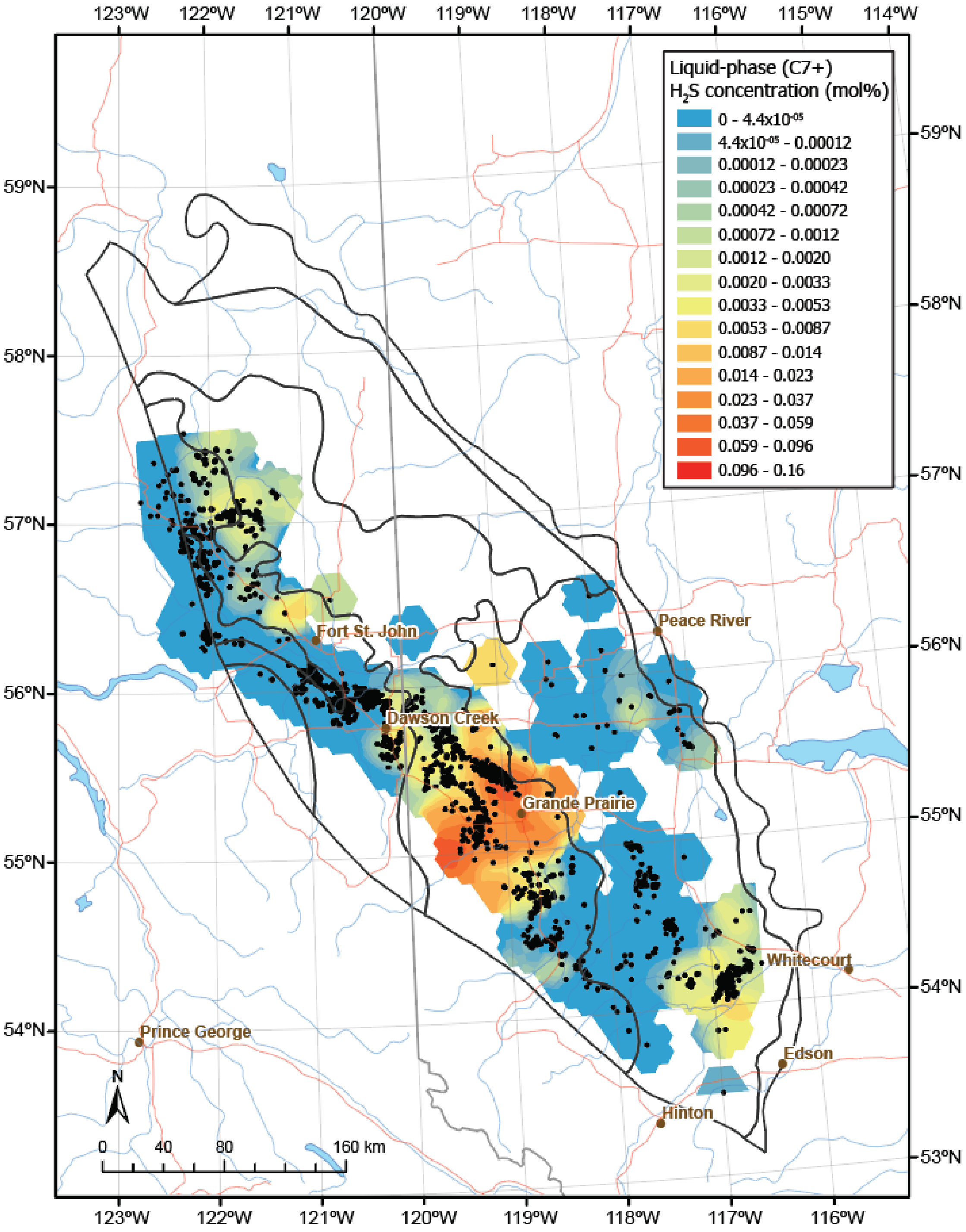

Figure 2. Hydrogen sulfide (H_2S) concentration in the liquid-phase. Liquid-phase samples are defined as those with a C7+ value equal to or greater than 0.1 mol%. Maximum H_2S concentrations were calculated for each surface X-Y location for interpolation.

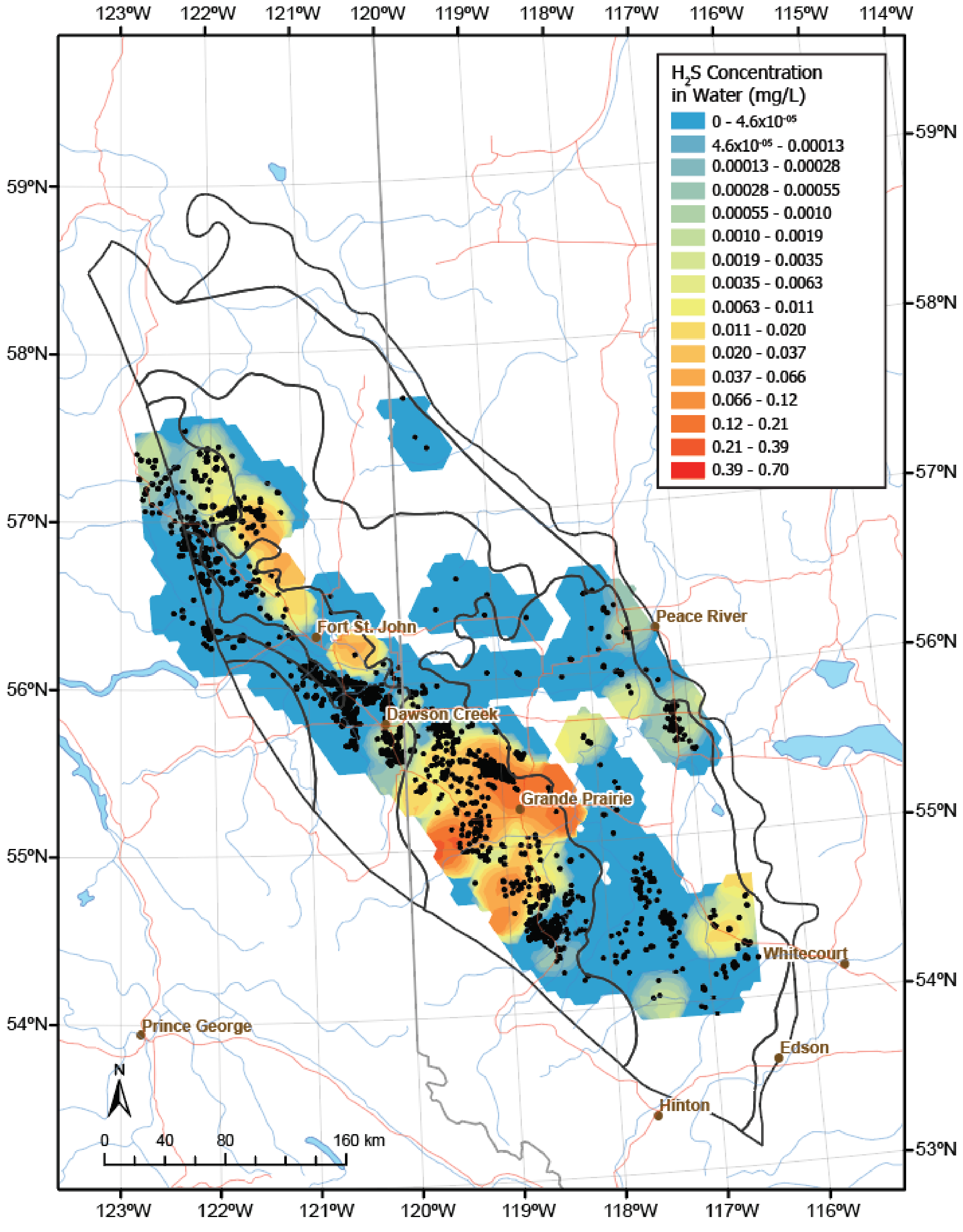

Figure 3. Hydrogen sulfide (H_2S) concentration in the aqueous phase. Maximum H_2S concentrations were calculated for each X-Y point and used for interpolation, see text for details.

Acknowledgements

Richard Nairn (Geological Survey of Canada) assisted with developing directional survey transformations and database management. Mark Hayes and Taylor Mennis (BCOGC) and Paulina Wozniakowska (University of Calgary) assisted with 3D modelling in BC. Christopher Lister (Geological Survey of Canada) provided helpful reviews of a previous version.

Discussions and remaining knowledge gaps

In this section the major topics discussed during Q&A and open discussion at the end of the workshop is summarized. This section covered major specific questions during different workshop themes as well as major scientific and technical gaps/challenges to better understand, predict and reduce the risk of exploration in high H_2S risk areas in Montney Formation in WCSB. Discussions presented here based on the workshop themes.

Diagenetic and Geochemical Controls

Geomicrobiology studies of Montney flow back and produced water is the first study to investigate the possible role of hydraulic fracturing fluids and its chemical composition contribution in generation of H_2S during hydraulic fracturing and production.

- Q: Has any hydrogen consuming microbes been identified in water samples and is there similarities between the H_2S and H_2 consuming microbes? *A: There are microorganisms that can consume hydrogen, and can even produce hydrogen sulfide later on in shale reservoirs (mainly Marcellus shale studies). I have not started looking into this yet, but once I do the metagenomes which allows me to look into the genomes of microorganisms, I will be able to identify genes related to hydrogen consumption/production.*
- Q: Do you have any inclinations how much H_2S can be generated by sulfur reducing microbes in the Montney Formation? *A: I do not have an indication yet as I will start very soon doing some microbial incubations in the laboratory to confirm this, but microorganisms have been identified as a major source of sour oil/gas in different reservoirs (conventional and unconventional).*
- Q: Did any gas samples also collected from the studied well and had any success correlating presence or concentration of measured H_2S with bacteria presence? *A: We have not collected gas samples unfortunately, only water samples. However, I believe that Andrew Kingston, which I collaborate with on this project, was able to distinguish between biogenic/thermogenic sulfide productions within the formation.*
- Q: Have you or anyone done experiments with produced water or cuttings at 80 to 90°C to see if you can measure H_2S and/or sulfur reducing microbes? *A: I have done some incubations at 85°C to see if any organisms would grow, which I was very pleased to see that they did. I tested them under fermentative conditions initially because it is easier for them to grow, but will move forward into "sulfide producing conditions" very soon now that I see there are souring microorganisms in the samples.*
- Q: Was there any accompanying H_2S data with the produced fluid time series? What was causing the darkening of the produced water? Was a water analysis done on the flow back/produced water samples? *A: We have collected a duplicate water sample set for chemical and isotope analysis. In samples obtained after several months we identified sulfide in the water.*
- Q: Is there any estimate on the speed of the reaction process led to H_2S generation? *A: The sulfate reduction pathway is conducted by enzymes, which can react almost instantly if they have the proper amount of substrate (sulfate in this case), and get slower as the products are appearing (sulfide in this case). Given an environment where the sulfate and nutrients are in abundant conditions, the reaction can be almost instantly, but it will get slower as the sulfide is accumulated since this slows the enzymes' activity. In the case of an oil reservoir, it is unclear if the microorganisms have contact with "enough" nutrients to react quite quickly. In our case, it seems that in September, the sulfide producing organisms got an abundant amount of it since we saw the sulfide increasing at that time. Sometimes bacteria need to wait for other bacteria to degrade compounds to get the nutrients they need, which might be why we saw the sulfide production only in September event though the well was flooded in May.*

Diagenetic history of the Montney Formation on a regional samples set and diagenetic sulfur cycle was investigated by Liseroudi (2021). This study expanded in terms of stratigraphy and detailed mineralogy, sulfur isotope analysis of different pyrite forms (bulk and *in situ*) to better understand the origin and distribution of H_2S as well as major mechanism of H_2S formation in the Montney Formation.

- Q: Does the sulfur content and $\delta^{34}S$ of bitumen measured and if those values are aligned with Paleozoic sulfate/anhydrite sulfur isotopic composition? How organic matter sulfur could play a role, especially for the low ppm H_2S values? Did you try to measure kerogen $\delta^{34}S$ in any of the higher TOC, possibly "self sourced" layers? *A: The organic matter (i.e., solid bitumen) sulfur content analysis are underway and we are exploring possibility to do bulk or in-situ $\delta^{34}S$ analysis on organic matter in the Montney Formation.*
- Q: What is the cause of high H_2S in Grand Prairie area? Is there any correlation on H_2S concentration to Vol. % of identified sources (either pyrite or anhydrite)? Can you predict a max expected concentration of H_2S based on in zone generation? Also, I noticed some really high $\delta^{34}S$ values (> +50‰). Can you comment on the origin? *A: possibly related to complex structural features and proximity to Devonian reef structures. Migration of sulfur-bearing fluids (sulfates or H_2S) through fault structures as shown by Liseroudi et al. (2020). It is uncertain, but could be related to updip migration of H_2S from the western edge, which generated more H_2S by thermochemical sulfate reduction.*
- Q: Tom Moslow has observed reworked bitumen clasts in the Montney. Perhaps this bitumen/degraded oil spewed out onto the sea floor from thermal vents and these also sourced the H_2S plumes hypothesised? *A: we did not find any direct evidence for reworked bitumen in our studied samples.*
- As part of the GNES H_2S project are there H_2S maps of formations other than the Montney? *A: This is in progress, we are working a manuscript to investigate all possibilities with regional mapping.*

Distribution and Mapping, Structural and Stratigraphic Controls

Another aspect of NRCan H_2S project was to investigate regional distribution of H_2S in the Montney Formation within the WCSB using public provincial gas datasets. The stratigraphic distribution of H_2S and the potential role of major structures in the basin in formation and possible migration of H_2S has investigated. In this session an overview of the BC Geoscience project led by the University of British Columbia on mapping and distribution and isotopic analysis presented.

- Q: Have you looked at Nordegg as source rock where Doig Phosphate is not present? *A: I have born the Nordegg in mind but with focus on gas isotopes thus far there are fewer available data to test this in Alberta where the Nordegg may well contribute, still molecular geochemistry of fluids being investigated but have not identified diagnostic indicators for the Nordegg in Montney fluids yet but believe it is highly likely that the Nordegg was a contributor.*
- Q: Have you observed any trends in the non-hydrocarbon gases that could relate to gas families? *A: I have very briefly looked at He where it has been measured as an indicator for vertical migration along deep faults but the data are all concentrated around the area of structural complexity (Dawson Creek graben complex, other structures related to PRA) and I have not looked at whether there are any more subtle trends. I have not yet looked at CO_2 but this will doubtless happen but significantly more contextual data is needed to constrain the origins and meaning of CO_2 occurrence.*
- Q: with pressure burial history presented in Dr. Mort's it has mentioned that the numbers worked out that Doig fluids could migrate to Montney. Could we also see gases/fluids from the Charlie Lake migrating downwards, or is the buoyancy too much to overcome? *A: I have not tested fluids higher up but it would be highly pertinent to ascertaining the source of H_2S with Charlie Lake as a candidate if pressure conditions allow. Faults are an unfortunate complication in the simple models I have built since it is very hard to attribute represent rock properties (K, phi) to faults. I am trying to find molecular diagnostics in fluids that would allow them to be correlated to their sources, however many of the fluids can be discriminated on the basis of maturity, but the information is far less specific on source. If we can find good*

evidence for fluid communication between Montney and Charlie Lake then we could make a more confident assumption that these fluids also carried H_2S.

- Q: Do you think a fracture will allow the various Montney zones to commingle or are the layers are enough apart. Alternatively, are the different compositions sharply contrasting or gradual? *A: I would imagine that a fracture would allow very effective communication vertically but I am not sure how well these fluids would be able to mix laterally so you may start seeing laterally heterogeneous fluids as you cross fracture zones - it's something I would like to look at more closely in the Heritage area example.*
- Q: Intriguing to see anti-correlation of induced seismicity with H_2S. Did you try looking at correlation with methane content? Is there any correlation of methane-rich gas migration with the stratigraphy? *A: Unfortunately, we do not tested the possible relationship between excess methane concentration and micro seismicity, for sure it worth to look into it. If you want to see a correlation/or lack of between stratigraphy and methane rich gas migration, a closer look at the Arc Dawson Upper Montney Pool would be the best option.*
- Q: How did you treat multiple analysis over time on a single well? Are you plotting the Max or an average for the well Orientation of transmitting faults/lineaments relative to current/past stress states? Alignment of conventional/turbidite features with structural features, combining structural and facies features for H_2S transmission. *A: We calculated the max from multiple analysis of a single well. Or from multiple wells with the same surface location. We used the max but we did check the standard deviation for multiple measurements and filtered out those where there was large variation since it's hard to get a representative value. These data are nonetheless worthy of separate analysis for this very reason.*
- Q: The “high” H_2S area is actually highly heterogeneous in H_2S content, which suggests much localized fault/fracture influence. Hydrothermal fluids rich in sulfate might have come up faults and result in local enhanced TSR “haloes” around faults/fractures. Seismic data would be needed to investigate further but may not be readily available. Maybe some fortunately located cores might shed some light? *A: one of the major challenges to fully investigate the structural controls on migration of sulfate-rich fluids and H2S is the lack of access to high quality seismic data. So far some cores (as shown in Liseroudi’s talk) cross those mineralized fractures that led to some insight in the origin of fluids that precipitated and healed those fractures.*
- Q: Intriguing and still unexplained: why the $\delta^{34}S$ isotope range of the produced H_2S is so uniform/constrained. *A: This is still one of the unanswered questions, possibly because multiple sources of H_2S in the study area and their mixing. This subject need more investigation.*
- Q: Many operators have wells that start off with no or extremely low H_2S content and then H_2S increases significantly with production time. So some time series of produced gas data with H_2S concentration and $\delta^{34}S$ isotope measurements would be really helpful to figure out what is going on. *A: This phenomenon has been observed in the Permian Basin, Bakken and Eagle Ford and was attributed to the drop in reservoir pressure during production which favoured the differential solution of H_2S relative to hydrocarbon gases. They also considered H_2S adsorption on mineral surfaces and the gradual connectivity to zones of high H_2S. We planned to collect time series gas sampling to investigate the isotopic evolution of H_2S and produced gases that may answer variations of H_2S during production. Possible compilation of geo-microbiological data and water geochemistry shed some light on this issue.*

In conclusion considering the research that have been done so far on the origin and distribution of H_2S in the Montney Formation the major unknowns are: (1) lack of control on sampling methodology, analysis of collected samples by industry and submitted to provincial regulators, which introduce an inherent bias into the regional datasets, (2) dominant mechanism(s) of H_2S generation and contribution of each possible mechanism, (3) lack of comprehensive understanding on contribution of organic matter sulfur in H_2S generation, (4) lack of data geochemical data to model the H_2S generation in order to predict high risk areas, and (5) lack of access to regional high quality data to better resolve structures in the WCSB.